

Synthetic Augmentation in Imbalanced Learning: When It Helps, When It Hurts, and How Much to Add

Zhengchi Ma

Department of Electrical & Computer Engineering, Duke University
and

Anru R. Zhang*

Department of Biostatistics and Department of Computer Science,
Duke University

Abstract

Imbalanced classification often causes standard training procedures to prioritize the majority class and perform poorly on rare but important cases. A classic and widely used remedy is to augment the minority class with synthetic samples, but two basic questions remain under-resolved: when does synthetic augmentation actually help, and how many synthetic samples should be generated?

We develop a unified statistical framework for synthetic augmentation in imbalanced learning, studying models trained on imbalanced data augmented with synthetic minority samples. Our theory shows that synthetic data is not always beneficial. In a “local symmetry” regime, imbalance is not the dominant source of error, so adding synthetic samples cannot improve learning rates and can even degrade performance by amplifying generator mismatch. When augmentation can help (“local asymmetry”), the optimal synthetic size depends on generator accuracy and on whether the generator’s residual mismatch is directionally aligned with the intrinsic majority–minority shift. This structure can make the best synthetic size deviate from naive full balancing. Practically, we recommend Validation-Tuned Synthetic Size (VTSS): select the synthetic size by minimizing balanced validation loss over a range centered near the fully balanced baseline, while allowing meaningful departures. Extensive simulations and real data analysis further support our findings.

Keywords: Data Imbalance, Synthetic Oversampling, Synthetic Data Size.

*Corresponding author: anru.zhang@duke.edu

1 Introduction

Imbalanced classification, where one class is observed far less frequently than the other, is a pervasive obstacle in modern statistical learning. Standard empirical risk minimization tends to favor overall accuracy, which often leads to systematically degraded detection of the minority class. This failure mode is especially consequential when the rare events are clinically, economically, or operationally important, as in medical data analysis (Salmi et al., 2024), finance (Chen, Calabrese and Martin-Barragan, 2024), and industrial anomaly detection (Bougaham et al., 2024). These challenges motivate a renewed statistical focus on mitigating imbalance in a principled way, without turning augmentation into a purely heuristic step (Chen, Yang, Yu, Shi and Chen, 2024).

A classic response to imbalance is to augment the minority class with additional (real or synthetic) samples, so that model training is less dominated by the majority class. The simplest mechanism is bootstrap-style oversampling, i.e., resampling minority observations with replacement (Efron and Tibshirani, 1994). A widely used alternative is SMOTE, which creates new minority examples by interpolating between a minority observation and its neighbors (Chawla et al., 2002). SMOTE has inspired many extensions, including ADASYN (He et al., 2008), Borderline-SMOTE (Han et al., 2005), safe-level-SMOTE (Bunkhumpornpat et al., 2009), and DBSMOTE (Bunkhumpornpat et al., 2012). Related augmentation strategies include Mixup (Zhang et al., 2017) and conditional data synthesis approaches (Tian and Shen, 2025). Beyond classical generators, modern deep generative models can also serve as synthetic sample generators, including VAEs (Kingma and Welling, 2013), normalizing flows (Papamakarios et al., 2021), GANs (Goodfellow et al., 2014), and diffusion/score-based models (Ho et al., 2020; Song, Sohl-Dickstein, Kingma, Kumar, Ermon and Poole, 2020). More recently, attention-based large language models have also been explored for synthetic data generation (Nakada et al., 2024). For a broad view of deep gen-

erative synthetic data across modalities and domains, see [Eigenschink et al. \(2023\)](#).

What remains unclear: when does augmentation help, and how much is enough?

Despite the breadth of methods and applications, two basic questions remain surprisingly under-resolved from a statistical perspective.

First, *synthetic augmentation is not guaranteed to help*. Because synthetic samples are generated from an estimated minority distribution, augmentation can reduce the impact of imbalance while also introducing *generator mismatch* and changing the effective variance. Its overall effect on the target performance criterion therefore depends on both the data geometry and the quality of the generator.

Second, *even when augmentation is beneficial, it is unclear how many synthetic samples should be added*. A common practice is *naive balancing*: generate enough synthetic minority samples so that the minority-plus-synthetic count matches the majority count. This rule is simple and often reasonable, but it is largely heuristic. Synthetic samples generally do not carry the same information as independent real samples, and their mismatch can interact with sample size in nontrivial ways.

Our perspective: treat augmentation as a controllable statistical operation.

This paper develops a unified framework that treats synthetic augmentation as a *controllable* statistical operation and analyzes the risk trade-offs it induces under a *balanced* evaluation criterion, i.e., one that treats the two classes symmetrically at the population level. This criterion is common in imbalanced learning when minority detection is a primary goal. Our framework applies to a broad class of training losses, classification rules, and synthetic-sample generators, and it is parameterized by two quantities: the *synthetic size* and the *generator mismatch*. Our results show how these two factors jointly determine the statistical value of augmentation.

Two guiding questions and the regimes they reveal. We use our framework to answer two high-level questions that map directly to practice.

Q1. Does augmenting with synthetic samples always help in imbalanced learning?

Not always. The key distinction is whether imbalance creates a *first-order* distortion of the learning objective near the population optimum under the balanced criterion. When the two classes exert different first-order influence in optimization-relevant directions, changing the effective class proportions can shift the learned solution toward the balanced target. We call this the *local asymmetry* regime, and it is precisely the setting in which synthetic augmentation can improve performance.

Our analysis also identifies an important complementary regime in which synthetic augmentation *cannot* help, even under severe imbalance. In this *local symmetry* regime, the two classes already exert equal first-order influence near the balanced optimum in the directions that matter for optimization. Then imbalance is not the bottleneck, so adding synthetic minority samples yields little benefit; if the generator is imperfect, it can instead amplify mismatch effects and degrade performance. We develop this phenomenon in detail in Section 5.

Q2. Is naive balancing truly the best?

Naive balancing is often a sensible default, but it is not universally optimal. Its optimality depends on generator quality and on whether the residual synthetic mismatch aligns with the intrinsic majority–minority difference in the learning problem. When the generator is consistent and its remaining mismatch has no exploitable directional structure, naive balancing is essentially rate-optimal: it removes the leading imbalance effect, and finer tuning can improve performance only by a constant factor. By contrast, when the mismatch is

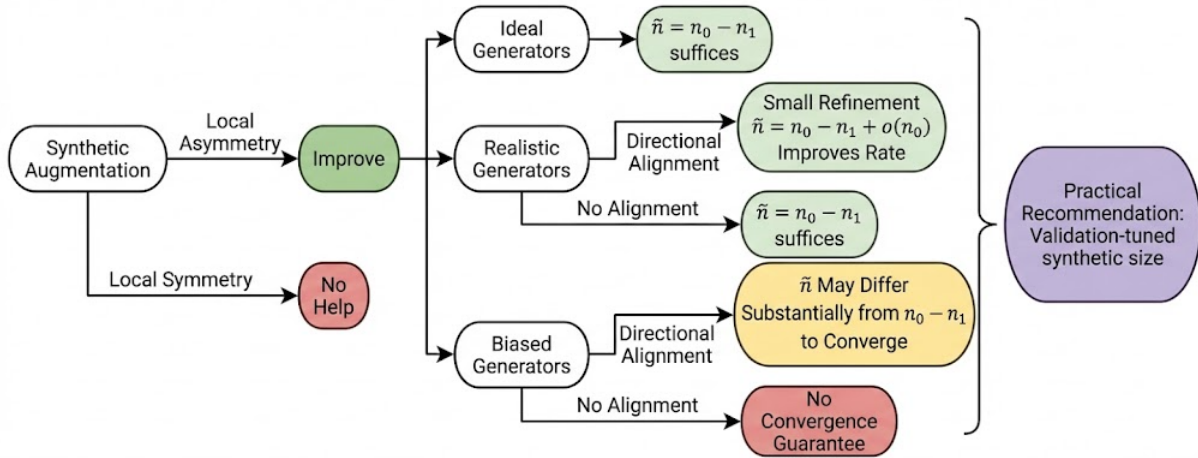


Figure 1: Flowchart of main results

directionally aligned with the majority–minority discrepancy, a *small* adjustment around naive balancing can further reduce the leading bias and produce a measurable gain. For systematically biased (inconsistent) generators, tuning the synthetic size may even be necessary for consistency, and the optimal choice can be far from naive balancing when bias cancelation is possible; when the mismatch direction is not aligned, changing the quantity alone cannot remove the bias.

A practical recommendation: treat synthetic size as a tunable hyperparameter. In real applications, the relevant regime and mismatch direction are rarely known a priori. Motivated by the theory, we propose a simple and robust procedure, *Validation-Tuned Synthetic Size (VTSS)*: sweep a range of synthetic sizes and choose the value that minimizes balanced validation loss. VTSS is implementation-friendly, captures potential gains from nontrivial sizing, and automatically avoids harmful over-synthesis in regimes where synthetic data does not help.

The main messages of our theory are summarized in Figure 1, which maps the local asymmetry/symmetry regimes and generator quality to when synthetic augmentation is helpful and how the synthetic size should be chosen.

Our framework accommodates a broad class of training losses, classification rules, and synthetic-sample generators. For completeness, the Supplementary Materials provide additional details and examples for the losses (Section 10), classifiers (Section 11), and generators (Section 12) considered in this work.

Related work. Synthetic minority augmentation has a long history in statistics and machine learning, including bootstrap-style oversampling (Efron and Tibshirani, 1994), SMOTE (Chawla et al., 2002) and its variants such as Borderline-SMOTE (Han et al., 2005), ADASYN (He et al., 2008), safe-level-SMOTE (Bunkhumpornpat et al., 2009), and DBSMOTE (Bunkhumpornpat et al., 2012), as well as related augmentation strategies such as Mixup (Zhang et al., 2017) and conditional synthesis (Tian and Shen, 2025). Deep generative approaches include VAEs (Kingma and Welling, 2013), normalizing flows (Papamakarios et al., 2021), GANs (Goodfellow et al., 2014), and diffusion/score-based models (Ho et al., 2020; Song, Sohl-Dickstein, Kingma, Kumar, Ermon and Poole, 2020); LLM-based oversampling has also been studied (Nakada et al., 2024). A broader survey of deep generative approaches to synthetic data can be found in Eigenschink et al. (2023).

Relatedly, class imbalance can also be addressed without generating data, through the choice of objective, decision rule, and evaluation metric. Existing work considered three common paradigms: (i) classical risk minimization (often paired with reweighting or resampling), (ii) cost-sensitive learning that minimizes a weighted combination of type I and type II errors, and (iii) the Neyman–Pearson (NP) paradigm, which controls type I error at a prespecified level while minimizing type II error (Rigollet and Tong, 2011; Tong et al., 2020; Feng et al., 2021). These perspectives motivate alternatives to oversampling such as loss reweighting, threshold adjustment, and constraint-based formulations.

Recent theoretical work has begun to clarify statistical properties of learning with synthetic data. Nakada et al. (2024) provides theoretical guarantees for when LLM-generated mi-

minority samples can improve learning under imbalance and discusses interactions between generator quality and augmentation size. [Lyu et al. \(2025\)](#) emphasizes that naively treating synthetic samples as real can introduce systematic bias and proposes bias-correction strategies with extensions beyond standard imbalanced classification. For uncertainty quantification and inference, [Keret and Shojaie \(2025\)](#) studies inference with AI-generated synthetic data for generalized linear models, while [Räisä et al. \(2025\)](#) develops a Bayesian framework that accounts for the synthetic generation mechanism and establishes conditions for consistent inference. [Xia and Klusowski \(2026\)](#) frames imbalanced classification as transfer learning under label shift and highlights settings in which oversampling incurs a cost, including curse-of-dimensionality effects for SMOTE. [Ahmad et al. \(2025\)](#) develops uniform concentration bounds comparing empirical risk on synthetic samples to the true minority risk and derives excess-risk guarantees for kernel-based classifiers.

A growing body of applied work illustrates synthetic augmentation in downstream analyses. In medical imaging, [Ktena et al. \(2024\)](#) uses conditional diffusion models for label-steerable augmentation and studies robustness and fairness under distribution shift. [Rodríguez-Almeida et al. \(2022\)](#) generates synthetic patient records for small, imbalanced disease prediction datasets, and [Wang et al. \(2025\)](#) studies self-improving generative foundation models for medical images and downstream gains from synthetic images. In finance, [Roy et al. \(2024\)](#) uses diffusion-generated transaction samples to augment scarce fraud cases. In time-series and industrial applications, [Stanton et al. \(2024\)](#) synthesizes time-series sensor datasets to support downstream predictive maintenance modeling.

Our work differs from these lines by providing a unified, risk-based characterization of when synthetic augmentation helps versus when it cannot, and by showing that the *choice of synthetic size* is a first-order practical decision rather than a fixed heuristic. Our theory isolates qualitative regimes (local asymmetry vs. local symmetry), explains the bias–variance

trade-offs induced by generator mismatch and synthetic size, and motivates VTSS as a robust practical procedure.

Organization. The rest of this paper is organized as follows. Section 2 introduces the notation and formal setup for imbalanced classification with synthetic minority augmentation, and defines the balanced evaluation objective used throughout. Section 3 develops our main excess-risk characterization, which makes explicit how performance depends on both class-proportion imbalance and generator-induced distributional mismatch. Section 4 studies the local asymmetry regime in which synthetic augmentation can improve learning, and shows how the optimal synthetic size depends on generator quality and the directional structure of its bias. Section 5 identifies a local symmetry regime in which imbalance is not the dominant bottleneck, so synthetic augmentation cannot improve rates and may degrade performance when the generator is imperfect. Section 6 then presents our practical procedure, Validation-Tuned Synthetic Size (VTSS), which selects the synthetic size by minimizing balanced validation loss. Section 7 provides simulation studies that verify the qualitative predictions of the theory and evaluate VTSS, and Section 8 reports a real-data application using electronic health records (EHR) data. Section 9 concludes with discussion and future directions. Proofs and additional technical details are deferred to the Supplementary Materials, which also include further examples for the losses (Section 10), classifiers (Section 11), and synthetic-sample generators (Section 12) covered by our framework.

2 Notation and Problem Formulation

Notation. For nonnegative sequences $\{a_n\}$ and $\{b_n\}$, we write $a_n \lesssim b_n$ (resp. $a_n \gtrsim b_n$) if there exists a universal constant $C > 0$ such that $a_n \leq Cb_n$ (resp. $a_n \geq Cb_n$). We write $a_n \asymp b_n$ if both $a_n \lesssim b_n$ and $b_n \lesssim a_n$ hold, and write $a_n \ll b_n$ (resp. $a_n \gg b_n$) if $a_n/b_n \rightarrow 0$

(resp. $a_n/b_n \rightarrow \infty$). Vectors are denoted by boldface letters (e.g., $\mathbf{x}, \mathbf{y}, \mathbf{u}, \mathbf{v}$), and $\|\cdot\|$ denotes the Euclidean norm. Gradients and Hessians with respect to $\boldsymbol{\theta}$ are denoted by ∇ and ∇^2 . For two nonzero vectors \mathbf{u}, \mathbf{v} of the same dimension, we denote their angle and the sine value by $\angle(\mathbf{u}, \mathbf{v}) := \arccos\left(\frac{\mathbf{u}^\top \mathbf{v}}{\|\mathbf{u}\|\|\mathbf{v}\|}\right)$, $\sin \angle(\mathbf{u}, \mathbf{v}) = \sqrt{1 - \left(\frac{\mathbf{u}^\top \mathbf{v}}{\|\mathbf{u}\|\|\mathbf{v}\|}\right)^2}$. For a symmetric matrix A , let $\lambda_{\max}(A)$ and $\lambda_{\min}(A)$ denote its largest and smallest eigenvalues. For symmetric matrices A and B , we write $A \succeq B$ (resp. $A \succ B$) if $A - B$ is positive semidefinite (resp. positive definite). Throughout, we work in an asymptotic regime where the data-generating distributions are fixed while the sample size grows. We use standard stochastic order notation $O_P(\cdot)$, $o_P(\cdot)$, $\Omega_P(\cdot)$, and $\Theta_P(\cdot)$. In particular, for sequences indexed by (n_0, n_1) , we write $x_{(n_0, n_1)} = O_P(a_{(n_0, n_1)})$ as $n_0, n_1 \rightarrow \infty$ if $x_{(n_0, n_1)}/a_{(n_0, n_1)}$ is stochastically bounded, and write $x_{(n_0, n_1)} = o_P(1)$ if $x_{(n_0, n_1)} \rightarrow 0$ in probability. We write $x_{(n_0, n_1)} = \Omega_P(a_{(n_0, n_1)})$ if $x_{(n_0, n_1)}/a_{(n_0, n_1)}$ is stochastically bounded away from zero, and $x_{(n_0, n_1)} = \Theta_P(a_{(n_0, n_1)})$ if both $O_P(\cdot)$ and $\Omega_P(\cdot)$ hold.

Problem formulation. We consider binary classification under class imbalance, where $y = 0$ denotes the majority class and $y = 1$ denotes the minority class. Let the class-conditional distributions be $\mathbf{x} \mid (y = 0) \sim \mathcal{P}_0$, $\mathbf{x} \mid (y = 1) \sim \mathcal{P}_1$. We observe n_0 majority samples and n_1 minority samples ($n_0 > n_1$), and we may augment the data with \tilde{n} synthetic minority samples. Synthetic covariates are drawn from a generator-induced distribution \mathcal{P}_{syn} ; since the generator is typically trained on the observed data, \mathcal{P}_{syn} may depend on (n_0, n_1) and should therefore be written more precisely as $\mathcal{P}_{\text{syn}, n_0, n_1}$. We suppress this dependence for notational simplicity.

Let $\ell(\boldsymbol{\theta}; \mathbf{x}, y)$ be a loss function with parameter $\boldsymbol{\theta} \in \Theta$. Common choices include cross-entropy/logistic loss, squared loss, hinge loss, and exponential loss (see Section 10 of the Supplementary Materials for detailed discussions). To treat the two classes symmetrically

at the population level, we define the **balanced population risk**

$$\mathcal{R}(\boldsymbol{\theta}) = \frac{1}{2} \mathbb{E}_{\mathcal{P}_0} \ell(\boldsymbol{\theta}; \mathbf{x}, 0) + \frac{1}{2} \mathbb{E}_{\mathcal{P}_1} \ell(\boldsymbol{\theta}; \mathbf{x}, 1), \quad (1)$$

and suppose there exists a minimizer $\boldsymbol{\theta}^* = \arg \min_{\boldsymbol{\theta} \in \Theta} \mathcal{R}(\boldsymbol{\theta})$. Augmenting the training data with \tilde{n} synthetic minority samples changes the effective class proportions (see Section 10 of the Supplement for a discussion of specific synthetic data generators used to produce these samples). Let $\pi_0 = \frac{n_0}{n_0+n_1+\tilde{n}}$, $\pi_1 = \frac{n_1}{n_0+n_1+\tilde{n}}$, $\tilde{\pi} = \frac{\tilde{n}}{n_0+n_1+\tilde{n}}$; so that $\pi_0 + \pi_1 + \tilde{\pi} = 1$. The resulting **synthetic population risk** is

$$\tilde{\mathcal{R}}(\boldsymbol{\theta}) = \pi_0 \mathbb{E}_{\mathcal{P}_0} \ell(\boldsymbol{\theta}; \mathbf{x}, 0) + \pi_1 \mathbb{E}_{\mathcal{P}_1} \ell(\boldsymbol{\theta}; \mathbf{x}, 1) + \tilde{\pi} \mathbb{E}_{\mathcal{P}_{\text{syn}}} \ell(\boldsymbol{\theta}; \mathbf{x}, 1),$$

with minimizer $\tilde{\boldsymbol{\theta}} = \arg \min_{\boldsymbol{\theta} \in \Theta} \tilde{\mathcal{R}}(\boldsymbol{\theta})$. In practice, we observe $\{(\mathbf{x}_i, y_i)\}_{i=1}^{n_0+n_1}$ and generate synthetic samples $\{\tilde{\mathbf{x}}_i\}_{i=1}^{\tilde{n}} \sim \mathcal{P}_{\text{syn}}$, $\tilde{y}_i \equiv 1$. We then minimize the **empirical augmented risk**

$$\begin{aligned} \hat{\mathcal{R}}(\boldsymbol{\theta}) &= \frac{1}{n_0 + n_1 + \tilde{n}} \left(\sum_{i=1}^{n_0+n_1} \ell(\boldsymbol{\theta}; \mathbf{x}_i, y_i) + \sum_{i=1}^{\tilde{n}} \ell(\boldsymbol{\theta}; \tilde{\mathbf{x}}_i, 1) \right) \\ &= \frac{1}{n_0 + n_1 + \tilde{n}} \left(\sum_{i=1}^{n_0} \ell(\boldsymbol{\theta}; \mathbf{x}_i^{(0)}, 0) + \sum_{i=1}^{n_1} \ell(\boldsymbol{\theta}; \mathbf{x}_i^{(1)}, 1) + \sum_{i=1}^{\tilde{n}} \ell(\boldsymbol{\theta}; \tilde{\mathbf{x}}_i, 1) \right), \end{aligned}$$

where $\{\mathbf{x}_i^{(0)}\}_{i=1}^{n_0}$ and $\{\mathbf{x}_i^{(1)}\}_{i=1}^{n_1}$ are the observed majority and minority samples. Let $\hat{\boldsymbol{\theta}} = \arg \min_{\boldsymbol{\theta} \in \Theta} \hat{\mathcal{R}}(\boldsymbol{\theta})$. Our goal is to estimate the balanced-risk optimizer $\boldsymbol{\theta}^*$ from imbalanced data, and to understand how synthetic augmentation, through \tilde{n} and \mathcal{P}_{syn} , affects the balanced excess risk $\mathcal{R}(\hat{\boldsymbol{\theta}}) - \mathcal{R}(\boldsymbol{\theta}^*)$.

3 Excess Risk Analysis for Imbalanced Classification

In this section, we establish a fundamental limitation on the balanced excess risk when training on imbalanced data augmented with synthetic minority samples. The key obstruction is a *distribution bias* induced by (i) the effective class weighting in the augmented

training population and (ii) the mismatch between the synthetic distribution \mathcal{P}_{syn} and the true minority distribution \mathcal{P}_1 . We begin by making these two effects explicit through a decomposition of the synthetic population risk, and then use it to characterize $\mathcal{R}(\hat{\boldsymbol{\theta}}) - \mathcal{R}(\boldsymbol{\theta}^*)$.

A key decomposition of the synthetic risk. Recall the balanced population risk $\mathcal{R}(\boldsymbol{\theta})$ and the synthetic population risk $\tilde{\mathcal{R}}(\boldsymbol{\theta})$. A direct calculation yields

$$\begin{aligned} \tilde{\mathcal{R}}(\boldsymbol{\theta}) &= \mathcal{R}(\boldsymbol{\theta}) \\ &+ \left(\pi_0 - \frac{1}{2}\right) \left[\mathbb{E}_{\mathcal{P}_0} \ell(\boldsymbol{\theta}; \mathbf{x}, 0) - \mathbb{E}_{\mathcal{P}_1} \ell(\boldsymbol{\theta}; \mathbf{x}, 1) \right] + \tilde{\pi} \left[\mathbb{E}_{\mathcal{P}_{\text{syn}}} \ell(\boldsymbol{\theta}; \mathbf{x}, 1) - \mathbb{E}_{\mathcal{P}_1} \ell(\boldsymbol{\theta}; \mathbf{x}, 1) \right]. \end{aligned} \quad (2)$$

To streamline notation, define

$$\phi(\boldsymbol{\theta}) := \mathbb{E}_{\mathcal{P}_0} \ell(\boldsymbol{\theta}; \mathbf{x}, 0) - \mathbb{E}_{\mathcal{P}_1} \ell(\boldsymbol{\theta}; \mathbf{x}, 1), \quad \psi(\boldsymbol{\theta}) := \mathbb{E}_{\mathcal{P}_{\text{syn}}} \ell(\boldsymbol{\theta}; \mathbf{x}, 1) - \mathbb{E}_{\mathcal{P}_1} \ell(\boldsymbol{\theta}; \mathbf{x}, 1), \quad (3)$$

where $\phi(\boldsymbol{\theta})$ measures the local majority–minority asymmetry under the loss and $\psi(\boldsymbol{\theta})$ quantifies the synthetic-to-minority discrepancy. With these definitions, (2) becomes

$$\tilde{\mathcal{R}}(\boldsymbol{\theta}) = \mathcal{R}(\boldsymbol{\theta}) + \left(\pi_0 - \frac{1}{2}\right) \phi(\boldsymbol{\theta}) + \tilde{\pi} \psi(\boldsymbol{\theta}). \quad (4)$$

Here, $\left(\pi_0 - \frac{1}{2}\right) \phi(\boldsymbol{\theta}) + \tilde{\pi} \psi(\boldsymbol{\theta})$ is the *risk-level* distribution bias induced by class-proportion mismatch and generator mismatch. Since our excess-risk analysis is driven by first-order optimality conditions, we will work with the gradient of this bias term. Accordingly, we define the corresponding *first-order bias vector* $\mathbf{b}(\boldsymbol{\theta}) := \left(\pi_0 - \frac{1}{2}\right) \nabla \phi(\boldsymbol{\theta}) + \tilde{\pi} \nabla \psi(\boldsymbol{\theta})$, which is exactly the $\boldsymbol{\theta}$ -gradient of the bias component in (4).

A lower bound for balanced excess risk. The next result shows that, even asymptotically, the estimator trained on the augmented population can incur a non-vanishing balanced excess risk unless the induced bias is controlled.

Theorem 1 (Excess Risk Lower Bound). *Assume the parameter space is bounded, $\boldsymbol{\theta} \in \{\boldsymbol{\theta} : \|\boldsymbol{\theta}\| < B\}$. Suppose the covariates \mathbf{x} have bounded support and the loss $\ell(\boldsymbol{\theta}; \mathbf{x}, y)$*

is continuous and differentiable in $\boldsymbol{\theta}$, and bounded on bounded $(\boldsymbol{\theta}, \boldsymbol{x})$. Assume $\mathcal{R}(\boldsymbol{\theta})$ is continuous and $\tilde{\mathcal{R}}(\boldsymbol{\theta})$ admits a unique minimizer. Further suppose that $\nabla\tilde{\mathcal{R}}(\boldsymbol{\theta})$ is Lipschitz at its minimizer $\tilde{\boldsymbol{\theta}}$, i.e., $\|\nabla\tilde{\mathcal{R}}(\boldsymbol{\theta}) - \nabla\tilde{\mathcal{R}}(\tilde{\boldsymbol{\theta}})\| \leq M\|\boldsymbol{\theta} - \tilde{\boldsymbol{\theta}}\|$, and $\mathcal{R}(\boldsymbol{\theta})$ satisfies at its minimizer $\boldsymbol{\theta}^*$ that for any $\boldsymbol{\theta}$: $\mathcal{R}(\boldsymbol{\theta}) \geq \mathcal{R}(\boldsymbol{\theta}^*) + \frac{\mu}{2}\|\boldsymbol{\theta} - \boldsymbol{\theta}^*\|^2$. Then the balanced excess risk satisfies

$$\mathcal{R}(\hat{\boldsymbol{\theta}}) - \mathcal{R}(\boldsymbol{\theta}^*) \geq \frac{\mu}{2M^2} \left\| \left(\pi_0 - \frac{1}{2} \right) \nabla\phi(\boldsymbol{\theta}^*) + \tilde{\pi} \nabla\psi(\boldsymbol{\theta}^*) \right\|^2 + o_P(1).$$

Theorem 1 shows that the leading lower bound is governed by the squared norm of the *first-order bias vector* $\mathbf{b}(\boldsymbol{\theta}^*) := \left(\pi_0 - \frac{1}{2} \right) \nabla\phi(\boldsymbol{\theta}^*) + \tilde{\pi} \nabla\psi(\boldsymbol{\theta}^*)$. The term proportional to $\pi_0 - \frac{1}{2}$ reflects the class-proportion mismatch in the augmented population, whereas the term proportional to $\tilde{\pi}$ captures generator mismatch via the discrepancy between \mathcal{P}_{syn} and \mathcal{P}_1 . In particular, a necessary condition for balanced-risk consistency, i.e., $\mathcal{R}(\hat{\boldsymbol{\theta}}) - \mathcal{R}(\boldsymbol{\theta}^*) \rightarrow 0$, is $\|\mathbf{b}(\boldsymbol{\theta}^*)\| \rightarrow 0$.

Excess Risk Asymptotic Representation. We next state the conditions under which the excess risk admits an explicit asymptotic representation. These assumptions are standard regularity conditions in statistical learning theory and allow us to refine the lower bound in Theorem 1 into an exact decomposition in Theorem 2.

Assumption 1 (Condition for Excess Risk Asymptotic Representation).

(A1) The balanced risk \mathcal{R} is differentiable and satisfies at its minimizer $\boldsymbol{\theta}^*$ for a constant

$$\mu > 0 \text{ that } \mathcal{R}(\boldsymbol{\theta}^*) \geq \mathcal{R}(\boldsymbol{\theta}) + \nabla\mathcal{R}(\boldsymbol{\theta})^\top(\boldsymbol{\theta}^* - \boldsymbol{\theta}) + \frac{\mu}{2}\|\boldsymbol{\theta}^* - \boldsymbol{\theta}\|^2. \text{ Also, it satisfies } \mathcal{R}(\boldsymbol{\theta}) - \mathcal{R}(\boldsymbol{\theta}^*) \geq L\|\boldsymbol{\theta} - \boldsymbol{\theta}^*\|^2 \text{ at the minimizer } \boldsymbol{\theta}^* \text{ for some constant } L > 0;$$

(A2) The covariates \boldsymbol{x} have bounded support and a finite third moment;

(A3) $\nabla^2\tilde{\mathcal{R}}(\boldsymbol{\theta}) \succeq \lambda I$ for some $\lambda > 0$, and satisfies $\|\nabla^2\tilde{\mathcal{R}}(\boldsymbol{\theta}) - \nabla^2\tilde{\mathcal{R}}(\tilde{\boldsymbol{\theta}})\| \leq L\|\boldsymbol{\theta} - \tilde{\boldsymbol{\theta}}\|$ at the minimizer $\tilde{\boldsymbol{\theta}}$ for a constant $L > 0$;

(A4) $\Sigma_0(\tilde{\boldsymbol{\theta}}), \Sigma_1(\tilde{\boldsymbol{\theta}}), \tilde{\Sigma}(\tilde{\boldsymbol{\theta}}) \succ \lambda I$ for some $\lambda > 0$, have finite largest eigenvalue. $\Sigma(\boldsymbol{\theta})$ satisfies

$\|\Sigma(\tilde{\boldsymbol{\theta}}) - \Sigma(\boldsymbol{\theta}^*)\| \leq L\|\tilde{\boldsymbol{\theta}} - \boldsymbol{\theta}^*\|$ at two minimizers $\tilde{\boldsymbol{\theta}}$ and $\boldsymbol{\theta}^*$ for a constant $L > 0$;

(A5) A finite gradient of total bias: $\|(\pi_0 - 1/2)\nabla^2\phi(\boldsymbol{\theta}) + \tilde{\pi}\nabla^2\psi(\boldsymbol{\theta})\| \leq C < \infty$.

Theorem 2 (Excess Risk Decomposition). *Define the covariance matrices of the loss gradients:*

$$\begin{aligned}\Sigma_0(\boldsymbol{\theta}) &= \text{Cov}_{\mathcal{P}_0}(\nabla_{\boldsymbol{\theta}}\ell(\boldsymbol{\theta}; \mathbf{x}, 0)), & \Sigma_1(\boldsymbol{\theta}) &= \text{Cov}_{\mathcal{P}_1}(\nabla_{\boldsymbol{\theta}}\ell(\boldsymbol{\theta}; \mathbf{x}, 1)), \\ \tilde{\Sigma}(\boldsymbol{\theta}) &= \text{Cov}_{\mathcal{P}_{\text{syn}}}(\nabla_{\boldsymbol{\theta}}\ell(\boldsymbol{\theta}; \mathbf{x}, 1)), & \Sigma(\boldsymbol{\theta}) &:= \frac{n_0\Sigma_0(\boldsymbol{\theta}) + n_1\Sigma_1(\boldsymbol{\theta}) + \tilde{n}\tilde{\Sigma}(\boldsymbol{\theta})}{n_0 + n_1 + \tilde{n}}.\end{aligned}\tag{5}$$

Suppose Assumption 1 holds. For large enough n_0 and n_1 , there exists a random vector $Z \sim \mathcal{N}(0, I_d)$ such that

$$\begin{aligned}\mathcal{R}(\hat{\boldsymbol{\theta}}) - \mathcal{R}(\boldsymbol{\theta}^*) &= \frac{1}{2}\mathbf{b}(\boldsymbol{\theta}^*)^\top \left[\nabla^2\mathcal{R}(\boldsymbol{\theta}^*) + \nabla\mathbf{b}(\boldsymbol{\theta}^*)\right]^{-1} \nabla^2\mathcal{R}(\boldsymbol{\theta}^*) \left[\nabla^2\mathcal{R}(\boldsymbol{\theta}^*) + \nabla\mathbf{b}(\boldsymbol{\theta}^*)\right]^{-1} \mathbf{b}(\boldsymbol{\theta}^*) \\ &\quad - \frac{1}{\sqrt{n_0 + n_1 + \tilde{n}}}\mathbf{b}(\boldsymbol{\theta}^*)^\top \left[\nabla^2\mathcal{R}(\boldsymbol{\theta}^*) + \nabla\mathbf{b}(\boldsymbol{\theta}^*)\right]^{-1} \nabla^2\mathcal{R}(\boldsymbol{\theta}^*) \left[\nabla^2\mathcal{R}(\boldsymbol{\theta}^*) + \nabla\mathbf{b}(\boldsymbol{\theta}^*)\right]^{-1} \Sigma(\boldsymbol{\theta}^*)^{\frac{1}{2}} Z \\ &\quad + \frac{1}{2(n_0 + n_1 + \tilde{n})} Z^\top \Sigma(\boldsymbol{\theta}^*)^{\frac{1}{2}} \left[\nabla^2\mathcal{R}(\boldsymbol{\theta}^*) + \nabla\mathbf{b}(\boldsymbol{\theta}^*)\right]^{-1} \nabla^2\mathcal{R}(\boldsymbol{\theta}^*) \left[\nabla^2\mathcal{R}(\boldsymbol{\theta}^*) + \nabla\mathbf{b}(\boldsymbol{\theta}^*)\right]^{-1} \Sigma(\boldsymbol{\theta}^*)^{\frac{1}{2}} Z + R.\end{aligned}$$

Here $\mathbf{b}(\boldsymbol{\theta}) = (\pi_0 - \frac{1}{2})\nabla\phi(\boldsymbol{\theta}) + \tilde{\pi}\nabla\psi(\boldsymbol{\theta})$, so $\nabla\mathbf{b}(\boldsymbol{\theta}) = (\pi_0 - \frac{1}{2})\nabla^2\phi(\boldsymbol{\theta}) + \tilde{\pi}\nabla^2\psi(\boldsymbol{\theta})$ denotes the Jacobian. The remainder term R satisfies

$$R = O_P\left(\|\mathbf{b}(\boldsymbol{\theta}^*)\|^3 + (n_0 + n_1 + \tilde{n})^{-3/2} + \frac{1}{n_0 + n_1 + \tilde{n}}\|\mathbf{b}(\boldsymbol{\theta}^*)\| + \frac{1}{\sqrt{n_0 + n_1 + \tilde{n}}}\|\mathbf{b}(\boldsymbol{\theta}^*)\|^2\right).$$

Theorem 2 expresses the excess risk as the sum of three leading terms and a higher-order remainder. The first term is a quadratic form in $\mathbf{b}(\boldsymbol{\theta}^*)$ and captures the deterministic *distribution bias* induced by the effective weights $(\pi_0, \pi_1, \tilde{\pi})$ and any discrepancy between \mathcal{P}_{syn} and \mathcal{P}_1 . The second and third terms quantify stochastic fluctuations through the covariance $\Sigma(\boldsymbol{\theta}^*)$ and the Gaussian limit Z , thereby making the bias–variance trade-off explicit as a function of (n_0, n_1, \tilde{n}) . This representation is useful in two ways. First, since the right-hand side depends on \tilde{n} through $\mathbf{b}(\boldsymbol{\theta}^*)$, $\nabla\mathbf{b}(\boldsymbol{\theta}^*)$, and $\Sigma(\boldsymbol{\theta}^*)$, it can be minimized with respect to \tilde{n} to obtain principled synthetic-size choices. Second, different generators

affect the expansion only through $\psi(\boldsymbol{\theta})$ and $\tilde{\Sigma}(\boldsymbol{\theta})$, providing a common asymptotic scale for comparing generators: holding (n_0, n_1, \tilde{n}) fixed, generators are preferable when they yield smaller bias $\mathbf{b}(\boldsymbol{\theta}^*)$ and/or more favorable covariance contributions.

Remark 1 (User-specific class weights). *Our presentation focuses on the balanced objective ($\rho = \frac{1}{2}$) for clarity, but all results extend directly to user-specified class weights. Fix $\rho \in (0, 1)$ as the weight on the majority class and define $\mathcal{R}^\rho(\boldsymbol{\theta}) = \rho \mathbb{E}_{\mathcal{P}_0} \ell(\boldsymbol{\theta}; \mathbf{x}, 0) + (1 - \rho) \mathbb{E}_{\mathcal{P}_1} \ell(\boldsymbol{\theta}; \mathbf{x}, 1)$. Then the synthetic population risk admits the decomposition $\tilde{\mathcal{R}}(\boldsymbol{\theta}) = \mathcal{R}^\rho(\boldsymbol{\theta}) + (\pi_0 - \rho) \phi(\boldsymbol{\theta}) + \tilde{\pi} \psi(\boldsymbol{\theta})$, so the corresponding first-order bias vector becomes $\mathbf{b}_\rho(\boldsymbol{\theta}) := (\pi_0 - \rho) \nabla \phi(\boldsymbol{\theta}) + \tilde{\pi} \nabla \psi(\boldsymbol{\theta})$. Consequently, Theorems 1 and 2 hold after replacing $\mathbf{b}(\boldsymbol{\theta})$ by $\mathbf{b}_\rho(\boldsymbol{\theta})$ (and replacing $\frac{1}{2}$ by ρ wherever it appears). Moreover, consistency under the ρ -weighted objective requires matching the target proportion $\pi_0 \rightarrow \rho$, i.e., $\tilde{n} = \frac{1-\rho}{\rho} n_0 - n_1 + o(n_0)$, and, as in the $\rho = \frac{1}{2}$ case, lower-order deviations of \tilde{n} around this target can affect rates.*

In the remainder of this paper, we distinguish two regimes described as follows.

- **Local asymmetry:** $\|\nabla \phi(\boldsymbol{\theta}^*)\| \geq c$ for a fixed constant $c > 0$. In this case, synthetic minority augmentation may improve performance. In this regime, both generator quality (through $\|\nabla \psi(\boldsymbol{\theta}^*)\|$) and synthetic size \tilde{n} matter: too few synthetic samples may not sufficiently mitigate imbalance, while too many may amplify generator-induced bias.
- **Local symmetry:** $\|\nabla \phi(\boldsymbol{\theta}^*)\| = 0$. In this case, synthetic minority samples typically do not help and may degrade performance.

4 Local Asymmetry: When Synthetic Minority Samples May Improve Performance

We now focus on the locally asymmetric regime, where $\|\nabla \phi(\boldsymbol{\theta}^*)\| \geq c > 0$. Here the choice of synthetic sample size \tilde{n} interacts with the generator mismatch $\|\nabla \psi(\boldsymbol{\theta}^*)\|$, leading

to a bias–variance trade-off that determines whether augmentation improves or harms performance. Accordingly, we organize the analysis by generator quality, considering the following three regimes in Sections 4.1, 4.2, and 4.3, respectively.

1. **Ideal synthetic minority-class sample generator:** $\|\nabla\psi(\boldsymbol{\theta}^*)\| \ll n_0^{-1/2}$. This regime primarily serves as a theoretical benchmark. If the generator is trained using only the available minority data, then even under favorable conditions that avoid the curse of dimensionality (as is often assumed in nonparametric settings), the estimation error of the learned minority distribution is fundamentally limited by the sample size n_1 , yielding at best a parametric-rate scaling of $n_1^{-1/2}$. More broadly, even when the majority and minority distributions share exploitable structure and the generator can, in principle, leverage information from both classes, the best achievable accuracy is still bounded by parametric scaling with the total sample size, namely $(n_0 + n_1)^{-1/2} \asymp n_0^{-1/2}$ in the imbalanced regime. Consequently, requiring $\|\nabla\psi(\boldsymbol{\theta}^*)\| \ll n_0^{-1/2}$ is generally unattainable for standard, data-trained generators.

2. **Realistic synthetic minority-class sample generator:** $n_0^{-1/2} \ll \|\nabla\psi(\boldsymbol{\theta}^*)\| \ll 1$. This corresponds to the practically relevant case, where the residual synthetic mismatch is non-negligible yet bounded.

3. **Inconsistent synthetic minority-class sample generator:** $\|\nabla\psi(\boldsymbol{\theta}^*)\| \gtrsim 1$.

The thresholds separating the ideal, realistic, and inconsistent regimes are well motivated: for standard data-trained generators, residual mismatch is typically limited by parametric-order scaling with the available sample size, making $\|\nabla\psi(\boldsymbol{\theta}^*)\| \ll n_0^{-1/2}$ unrealistic. At the other extreme, a mismatch bounded away from zero (i.e., $\|\nabla\psi(\boldsymbol{\theta}^*)\| \gtrsim 1$) indicates persistent distributional error and may compromise consistency. Nevertheless, the ideal and inconsistent regimes provide useful benchmarks for isolating algorithmic and statistical behavior.

4.1 With Ideal Synthetic Sample Generators

We first study the regime of *ideal* synthetic generators, where the synthetic distribution \mathcal{P}_{syn} closely matches the true minority distribution \mathcal{P}_1 . Intuitively, when the generator-induced mismatch is negligible, the precise choice of the synthetic sample size \tilde{n} should matter only weakly: as long as \tilde{n} is chosen at the appropriate order of $n_0 - n_1$ (so that the effective class proportions are approximately balanced), the estimator based on synthetic augmentation should perform well.

The next theorem formalizes this intuition. It shows that, under an ideal generator, any synthetic size \tilde{n} that stays sufficiently close to the balancing choice $\tilde{n} = n_0 - n_1$ yields the same $1/n_0$ convergence rate. In this regime, tuning \tilde{n} can at best improve constant factors, but cannot improve the rate.

Theorem 3 (Excess risk under an ideal synthetic generator). *Assume the conditions of Theorem 2. Suppose that the curvature contribution from the synthetic mismatch is controlled in the sense that $\|\nabla^2\psi(\boldsymbol{\theta}^*)\| \leq \lambda_{\min}(\nabla^2\mathcal{R}(\boldsymbol{\theta}^*))$. If the generator is ideal, satisfying $\|\nabla\psi(\boldsymbol{\theta}^*)\| \ll n_0^{-1/2}$, then for any synthetic size $\tilde{n} \in \mathcal{C} := \{\tilde{n} : \tilde{n} = n_0 - n_1 + o(\sqrt{n_0})\}$, we have $\mathcal{R}(\hat{\boldsymbol{\theta}}) - \mathcal{R}(\boldsymbol{\theta}^*) = \Theta_P(n_0^{-1})$.*

The set \mathcal{C} requires the effective class proportions to be balanced around 1/2 up to the natural $n_0^{-1/2}$ scale of stochastic fluctuations. Under an ideal generator, the leading bias term in Theorem 2 is dominated by the stochastic term as long as $\tilde{n} \in \mathcal{C}$, and the excess risk attains the classical balanced parametric rate $\mathcal{R}(\hat{\boldsymbol{\theta}}) - \mathcal{R}(\boldsymbol{\theta}^*) = \Theta_P(n_0^{-1})$. In particular, the naive balancing choice $\tilde{n} = n_0 - n_1$ already achieves the optimal rate. Adjusting \tilde{n} within \mathcal{C} may improve constants, but cannot surpass the n_0^{-1} rate.

4.2 With Realistic Synthetic Sample Generators

We next consider a more realistic regime in which the synthetic generator is statistically consistent, but its residual mismatch decays more slowly than the parametric rate: $n_0^{-1/2} \ll \|\nabla\psi(\boldsymbol{\theta}^*)\| \ll 1$. Our goal is to understand how the interaction between the intrinsic majority–minority imbalance and the generator-induced bias determines the appropriate order of the synthetic sample size \tilde{n} . To build intuition, we consider the following toy example.

Example 1 (Toy collinear case). *Assume the generator is consistent with $\|\nabla\psi(\boldsymbol{\theta}^*)\| \asymp (\log n_1)^{-1/2}$, so $\|\nabla\psi(\boldsymbol{\theta}^*)\| \gg n_0^{-1/2}$. Write the leading terms in Theorem 2 as $\mathcal{R}(\hat{\boldsymbol{\theta}}) - \mathcal{R}(\boldsymbol{\theta}^*) = T_1 + T_2 + T_3 + R$, where $T_1 \asymp \|\mathbf{b}(\boldsymbol{\theta}^*)\|^2$, $T_2 = \Theta_P(n^{-1/2}\|\mathbf{b}(\boldsymbol{\theta}^*)\|)$, and $T_3 = \Theta_P(n^{-1})$, with $n = n_0 + n_1 + \tilde{n}$. Since consistency requires $\tilde{n} \approx n_0 - n_1$, let $\tilde{n} = (n_0 - n_1)(1 + \delta_n)$ with $\delta_n \rightarrow 0$. If $\nabla\psi(\boldsymbol{\theta}^*)$ is collinear with $\nabla\phi(\boldsymbol{\theta}^*)$, i.e., $\nabla\psi(\boldsymbol{\theta}^*) = s(\log n_1)^{-1/2}\nabla\phi(\boldsymbol{\theta}^*)$ for $s \in \{\pm 1\}$, then one can choose $\delta_n = \Theta((\log n_1)^{-1/2})$ so that $\mathbf{b}(\boldsymbol{\theta}^*) = 0$. Consequently, $T_1 = T_2 = 0$ and $\mathcal{R}(\hat{\boldsymbol{\theta}}) - \mathcal{R}(\boldsymbol{\theta}^*) = \Theta_P(n_0^{-1})$. In contrast, the naive balancing choice $\tilde{n} = n_0 - n_1$ leaves $\|\mathbf{b}(\boldsymbol{\theta}^*)\| = \Theta((\log n_1)^{-1/2})$, yielding a slower rate $\mathcal{R}(\hat{\boldsymbol{\theta}}) - \mathcal{R}(\boldsymbol{\theta}^*) = \Theta_P((\log n_1)^{-1})$.*

Example 1 highlights two points. First, while $\tilde{n} \approx n_0 - n_1$ is necessary for consistency, the lower-order refinement of \tilde{n} around $n_0 - n_1$ can change the convergence rate. Second, the relative direction of $\nabla\psi(\boldsymbol{\theta}^*)$ and $\nabla\phi(\boldsymbol{\theta}^*)$ matters: alignment can either amplify or cancel the leading bias term $\mathbf{b}(\boldsymbol{\theta}^*)$. We next formalize these insights in a general setting.

Theorem 4 (Excess risk under a realistic synthetic generator). *Suppose the assumptions of Theorem 2 hold and $\|\nabla^2\psi(\boldsymbol{\theta}^*)\| < \infty$. Assume the generator is realistic in the sense that $\|\nabla\psi(\boldsymbol{\theta}^*)\| \gg n_0^{-1/2}$, and that the alignment condition $\sin \angle(\nabla\phi(\boldsymbol{\theta}^*), \nabla\psi(\boldsymbol{\theta}^*)) \lesssim \frac{1}{\|\nabla\psi(\boldsymbol{\theta}^*)\|\sqrt{n_0}}$ holds. Then, if we choose $\tilde{n} = \frac{n_0 - n_1 + O_P(\sqrt{n_0})}{1 - 2\|\nabla\psi(\boldsymbol{\theta}^*)\|/\|\nabla\phi(\boldsymbol{\theta}^*)\| \cos \angle(\nabla\phi(\boldsymbol{\theta}^*), \nabla\psi(\boldsymbol{\theta}^*)) + O_P(1/\sqrt{n_0})}$, we have $\mathcal{R}(\hat{\boldsymbol{\theta}}) - \mathcal{R}(\boldsymbol{\theta}^*) = \Theta_P(n_0^{-1})$. If we choose the naive balancing rule $\tilde{n} = n_0 - n_1$, then $\mathcal{R}(\hat{\boldsymbol{\theta}}) - \mathcal{R}(\boldsymbol{\theta}^*) = \Theta_P(\|\nabla\psi(\boldsymbol{\theta}^*)\|^2) \gg \Theta_P(n_0^{-1})$.*

Theorem 4 formalizes a “bias-cancellation” phenomenon. When the generator mismatch $\nabla\psi(\boldsymbol{\theta}^*)$ is sufficiently aligned with the intrinsic shift $\nabla\phi(\boldsymbol{\theta}^*)$, a small refinement of \tilde{n} around $n_0 - n_1$ cancels the leading distribution bias and restores the parametric rate $\Theta_P(n_0^{-1})$. In contrast, the naive balancing rule $\tilde{n} = n_0 - n_1$ leaves a residual bias of order $\|\nabla\psi(\boldsymbol{\theta}^*)\|$, resulting in a slower excess-risk rate.

Practically, the result suggests treating \tilde{n} as a tuning parameter rather than a fixed balancing heuristic: useful directional information between $\nabla\phi(\boldsymbol{\theta}^*)$ and $\nabla\psi(\boldsymbol{\theta}^*)$ can guide a choice of \tilde{n} that reduces generator-induced bias and improve the performance.

4.3 With Inconsistent Synthetic Sample Generators

In this subsection, we aim to study the inconsistent regime as a robustness and failure-mode analysis. In practice, generators may be misspecified, capacity-limited, or trained with insufficient data, leading to a non-vanishing distributional mismatch even asymptotically. In this case, we consider the setting in which the mismatch does not vanish, e.g., $\liminf_{n_0, n_1 \rightarrow \infty} \|\nabla\psi(\boldsymbol{\theta}^*)\| \gtrsim 1$, where $\psi(\cdot)$ is defined in equation (3). This implies that the total synthetic bias term $\mathbf{b}(\boldsymbol{\theta}^*)$ defined in Theorem 2 generally need not converge to zero, so the estimator may retain a non-vanishing bias unless additional directional structure between $\nabla\phi(\boldsymbol{\theta}^*)$ and $\nabla\psi(\boldsymbol{\theta}^*)$ is available and the synthetic size \tilde{n} is tuned accordingly.

The next theorem shows that (a) if $\mathbf{b}(\boldsymbol{\theta}^*)$ remains bounded away from zero, then the excess risk cannot converge to zero; (b) when $\nabla\phi(\boldsymbol{\theta}^*)$ and $\nabla\psi(\boldsymbol{\theta}^*)$ are approximately aligned, an appropriate choice of \tilde{n} can partially offset the persistent mismatch and restore consistency of the excess risk.

Theorem 5 (Excess risk under an inconsistent synthetic generator). *Suppose synthetic bias satisfies $\liminf_{n_0, n_1 \rightarrow \infty} \|\nabla\psi(\boldsymbol{\theta}^*)\| \geq c$ for constant $c > 0$, and $\|\nabla\psi(\boldsymbol{\theta}^*)\|/\|\nabla\phi(\boldsymbol{\theta}^*)\| < 1/2$.*

- *When synthetic direction is well aligned such that $\sin \angle(\nabla\phi(\boldsymbol{\theta}^*), \nabla\psi(\boldsymbol{\theta}^*)) = o_P(1)$, by*

selecting synthetic size $\tilde{n} = \frac{n_0 - n_1 + (n_0 + n_1)o(1)}{1 - 2\|\nabla\psi(\boldsymbol{\theta}^*)\|/\|\nabla\phi(\boldsymbol{\theta}^*)\|\cos\angle(\nabla\phi(\boldsymbol{\theta}^*),\nabla\psi(\boldsymbol{\theta}^*)) + o(1)}$, the excess risk satisfies $\mathcal{R}(\hat{\boldsymbol{\theta}}) - \mathcal{R}(\boldsymbol{\theta}^*) = o_P(1)$.

- If either (i) the generator mismatch is not asymptotically aligned with the intrinsic shift, in the sense that there exists $c_0 > 0$ such that $\sin\angle(\nabla\phi(\boldsymbol{\theta}^*),\nabla\psi(\boldsymbol{\theta}^*)) > c_0 > 0$ in probability and $\tilde{n}/n_0 \rightarrow \rho$ for some $\rho \geq 0$, or (ii) the directions are aligned but we nevertheless choose the naive balancing rule $\tilde{n} = n_0 - n_1$, then there exists $c_1 > 0$ such that $\mathcal{R}(\hat{\boldsymbol{\theta}}) - \mathcal{R}(\boldsymbol{\theta}^*) \geq c_1 + o_P(1)$.

Next, we provide two examples that illustrate the phenomena characterized by Theorem 5.

All derivations are given in Section 13.2 of the Supplementary Materials.

Example 2 (Two-dimensional Gaussian model). Let $d = 2$. Suppose $\mathbf{x} \mid y = 0 \sim \mathcal{P}_0 = \mathcal{N}(\mathbf{0}, I_2)$, $\mathbf{x} \mid y = 1 \sim \mathcal{P}_1 = \mathcal{N}(\boldsymbol{\mu}_1, I_2)$, and synthetic minority samples are generated from $\tilde{\mathbf{x}} \sim \mathcal{P}_{\text{syn}} = \mathcal{N}(\boldsymbol{\mu}_s, I_2)$. We consider the squared loss $\ell(\boldsymbol{\theta}; \mathbf{x}, y) = (\boldsymbol{\theta}^\top \mathbf{x} - y)^2$.

(i) Aligned bias directions. Take $\boldsymbol{\mu}_1 = (\mu, 0)^\top$ and $\boldsymbol{\mu}_s = (a, 0)^\top$ with $a \notin \{\mu, 2/\mu\}$ to avoid degeneracy. In this case, $\nabla\phi(\boldsymbol{\theta}^*)$ and $\nabla\psi(\boldsymbol{\theta}^*)$ are collinear. Consequently, there exists a choice of synthetic sample size, $\tilde{n} = \frac{\mu(n_0 - n_1)}{a(\mu^2 + 2) - \mu(a^2 + 1)}$, for which the leading bias cancels and the balanced excess risk satisfies $\mathcal{R}(\hat{\boldsymbol{\theta}}) - \mathcal{R}(\boldsymbol{\theta}^*) = O_P((n_0 + n_1 + \tilde{n})^{-1})$. However, the naive ‘‘balancing’’ choice $\tilde{n} = n_0 - n_1$ need not be sufficient for consistency. For example, when $\mu = 1$ and $a = \frac{1}{2}$, the bias-cancelling choice equals $\tilde{n} = 4(n_0 - n_1)$, whereas using $\tilde{n} = n_0 - n_1$ yields $\mathcal{R}(\hat{\boldsymbol{\theta}}) - \mathcal{R}(\boldsymbol{\theta}^*) \rightarrow c > 0$ in probability.

(ii) Orthogonal bias directions. Take $\boldsymbol{\mu}_1 = (\mu, 0)^\top$ and $\boldsymbol{\mu}_s = (\mu, \mu)^\top$ with $\mu^2 \leq 2$. Then $\nabla\phi(\boldsymbol{\theta}^*)$ and $\nabla\psi(\boldsymbol{\theta}^*)$ are orthogonal. If the synthetic fraction does not vanish (i.e., $\liminf \tilde{\pi} \geq \tau > 0$), the balanced excess risk remains bounded away from zero: $\mathcal{R}(\hat{\boldsymbol{\theta}}) - \mathcal{R}(\boldsymbol{\theta}^*) \rightarrow c > 0$ in probability. Thus, when the synthetic mismatch introduces a bias component orthogonal to $\nabla\phi(\boldsymbol{\theta}^*)$, tuning \tilde{n} cannot eliminate the leading bias

and consistency fails whenever synthetic augmentation has non-negligible weight.

5 Local Symmetry: When Synthetic Minority Samples May Degrade Performance

Synthetic minority augmentation is often motivated as a remedy for class imbalance. However, there is an important regime in which augmentation cannot help, and may even hurt, despite severe imbalance. The key phenomenon is a form of *local symmetry* at the balanced-risk minimizer, under which the two classes already contribute equally along the optimization-relevant directions. In such cases, imbalance is not the bottleneck, and any additional synthetic samples can only introduce distributional bias if the generator is imperfect.

Recall we say the problem exhibits *local symmetry* at $\boldsymbol{\theta}^*$ if

$$\nabla\phi(\boldsymbol{\theta}^*) = \nabla_{\boldsymbol{\theta}} \left\{ \mathbb{E}_{\mathcal{P}_0} \ell(\boldsymbol{\theta}; \mathbf{x}, 0) - \mathbb{E}_{\mathcal{P}_1} \ell(\boldsymbol{\theta}; \mathbf{x}, 1) \right\} \Big|_{\boldsymbol{\theta}=\boldsymbol{\theta}^*} = 0. \quad (6)$$

Condition (6) means that, at the balanced-risk optimum, the (population) gradient contributions from the majority and minority classes coincide; hence reweighting the classes provides little first-order benefit near $\boldsymbol{\theta}^*$. In this regime, the leading bias term that governs the excess risk reduces to the generator-mismatch component. Specifically, writing the (vector) bias as $\mathbf{b}(\boldsymbol{\theta}^*) := \left(\pi_0 - \frac{1}{2}\right) \nabla\phi(\boldsymbol{\theta}^*) + \tilde{\pi} \nabla\psi(\boldsymbol{\theta}^*)$, local symmetry implies $\mathbf{b}(\boldsymbol{\theta}^*) = \tilde{\pi} \nabla\psi(\boldsymbol{\theta}^*)$. Thus, setting $\tilde{\pi} = 0$ eliminates the synthetic component entirely, whereas adding many synthetic samples can amplify the mismatch bias through $\tilde{\pi}$. The next theorem quantifies this trade-off under a *realistic* generator that is imperfect but improving with sample size.

Theorem 6 (Realistic synthetic augmentation can degrade performance). *Under the assumptions of Theorem 2, suppose the local symmetry condition (6) holds, and the synthetic generator is realistic in the sense that $n_0^{-1/2} \ll \|\nabla\psi(\boldsymbol{\theta}^*)\| \ll 1$. Then for diminishing*

synthetic size $\tilde{n} = O(\sqrt{n_0}/\|\nabla\psi(\boldsymbol{\theta}^*)\|) \ll n_0$, we have $\mathcal{R}(\hat{\boldsymbol{\theta}}) - \mathcal{R}(\boldsymbol{\theta}^*) = O_P(n_0^{-1})$. For non-diminishing synthetic size $\tilde{n} \gtrsim n_0$, we have $\mathcal{R}(\hat{\boldsymbol{\theta}}) - \mathcal{R}(\boldsymbol{\theta}^*) = \Omega_P(\|\nabla\psi(\boldsymbol{\theta}^*)\|^2) \gg \Theta_P(n_0^{-1})$.

Theorem 6 shows that, under local symmetry, synthetic augmentation cannot improve the balanced excess risk when the generator mismatch is non-negligible. If the synthetic size is diminishing, the estimator already achieves the baseline $O_P(n_0^{-1})$ rate, indicating that little or no augmentation is sufficient. In contrast, if the synthetic size is non-diminishing (of order n_0 or larger), the mismatch bias accumulates and the excess risk scales at least as $\|\nabla\psi(\boldsymbol{\theta}^*)\|^2$, which dominates the baseline n_0^{-1} rate. Intuitively, because the two classes already exert equal first-order influence near $\boldsymbol{\theta}^*$, adding synthetic minority samples provides no imbalance-related benefit and can only degrade performance by injecting distributional bias.

We next present two examples that satisfy the local symmetry condition (6). Details are provided in Sections 13.3 and 13.4 of the Supplementary Materials, and Section 7 further corroborates the theory via simulation.

Example 3 (Mean-shift model). Consider a mean-shift model with $\mathbb{P}(y = 1) = \pi$ and $\mathbb{P}(y = 0) = 1 - \pi$, and class-conditionals $\mathbf{x} \mid (y = 1) \sim \boldsymbol{\mu} + \boldsymbol{\xi}$, $\mathbf{x} \mid (y = 0) \sim -\boldsymbol{\mu} + \boldsymbol{\xi}$, where $\boldsymbol{\mu} \in \mathbb{R}^d$ is fixed and $\boldsymbol{\xi} \in \mathbb{R}^d$ has mean zero, bounded support, and full-rank covariance. Under the linear score $f_{\boldsymbol{\theta}}(\mathbf{x}) = \boldsymbol{\theta}^\top \mathbf{x}$ and squared loss $\ell(\boldsymbol{\theta}; \mathbf{x}, y) = (y - \frac{1}{2} - \boldsymbol{\theta}^\top \mathbf{x})^2$, the local symmetry condition (6) holds, i.e., $\nabla\phi(\boldsymbol{\theta}^*) = \mathbf{0}$.

Example 4 (Sigmoid Bernoulli logistic regression). Consider the sigmoid Bernoulli model (without intercept) with $\mathbf{x} \sim p(\mathbf{x})$ and $\mathbb{P}(y = 1 \mid \mathbf{x}) = \sigma(\mathbf{x}^\top \boldsymbol{\theta}_{\text{true}})$, $\mathbb{P}(y = 0 \mid \mathbf{x}) = 1 - \sigma(\mathbf{x}^\top \boldsymbol{\theta}_{\text{true}})$, and logistic loss $\ell(\boldsymbol{\theta}; \mathbf{x}, y) = \log(1 + \exp\{\boldsymbol{\theta}^\top \mathbf{x}\}) - y\boldsymbol{\theta}^\top \mathbf{x}$. If $\mathbb{E}_{p(\mathbf{x})} \left[\mathbf{x} \sigma(\boldsymbol{\theta}_{\text{true}}^\top \mathbf{x}) (1 - \sigma(\boldsymbol{\theta}_{\text{true}}^\top \mathbf{x})) \right] = \mathbf{0}$, then the local symmetry condition (6) holds, i.e., $\nabla\phi(\boldsymbol{\theta}^*) = \mathbf{0}$.

6 Practical Method: Validation-Tuned Synthetic Size (VTSS)

Our theory indicates that the common balancing rule $\tilde{n} = n_0 - n_1$ is not always optimal. In particular, Theorem 2 expresses the leading behavior of the excess risk as a function of the synthetic size \tilde{n} , implying that different choices of \tilde{n} (even when all are of the same order as $n_0 - n_1$) can yield materially different performance. While Theorem 2 also suggests an “optimal” \tilde{n} by minimizing the leading-term approximation, the resulting objective depends on population-level quantities, such as derivatives of the risk at $\boldsymbol{\theta}^*$, local symmetry $\nabla\phi(\boldsymbol{\theta}^*)$, and the generator-induced discrepancy $\nabla\psi(\boldsymbol{\theta}^*)$, that are not directly observable from finite samples. Hence, direct optimization is infeasible in practice.

Nevertheless, the theorem provides a clear operational message: *the choice of \tilde{n} is important*, and naive balancing may be suboptimal. Motivated by the fact that, in locally asymmetric regimes, consistency typically requires \tilde{n} to be close to $n_0 - n_1$ (equivalently, $\tilde{n}/(n_0 - n_1) \rightarrow 1$), we restrict attention to a neighborhood of the balancing choice. Specifically, we consider candidates $\tilde{n}(\gamma) = \text{round}(\gamma(n_0 - n_1))$, $\gamma \in \Gamma$, where $\Gamma \subset \mathbb{R}_+$ is centered at 1. For each γ , we augment the training set to achieve a target minority count $n_1^{\text{tar}} = n_1 + \tilde{n}(\gamma)$, train the downstream classifier, and select the γ that minimizes the average *balanced* validation loss in a K -fold cross-validation. We refer to this procedure as *Validation-Tuned Synthetic Size (VTSS)* and summarize it in Algorithm 1.

Remark 2. *Algorithm 1 uses K -fold cross-validation to select the synthetic multiplier γ by minimizing the average validation risk. In settings where the validation criterion is noisy (e.g., limited sample size, high outcome variability, or substantial measurement noise), the selection can be further stabilized by repeating the entire K -fold procedure m times with independent fold partitions and choosing γ that minimizes the aggregated mean over all mK fold evaluations, which reduces variance in the estimated criterion. Moreover,*

Algorithm 1 Validation-Tuned Synthetic Size (VTSS)

Require: Imbalanced dataset $\mathcal{D} = \{(\mathbf{x}_i, y_i)\}_{i=1}^{n_0+n_1}$ with class counts (n_0, n_1) ; number of folds K ; candidate multipliers $\Gamma \subset \mathbb{R}_+$ (centered at 1); classifier training routine $\text{Fit}(\cdot)$; balanced log-loss $\hat{L}_{\text{bal}}(\boldsymbol{\theta}; \mathcal{D}_{\text{val}}) = \frac{1}{2n_{0,\text{val}}} \sum_{i=1}^{n_{0,\text{val}}} \ell(\boldsymbol{\theta}; \mathbf{x}_i^{0,\text{val}}, 0) + \frac{1}{2n_{1,\text{val}}} \sum_{i=1}^{n_{1,\text{val}}} \ell(\boldsymbol{\theta}; \mathbf{x}_i^{1,\text{val}}, 1)$ synthetic generator $\text{Syn}(\cdot; n_1^{\text{tar}})$.

Ensure: Selected synthetic size \tilde{n}^{VTSS} (equivalently γ^{VTSS}) and $\hat{\boldsymbol{\theta}}^{\text{VTSS}}$.

- 1: Partition \mathcal{D} into K folds $\{\mathcal{D}^{(k)}\}_{k=1}^K$. Initialize best CV loss $L^{\text{VTSS}} \leftarrow +\infty$.
 - 2: **for** each $\gamma \in \Gamma$ **do**
 - 3: Compute candidate synthetic size $\tilde{n} \leftarrow \text{round}(\gamma(n_0 - n_1))$.
 - 4: Set target minority count $n_1^{\text{tar}} \leftarrow n_1 + \tilde{n}$. Initialize CV loss accumulator $S_\gamma \leftarrow 0$.
 - 5: **for** $k = 1, \dots, K$ **do**
 - 6: Set validation fold $\mathcal{D}_{\text{val}}^{(k)} \leftarrow \mathcal{D}^{(k)}$ and training folds $\mathcal{D}_{\text{tr}}^{(k)} \leftarrow \mathcal{D} \setminus \mathcal{D}^{(k)}$.
 - 7: Augment training data: $\tilde{\mathcal{D}}_{\text{tr}}^{(k)}(\gamma) \leftarrow \text{Syn}(\mathcal{D}_{\text{tr}}^{(k)}; n_1^{\text{tar}})$.
 - 8: Train classifier $\hat{\boldsymbol{\theta}}_\gamma^{(k)} \leftarrow \text{Fit}(\tilde{\mathcal{D}}_{\text{tr}}^{(k)}(\gamma))$.
 - 9: Compute balanced validation log-loss $L_\gamma^{(k)} \leftarrow \hat{L}_{\text{bal}}(\hat{\boldsymbol{\theta}}_\gamma^{(k)}; \mathcal{D}_{\text{val}}^{(k)})$.
 - 10: Update $S_\gamma \leftarrow S_\gamma + L_\gamma^{(k)}$.
 - 11: **end for**
 - 12: Compute average CV loss $\bar{L}_\gamma \leftarrow \frac{1}{K} S_\gamma$.
 - 13: **if** $\bar{L}_\gamma < L^{\text{VTSS}}$ **then**
 - 14: Update $L^{\text{VTSS}} \leftarrow \bar{L}_\gamma, \gamma^{\text{VTSS}} \leftarrow \gamma$.
 - 15: **end if**
 - 16: **end for**
 - 17: Set $\tilde{n}^{\text{VTSS}} \leftarrow \text{round}(\gamma^{\text{VTSS}}(n_0 - n_1))$ and $n_1^{\text{tar}} \leftarrow n_1 + \tilde{n}^{\text{VTSS}}$.
 - 18: Train final model on the full augmented data: $\tilde{\mathcal{D}}(\gamma^{\text{VTSS}}) \leftarrow \text{Syn}(\mathcal{D}; n_1^{\text{tar}})$ and $\hat{\boldsymbol{\theta}}^{\text{VTSS}} \leftarrow \text{Fit}(\tilde{\mathcal{D}}(\gamma^{\text{VTSS}}))$.
 - 19: Output \tilde{n}^{VTSS} and $\hat{\boldsymbol{\theta}}^{\text{VTSS}}$.
-

while we present VTSS using the balanced log-loss, the same framework applies to any problem-relevant validation objective. One may replace \hat{L}_{bal} with an alternative metric (e.g., maximize balanced accuracy, minimize a cost-sensitive loss etc.) depending on the downstream goal. Thus, VTSS should be viewed as a general tuning framework that selects γ by optimizing a user-specified, task-dependent validation criterion.

7 Simulation Studies

In this section, we use controlled simulations to validate the theory developed above and to evaluate the practical benefits of Validation-Tuned Synthetic Size (VTSS) (Section 6). Due to space constraints, we defer the detailed simulation study settings to Section 15 of the Supplement.

7.1 Under Local Asymmetry

In the local asymmetry case, we study the classification with directional alignment. To illustrate the directional-alignment phenomenon for biased synthetic generator discussed in Section 4.3, we consider a 2D Gaussian setting as in Example 2, with a linear predictor. We compare two fixed synthetic-size rules: the naive balancing choice $\tilde{n} = n_0 - n_1$ and the bias-canceling choice $\tilde{n} = 4(n_0 - n_1)$ (from the analysis of Example 2). We evaluate parameter error $\|\hat{\boldsymbol{\theta}} - \boldsymbol{\theta}^*\|_2$ and balanced excess risk.

The simulation in Figure 2 confirms the theoretical analysis in Example 2. When $\tilde{n} = 4(n_0 - n_1)$, both the balanced excess risk and the parameter error $\|\hat{\boldsymbol{\theta}} - \boldsymbol{\theta}^*\|_2$ decay to zero as the sample size grows, whereas under naive balancing they converge to a strictly positive level. This demonstrates that naive balance can be inconsistent in the presence of biased synthetic data.

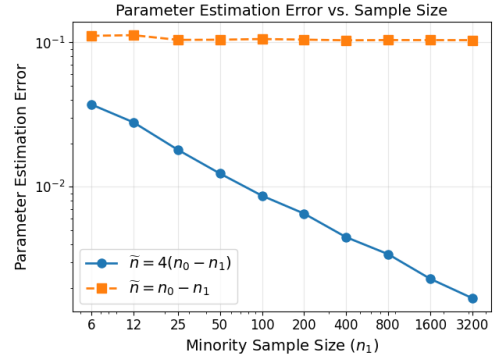
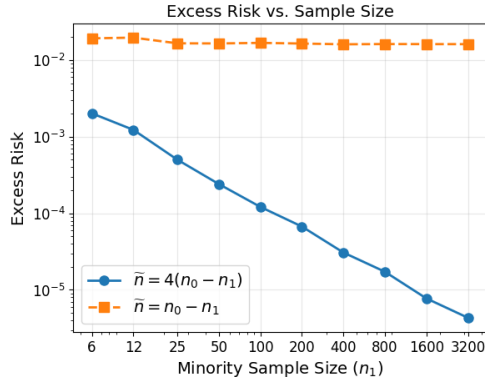


Figure 2: Balanced excess risk and parameter estimation error in a 2D Gaussian model with aligned synthetic bias based on 100 simulations.

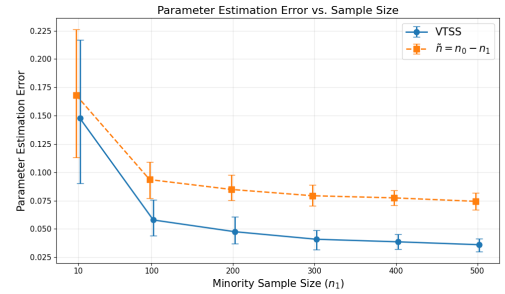
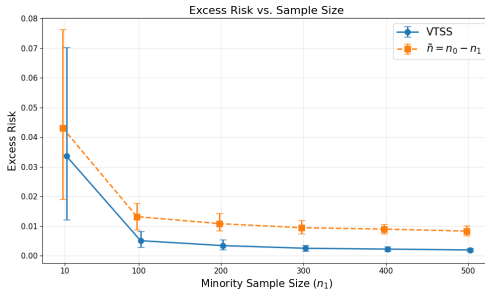


Figure 3: Excess risk and parameter error versus minority sample size under a 2D Gaussian mean-shift model (squared loss) based 100 simulations.

For directional alignment with a realistic and consistent synthetic generator (Section 4.2), we simulate the same 2D Gaussian setup with squared loss. Synthetic minority samples are produced by a realistic, consistent, and directionally aligned generator: for a requested synthetic size k , draw $\mathbf{x}_{\text{syn}} \sim \mathcal{N}(\boldsymbol{\mu}_{\text{syn}}, I_2)$ with $\boldsymbol{\mu}_{\text{syn}} = (1 - (\log n_1)^{-1/2}) \boldsymbol{\mu}_1$, so that the synthetic mean approaches $\boldsymbol{\mu}_1$ as n_1 increases while remaining aligned with $\boldsymbol{\mu}_1$. We compare VTSS with the naive balancing rule $\tilde{n} = n_0 - n_1$, and evaluate population balanced excess risk and parameter error.

The results are shown in Figure 3. Across all values of n_1 , VTSS achieves substantially smaller errors and a faster decay rate, supporting our theory that, under a realistic but consistent generator, directional information can be exploited to select \tilde{n} that outperforms

naive balancing.

7.2 Under Local Symmetry

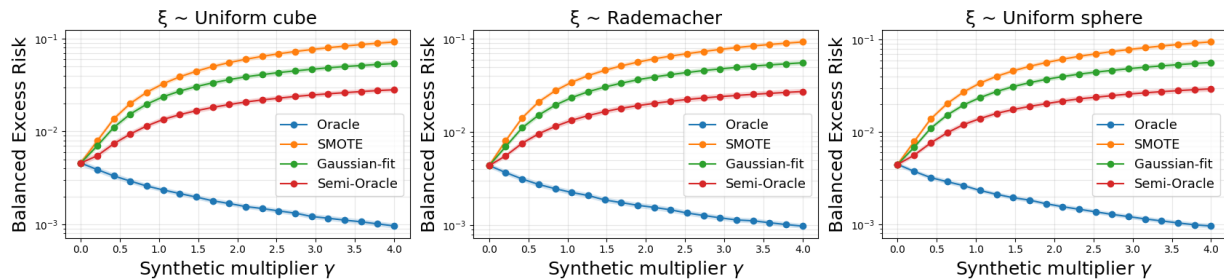


Figure 4: Balanced excess risk $\mathcal{R}(\hat{\theta}) - \mathcal{R}(\theta^*)$ (log scale) versus the synthetic multiplier γ .

To further illustrate local symmetry (Section 5), we conduct a simulation study based on the mean-shift model in Example 3 with a linear predictor. We consider three choices of ξ : Uniform cube, Rademacher, and Uniform sphere. We start from an imbalanced training sample with $n_1 = 100$ and $n_0 = 2000$, and augment the minority class with $\tilde{n} = \text{round}(\gamma(n_0 - n_1))$ synthetic samples, where γ ranges over 20 values in $[0, 4]$. We compare four synthetic generators: (i) **Oracle**; (ii) **SMOTE**; (iii) **Gaussian-fit**; and (iv) **Semi-Oracle**, which samples ξ from the true noise distribution but centers at the empirical minority mean $\hat{\mu}_1$ (i.e., $\hat{\mu}_1 + \xi$).

The results in Figure 4 align with the theoretical analysis. In the mean-shift setting, the majority–minority difference cancels at the balanced optimum ($\nabla\phi(\theta^*) = 0$), so adding synthetic data from a realistic generator cannot reduce this part of the error. Instead, any mismatch between the synthetic and true minority distributions introduces bias and can only worsen balanced excess risk. Empirically, realistic generators, including the Semi-Oracle generator that is already close to the truth, fail to improve performance and typically degrade it as more synthetic samples are added. In contrast, only the Oracle generator improves monotonically with increasing γ , reflecting that it avoids generator-induced mis-

match and helps by adding correctly distributed minority samples. For the VTSS, we plot the empirical distribution of the selected γ^* in Figure 9 of the Supplementary Materials. VTSS selects a very small γ^* in the vast majority of runs and frequently chooses $\gamma^* = 0$ exactly, further demonstrating the effectiveness of the proposed VTSS framework.

We also have analogous local symmetry results showing that synthetic data provides no benefit for the sigmoid Bernoulli logistic model as in Example 4 these results are presented in Section 15.2.2 of the supplementary materials.

7.3 Further Evaluation of VTSS

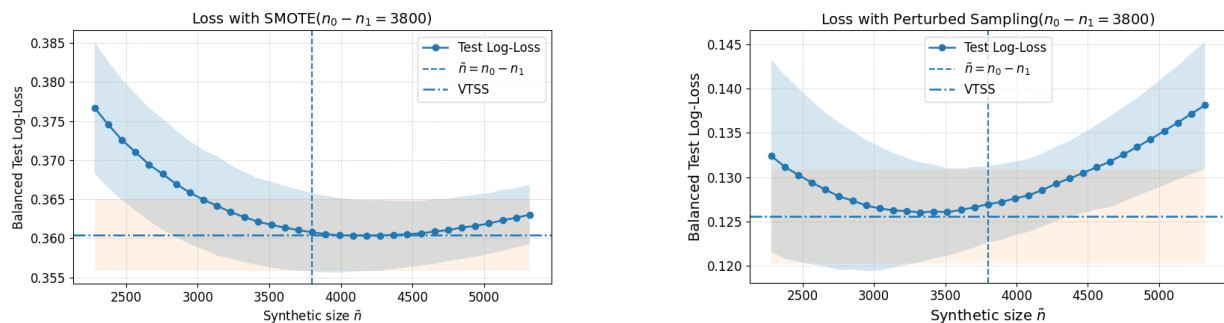


Figure 5: Balanced test log-loss as a function of the synthetic size \tilde{n} . **Left:** logistic regression with SMOTE as the synthetic generator. **Right:** kernel logistic regression with perturbed sampling as the synthetic generator.

In this subsection, we further illustrate the advantage of VTSS by plotting the test loss as a function of the synthetic size \tilde{n} and comparing it with the loss achieved by VTSS. We consider two configurations. (i) Linear classification (SMOTE + logistic regression) and (ii) Nonlinear classification (perturbed sampling + kernel logistic).

In both configurations of Figure 5, the empirical curves confirm the theoretical insight that, although the naive balancing choice $\tilde{n} = n_0 - n_1$ often lies near the optimum, it is generally not the loss-minimizing synthetic size. Moreover, VTSS, which selects \tilde{n} by minimizing

balanced validation loss on each dataset, can always capture the lowest average loss. This highlights the benefit of data-dependent tuning around a theory-guided target.

8 Real Data Applications

In this section, we present real data applications to further illustrate our theoretical findings and evaluate the proposed VTSS method.

Data source, cohort construction, features. We study prediction of sepsis-related outcomes using the MIMIC-III critical care database. Clinically, sepsis is a life-threatening condition arising from a dysregulated response to infection that can rapidly progress to organ dysfunction, making timely identification essential for improving outcomes (Singer et al., 2016). We conduct experiments on MIMIC-III (Medical Information Mart for Intensive Care), a large, de-identified, single-center ICU dataset covering admissions at Beth Israel Deaconess Medical Center from 2001–2012, with rich clinical information including demographics, bedside vital signs, laboratory results, medications, clinical notes, and mortality outcomes (Johnson et al., 2016).

Using MIMIC-III, we construct an adult admission cohort (age > 15 years at admission). We consider three binary prediction tasks, with in-hospital mortality, sepsis, and septic shock as responses. These represent clinically consequential outcomes capturing (i) overall patient prognosis, (ii) infection-related critical illness, and (iii) progression to the most severe end of the sepsis spectrum. Sepsis status is identified using ICD-9 diagnosis codes, labeling admissions with severe sepsis or septic shock as sepsis cases.

To capture early physiologic trajectories, we extract 10 clinical variables measured during the first 120 hours after admission and use binned averages to stabilize irregularly sampled measurements:

	Positive Samples (n_1)	Negative Samples (n_0)	Imbalance Ratio (n_0/n_1)
Mortality	5,789	45,068	7.785
Sepsis	4,084	46,773	11.45
Septic Shock	2,585	48,272	18.67

Table 1: Class imbalance for the mortality, sepsis, and septic shock prediction tasks.

- Bedside vital signs from CHARTEVENTS, averaged into 6-hour bins (20 bins): heart rate, respiratory rate, temperature, and systolic blood pressure.
- Laboratory measurements from LABEVENTS, averaged into 24-hour bins (5 bins): white blood cell count, platelets, creatinine, INR, lactate, and total bilirubin.

For each admission, we convert the multivariate time series into a mean feature vector over the observation window. Missing features are imputed using the corresponding cohort-level feature means. After preprocessing, all three datasets are substantially imbalanced; the class counts and imbalance ratios are summarized in Table 1.

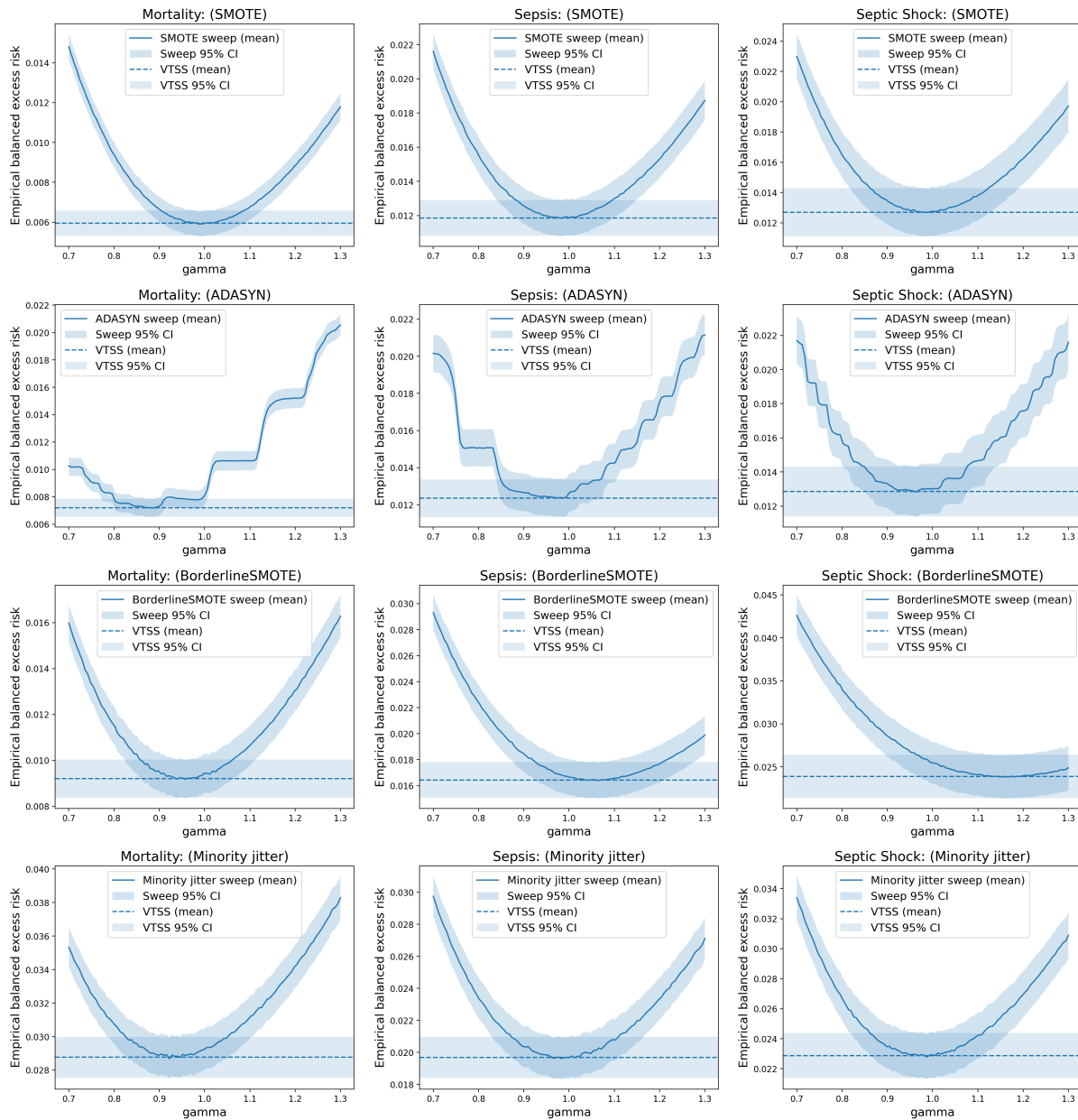
We train (i) logistic regression and (ii) support vector machine (SVM) classifiers on these features to predict each outcome.

Evaluation metric: balanced excess risk. Performance is primarily assessed using the balanced excess risk. Because the population minimizer $\theta^* = \arg \min_{\theta} \mathcal{R}(\theta)$ depends on unknown population expectations, we approximate the subtractive term using an oracle plug-in estimate on each test split. Specifically, we compute $\theta_{\text{test}}^* = \arg \min_{\theta} \hat{\mathcal{R}}_{\text{test}}(\theta)$ (the parameter that minimizes the balanced loss on the test set) and report the balanced excess risk as $\hat{\mathcal{R}}_{\text{test}}(\hat{\theta}) - \hat{\mathcal{R}}_{\text{test}}(\theta_{\text{test}}^*)$. To account for sampling variability, we repeat the train-test split 100 times with different random seeds and report the average balanced excess risk across repetitions.

Synthetic data generation and tuning protocol. We compare four synthetic data generators: SMOTE, ADASYN, Borderline-SMOTE, and Minority Jitter (randomly sampling a minority instance and adding feature-wise Gaussian perturbations). Let γ denote the synthetic size multiplier. For each task–classifier–generator combination, we tune γ via 5-fold cross-validation and repeat the cross-validation procedure 10 times. We sweep γ over a range centered around 1 and report the mean balanced excess risk with a 95% confidence interval at each γ . For reference, we also plot a horizontal dashed line (with 95% confidence interval) corresponding to the average balanced excess risk achieved by VTSS.

Results for logistic regression. Figure 6 highlights that the optimal synthetic sample size is highly sensitive to both the clinical endpoint and the chosen generator. Training on the raw imbalanced data without any synthetic augmentation (corresponding to the $\gamma = 0$ case) can yield substantially worse performance, as suggested the bottom row of Figure 6, underscoring the need to address class imbalance in these tasks. Across mortality, sepsis, and septic shock, the balanced excess risk curves as a function of the synthetic multiplier γ exhibit minima at markedly different locations: depending on the task and generator, the best-performing γ can be less than 1 (conservative oversampling), close to 1, or greater than 1 (aggressive oversampling). This variability indicates that naively fixing $\gamma = 1$ may incur a nontrivial excess-risk penalty in some settings. In contrast, VTSS provides a stable and reliable choice for selecting synthetic size. Its performance matches (within uncertainty) the best achievable risk across the candidate γ values considered, effectively recovering the balanced excess risk at optimal synthetic size. Therefore, VTSS can be used as a robust default when choosing the synthetic multiplier across different prediction tasks and generators.

Results for SVM. We next repeat the same experimental pipeline under the identical framework, replacing logistic regression with an SVM classifier. The results are summarized



Raw-Mortality

0.3825 [0.3809, 0.3842]

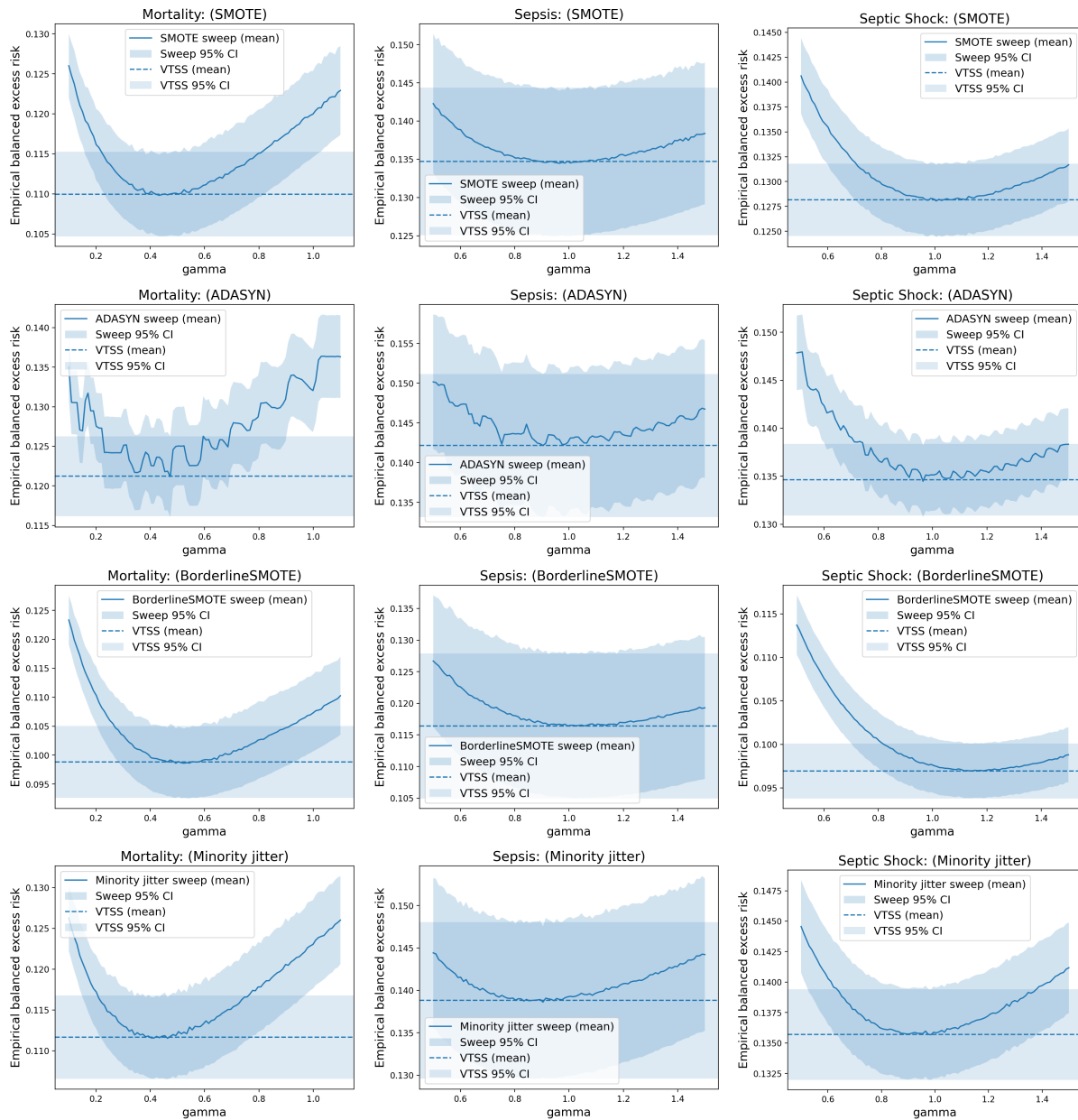
Raw-Sepsis

0.5721 [0.5700, 0.5742]

Raw-Septic shock

0.7786 [0.7761, 0.7810]

Figure 6: Excess risk in predicting hospital mortality, sepsis and septic shock across four synthetic generators using logistic regression. Bottom row is the excess risk obtained by training with raw imbalanced data without synthetic data augmentation.



Raw-Mortality

0.1463 [0.1428, 0.1497]

Raw-Sepsis

0.2138 [0.2091, 0.2185]

Raw-Septic shock

0.2478 [0.2427, 0.2529]

Figure 7: Excess risk in predicting hospital mortality, sepsis and septic shock across four synthetic generators using SVM. Bottom row is the excess risk obtained by training with raw imbalanced data without synthetic data augmentation.

in Figure 7. The qualitative conclusions remain consistent: performance is sensitive to γ , the optimal γ depends on both the endpoint and generator, and training on the raw imbalanced data is frequently suboptimal according to the bottom row of Figure 7. Notably, for in-hospital mortality the risk-minimizing multipliers are often concentrated around $\gamma \in [0.4, 0.6]$, suggesting that under SVM this task favors substantially less oversampling than the naive balancing choice $\gamma = 1$. VTSS captures this behavior and consistently recovers near-minimal balanced excess risk, supporting its use as a robust default across classifiers, tasks, and generators.

Alternative validation objective: balanced accuracy. To further assess the flexibility of VTSS, we also consider an alternative validation objective motivated by Remark 2. Instead of selecting γ by minimizing validation balanced log-loss, we instantiate VTSS with a decision-oriented criterion and choose γ to maximize validation balanced accuracy, keeping all other components of the pipeline unchanged. Figure 8 reports balanced accuracy as a function of γ for each generator, along with the VTSS-selected operating point and associated uncertainty.

Figure 8 shows that VTSS consistently selects γ values achieving near-optimal balanced accuracy across generators, while the naive balancing choice can be noticeably suboptimal. We also observe that VTSS does not always coincide exactly with the global maximizer of the balanced accuracy curve. A plausible explanation is that balanced accuracy is a thresholded, non-smooth metric that can exhibit flat or step-like validation profiles across nearby γ values, making the exact maximizer difficult to localize under finite-sample variability. Nevertheless, VTSS remains consistently close to the best achievable balanced accuracy while improving upon naive balancing, supporting its use as a robust default for synthetic-size selection under alternative evaluation metrics.

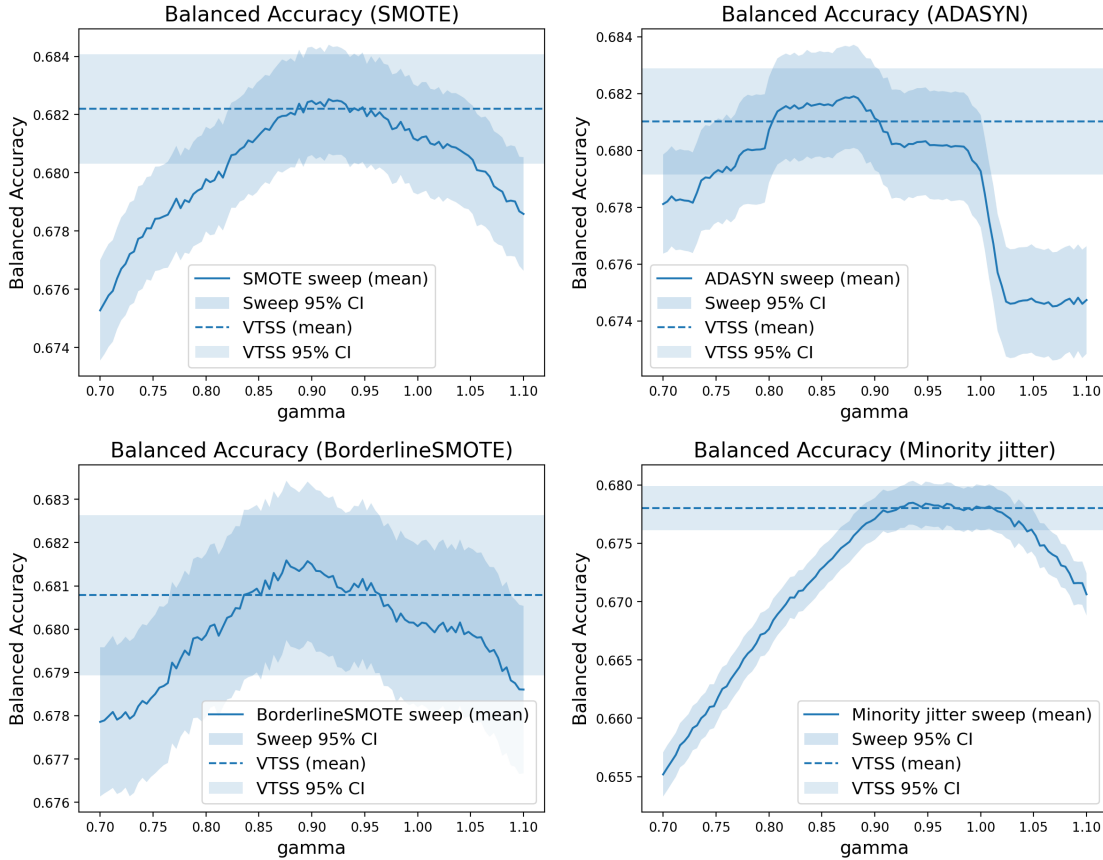


Figure 8: Balanced accuracy in predicting hospital mortality across four synthetic generators.

9 Discussion

This paper develops a unified risk-based theory for synthetic minority augmentation in imbalanced classification under a balanced evaluation objective. We derive an excess-risk decomposition that separates imbalance-induced objective distortion from generator-induced mismatch, and show how the synthetic size \tilde{n} governs the resulting bias–variance trade-off. The theory identifies two regimes: under local asymmetry, augmentation can help, but the optimal \tilde{n} depends on generator quality and may deviate from naive full balancing (especially under directional alignment); under local symmetry, imbalance is not the first-order bottleneck, so realistic augmentation typically cannot help and may hurt by amplifying mismatch. These insights motivate Validation-Tuned Synthetic Size (VTSS), which se-

lects \tilde{n} using balanced validation loss to capture gains when tuning matters while avoiding over-synthesis when augmentation is unhelpful.

Our analysis focuses on a classical low-dimensional asymptotic regime with fixed covariate dimension d . Extending the framework to high-dimensional settings, where both downstream learning and generator mismatch can change qualitatively, and where mismatch may worsen due to curse-of-dimensionality effects, is an important direction. In such regimes, understanding how mismatch scales with d , how the bias–variance trade-off shifts, and how to adapt VTSS when validation is noisy or limited remain open problems.

Our results also clarify settings where oversampling is less likely to help even in low dimensions. For likelihood-based generative discriminant models such as LDA, class imbalance primarily enters through an explicit prior term, so balanced or cost-sensitive operating points can often be achieved by adjusting priors at prediction time rather than altering the training sample composition. Moreover, because these methods are sensitive to moment misspecification, synthetic samples can be counterproductive if they introduce even mild mean or covariance distortions.

A key message is that the direction of generator mismatch matters. This connects naturally to guided generative modeling (e.g., guided diffusion or instruction-tuned LLMs): if guidance can steer the dominant mismatch component toward the imbalance-relevant direction, augmentation becomes more effective and modest deviations from naive balancing can yield measurable gains. This suggests future work on augmentation-aware generator training that optimizes not only sample realism but also mismatch in the directions most relevant to the downstream balanced risk.

In many technical and empirical analyses that combine true minority data with synthetic minority samples, it is common (often implicitly) to treat the two as independent. However, this independence generally fails when the synthetic generator is trained on the same target

minority dataset. The induced synthetic distribution can depend on the true minority samples. A simple way to restore the independence condition needed by many arguments is the data-splitting scheme. One randomly partitions the available minority data into two disjoint parts, trains the synthetic generator only on the first part, and reserves the second part as the true minority samples used for downstream estimation. When minority data are extremely scarce, this idea can be extended via K -fold cross-fitting, rotating which fold is held out so that every real observation is used for both generator training and downstream analysis, but never in the same fold. The data-splitting scheme is commonly used in the analysis of synthetic data. For example, [Tian and Shen \(2025\)](#) explicitly randomly partitions the training sample into two subsamples, with one for training the generator and one reserved for augmentation. [Xia et al. \(2024\)](#) Uses a Train–Holdout–Evaluation split, where the synthetic data generator is trained only on the training set while the holdout set remains untouched during the synthetic data generation process. These practices provide a straightforward and widely adopted way to justify the independence assumption when synthetic data are learned from observed minority samples.

Finally, synthetic data is widely used beyond imbalance, including in fairness and privacy settings ([Ktena et al., 2024](#)). Our analysis suggests a common principle across these applications: benefits depend jointly on how the synthetic distribution differs from the target and how much synthetic data is introduced. Extending our risk decomposition to group-weighted objectives and integrating mismatch control with privacy notions are promising directions, but the practical takeaway remains: treat the synthetic size as a tunable decision rather than a fixed balancing heuristic.

Data Availability Statement

The MIMIC-III database is publicly available, but access is restricted due to patient privacy concerns. Access can be obtained by completing the required CITI training and a data use agreement through PhysioNet. See details at <https://physionet.org/content/mimiciii/1.4/>.

Acknowledgments

The authors thank Pengfei Lyu for helpful discussions. The research was supported in part by NIH Grants R01HL169347 and R01HL168940.

References

- Ahmad, T., Kalan, M. M., Portier, F. and Stupfler, G. (2025), ‘Concentration and excess risk bounds for imbalanced classification with synthetic oversampling’, *arXiv preprint arXiv:2510.20472* .
- Bobkov, S. and Götze, F. (2024), ‘Berry-esseen bounds in local limit theorems’, *arXiv preprint arXiv:2407.20744* .
- Boser, B. E., Guyon, I. M. and Vapnik, V. N. (1992), A training algorithm for optimal margin classifiers, *in* ‘Proceedings of the fifth annual workshop on Computational learning theory’, pp. 144–152.
- Bougaham, A., El Adoui, M., Linden, I. and Frénay, B. (2024), ‘Composite score for anomaly detection in imbalanced real-world industrial dataset’, *Machine Learning* **113**(7), 4381–4406.
- Breiman, L. (2001), ‘Random forests’, *Machine learning* **45**(1), 5–32.

- Bunghumpornpat, C., Sinapiromsaran, K. and Lursinsap, C. (2009), Safe-level-SMOTE: Safe-level-synthetic minority over-sampling technique for handling the class imbalanced problem, *in* ‘Pacific-Asia Conference on Knowledge Discovery and Data Mining’, Springer, pp. 475–482.
- Bunghumpornpat, C., Sinapiromsaran, K. and Lursinsap, C. (2012), ‘Dbstmote: density-based synthetic minority over-sampling technique’, *Applied Intelligence* **36**(3), 664–684.
- Burda, Y., Grosse, R. and Salakhutdinov, R. (2015), ‘Importance weighted autoencoders’, *arXiv preprint arXiv:1509.00519* .
- Chawla, N. V., Bowyer, K. W., Hall, L. O. and Kegelmeyer, W. P. (2002), ‘SMOTE: Synthetic minority over-sampling technique’, *Journal of Artificial Intelligence Research* **16**, 321–357.
- Chen, W., Yang, K., Yu, Z., Shi, Y. and Chen, C. P. (2024), ‘A survey on imbalanced learning: latest research, applications and future directions’, *Artificial Intelligence Review* **57**(6), 137.
- Chen, X., Duan, Y., Houthoofd, R., Schulman, J., Sutskever, I. and Abbeel, P. (2016), ‘Infogan: Interpretable representation learning by information maximizing generative adversarial nets’, *Advances in neural information processing systems* **29**.
- Chen, Y., Calabrese, R. and Martin-Barragan, B. (2024), ‘Interpretable machine learning for imbalanced credit scoring datasets’, *European Journal of Operational Research* **312**(1), 357–372.
- Cortes, C. and Vapnik, V. (1995), ‘Support-vector networks’, *Machine learning* **20**(3), 273–297.

- Efron, B. and Tibshirani, R. J. (1994), *An introduction to the bootstrap*, Chapman and Hall/CRC.
- Eigenschink, P., Reutterer, T., Vamosi, S., Vamosi, R., Sun, C. and Kalcher, K. (2023), ‘Deep generative models for synthetic data: A survey’, *IEEE Access* **11**, 47304–47320.
- Feng, Y., Zhou, M. and Tong, X. (2021), ‘Imbalanced classification: a paradigm-based review’, *Statistical Analysis and Data Mining: The ASA Data Science Journal* **14**(5), 383–406.
- Freund, Y. and Schapire, R. E. (1997), ‘A decision-theoretic generalization of on-line learning and an application to boosting’, *Journal of computer and system sciences* **55**(1), 119–139.
- Goodfellow, I. J., Pouget-Abadie, J., Mirza, M., Xu, B., Warde-Farley, D., Ozair, S., Courville, A. and Bengio, Y. (2014), ‘Generative adversarial nets’, *Advances in neural information processing systems* **27**.
- Han, H., Wang, W. Y. and Mao, B. H. (2005), Borderline-SMOTE: A new over-sampling method in imbalanced data sets learning, *in* ‘International Conference on Intelligent Computing’, Springer, pp. 878–887.
- He, H., Bai, Y., Garcia, E. A. and Li, S. (2008), ADASYN: Adaptive synthetic sampling approach for imbalanced learning, *in* ‘2008 IEEE International Joint Conference on Neural Networks (IEEE World Congress on Computational Intelligence)’, IEEE, pp. 1322–1328.
- He, H. and Garcia, E. A. (2009), ‘Learning from imbalanced data’, *IEEE Transactions on knowledge and data engineering* **21**(9), 1263–1284.
- Higgins, I., Matthey, L., Pal, A., Burgess, C., Glorot, X., Botvinick, M., Mohamed, S.

- and Lerchner, A. (2017), beta-vae: Learning basic visual concepts with a constrained variational framework, *in* ‘International conference on learning representations’.
- Ho, J., Jain, A. and Abbeel, P. (2020), ‘Denoising diffusion probabilistic models’, *Advances in neural information processing systems* **33**, 6840–6851.
- Johnson, A. E., Pollard, T. J., Shen, L., Lehman, L.-w. H., Feng, M., Ghassemi, M., Moody, B., Szolovits, P., Anthony Celi, L. and Mark, R. G. (2016), ‘Mimic-iii, a freely accessible critical care database’, *Scientific data* **3**(1), 1–9.
- Keret, N. and Shojaie, A. (2025), ‘Glm inference with ai-generated synthetic data using misspecified linear regression’, *arXiv preprint arXiv:2503.21968* .
- Kingma, D. P. and Welling, M. (2013), ‘Auto-encoding variational Bayes’, *arXiv preprint arXiv:1312.6114* .
- Kleiner, A., Talwalkar, A., Sarkar, P. and Jordan, M. I. (2014), ‘A scalable bootstrap for massive data’, *Journal of the Royal Statistical Society Series B: Statistical Methodology* **76**(4), 795–816.
- Ktena, I., Wiles, O., Albuquerque, I., Rebuffi, S.-A., Tanno, R., Roy, A. G., Azizi, S., Belgrave, D., Kohli, P., Cemgil, T. et al. (2024), ‘Generative models improve fairness of medical classifiers under distribution shifts’, *Nature Medicine* **30**(4), 1166–1173.
- Last, F., Douzas, G. and Bacao, F. (2017), ‘Oversampling for imbalanced learning based on k-means and smote’, *arXiv preprint arXiv:1711.00837* .
- Lipman, Y., Chen, R. T., Ben-Hamu, H., Nickel, M. and Le, M. (2022), ‘Flow matching for generative modeling’, *arXiv preprint arXiv:2210.02747* .
- Lyu, P., Ma, Z., Zhang, L. and Zhang, A. R. (2025), ‘Bias-corrected data synthesis for imbalanced learning’, *arXiv preprint arXiv:2510.26046* .

- Matharaarachchi, S., Domaratzki, M. and Muthukumarana, S. (2024), ‘Enhancing smote for imbalanced data with abnormal minority instances’, *Machine Learning with Applications* **18**, 100597.
- Mirza, M. and Osindero, S. (2014), ‘Conditional generative adversarial nets’, *arXiv preprint arXiv:1411.1784* .
- Nakada, R., Xu, Y., Li, L. and Zhang, L. (2024), ‘Synthetic oversampling: Theory and a practical approach using llms to address data imbalance’, *arXiv preprint arXiv:2406.03628* .
- Newey, W. K. and McFadden, D. (1994), ‘Large sample estimation and hypothesis testing’, *Handbook of econometrics* **4**, 2111–2245.
- Papamakarios, G., Nalisnick, E., Rezende, D. J., Mohamed, S. and Lakshminarayanan, B. (2021), ‘Normalizing flows for probabilistic modeling and inference’, *Journal of Machine Learning Research* **22**(57), 1–64.
- Radford, A., Metz, L. and Chintala, S. (2015), ‘Unsupervised representation learning with deep convolutional generative adversarial networks’, *arXiv preprint arXiv:1511.06434* .
- Räisä, O., Jälkö, J. and Honkela, A. (2025), ‘On consistent bayesian inference from synthetic data’, *Journal of Machine Learning Research* **26**(74), 1–65.
- Rigollet, P. and Tong, X. (2011), ‘Neyman-pearson classification, convexity and stochastic constraints’, *Journal of machine learning research* .
- Rodriguez-Almeida, A. J., Fabelo, H., Ortega, S., Deniz, A., Balea-Fernandez, F. J., Quevedo, E., Soguero-Ruiz, C., Wägner, A. M. and Callico, G. M. (2022), ‘Synthetic patient data generation and evaluation in disease prediction using small and imbalanced datasets’, *IEEE journal of biomedical and health informatics* **27**(6), 2670–2680.

- Rombach, R., Blattmann, A., Lorenz, D., Esser, P. and Ommer, B. (2022), High-resolution image synthesis with latent diffusion models, *in* ‘Proceedings of the IEEE/CVF conference on computer vision and pattern recognition’, pp. 10684–10695.
- Rosenblatt, F. (1958), ‘The perceptron: a probabilistic model for information storage and organization in the brain.’, *Psychological review* **65**(6), 386.
- Roy, R., Tiwari, D. and Pandey, A. (2024), Frauddiffuse: Diffusion-aided synthetic fraud augmentation for improved fraud detection, *in* ‘Proceedings of the 5th ACM International Conference on AI in Finance’, pp. 90–98.
- Rubin, D. B. (1981), ‘The bayesian bootstrap’, *The annals of statistics* pp. 130–134.
- Salmi, M., Atif, D., Oliva, D., Abraham, A. and Ventura, S. (2024), ‘Handling imbalanced medical datasets: review of a decade of research’, *Artificial intelligence review* **57**(10), 273.
- Schapire, R. E. (1990), ‘The strength of weak learnability’, *Machine learning* **5**(2), 197–227.
- Singer, M., Deutschman, C. S., Seymour, C. W., Shankar-Hari, M., Annane, D., Bauer, M., Bellomo, R., Bernard, G. R., Chiche, J.-D., Coopersmith, C. M. et al. (2016), ‘The third international consensus definitions for sepsis and septic shock (sepsis-3)’, *Jama* **315**(8), 801–810.
- Sohl-Dickstein, J., Weiss, E., Maheswaranathan, N. and Ganguli, S. (2015), Deep unsupervised learning using nonequilibrium thermodynamics, *in* ‘International conference on machine learning’, pmlr, pp. 2256–2265.
- Sohn, K., Lee, H. and Yan, X. (2015), ‘Learning structured output representation using deep conditional generative models’, *Advances in neural information processing systems* **28**.

- Song, J., Meng, C. and Ermon, S. (2020), ‘Denoising diffusion implicit models’, *arXiv preprint arXiv:2010.02502* .
- Song, Y., Sohl-Dickstein, J., Kingma, D. P., Kumar, A., Ermon, S. and Poole, B. (2020), ‘Score-based generative modeling through stochastic differential equations’, *arXiv preprint arXiv:2011.13456* .
- Stanton, I., Munir, K., Ikram, A. and El-Bakry, M. (2024), ‘Data augmentation for predictive maintenance: Synthesising aircraft landing gear datasets’, *Engineering Reports* **6**(12), e12946.
- Tian, X. and Shen, X. (2025), ‘Conditional data synthesis augmentation’, *arXiv preprint arXiv:2504.07426* .
- Tong, X., Xia, L., Wang, J. and Feng, Y. (2020), ‘Neyman-pearson classification: parameters and sample size requirement’, *Journal of Machine Learning Research* **21**(12), 1–48.
- Vaswani, A., Shazeer, N., Parmar, N., Uszkoreit, J., Jones, L., Gomez, A. N., Kaiser, Ł. and Polosukhin, I. (2017), ‘Attention is all you need’, *Advances in neural information processing systems* **30**.
- Wang, J., Wang, K., Yu, Y., Lu, Y., Xiao, W., Sun, Z., Liu, F., Zou, Z., Gao, Y., Yang, L. et al. (2025), ‘Self-improving generative foundation model for synthetic medical image generation and clinical applications’, *Nature Medicine* **31**(2), 609–617.
- Xia, E. and Klusowski, J. M. (2026), ‘Classification imbalance as transfer learning’, *arXiv preprint arXiv:2601.10630* .
- Xia, Y., Wang, C.-H., Mabry, J. and Cheng, G. (2024), ‘Advancing retail data science: Comprehensive evaluation of synthetic data’, *arXiv preprint arXiv:2406.13130* .

Zhang, H., Cisse, M., Dauphin, Y. N. and Lopez-Paz, D. (2017), ‘Mixup: Beyond empirical risk minimization’, *arXiv preprint arXiv:1710.09412* .

Supplementary Materials for “Synthetic Augmentation in Imbalanced Learning: When It Helps, When It Hurts, and How Much to Add” Zhengchi Ma

Department of Electrical & Computer Engineering, Duke University

and

Anru R. Zhang

Department of Biostatistics and Department of Computer Science,

Duke University

Abstract

In the supplementary materials, we discuss related classifiers and synthetic data generators and provide proofs of all technical results.

10 Examples for Choice of Loss

In this section, we summarize common choices of loss functions for classification.

Cross-entropy/logistic loss. If the model outputs a probability $p_{\theta}(\mathbf{x}) \in (0, 1)$, the cross-entropy loss is $\ell(\theta; \mathbf{x}, y) = -y \log p_{\theta}(\mathbf{x}) - (1 - y) \log(1 - p_{\theta}(\mathbf{x}))$. A common parameterization is $p_{\theta}(\mathbf{x}) = \sigma(f_{\theta}(\mathbf{x}))$ with sigmoid $\sigma(t) = 1/(1 + e^{-t})$. This is equivalent to maximum likelihood for a Bernoulli model and typically yields well-calibrated probabilities when the model is correctly specified. Under oversampling, however, the effective class prior in training changes (because $\tilde{\pi}$ increases the frequency of label 1), so probability calibration may require adjustment if one wants probabilities under the original prior.

Square loss. With the square loss $\ell(\boldsymbol{\theta}; \mathbf{x}, y) = (y - p_{\boldsymbol{\theta}}(\mathbf{x}))^2$, binary classification is treated as regression to the label $y \in \{0, 1\}$ using the model output $p_{\boldsymbol{\theta}}(\mathbf{x})$ as a real-valued prediction. This objective is simple to optimize and often convenient analytically. However, it is less robust to outliers in probability space.

Hinge loss. For output score $f_{\boldsymbol{\theta}}(\mathbf{x})$, the hinge loss can be written as $\ell(\boldsymbol{\theta}; \mathbf{x}, y) = \max(0, 1 - (2y - 1)f_{\boldsymbol{\theta}}(\mathbf{x}))$. It encourages a large margin between classes and underlies SVMs. Margin-based losses tend to be less sensitive to probability calibration but are sensitive to the geometry of the feature distribution. Synthetic samples that distort the minority geometry can therefore affect the margin and support vectors. When labels are written in $\{-1, +1\}$, we can map $y \in \{0, 1\}$ to $y' \in \{-1, +1\}$ via $y' = 2y - 1$, the hinge loss becomes $\ell(\boldsymbol{\theta}; \mathbf{x}, y') = \max(0, 1 - y'f_{\boldsymbol{\theta}}(\mathbf{x}))$.

Exponential loss (boosting). The exponential loss is $\ell_{\text{exp}}(\boldsymbol{\theta}; \mathbf{x}, y) = \exp(-(2y - 1)f_{\boldsymbol{\theta}}(\mathbf{x}))$, where $f_{\boldsymbol{\theta}}(\mathbf{x})$ is a real-valued score. This loss heavily penalizes misclassified points with large negative margins and is associated with AdaBoost-like algorithms. Because it emphasizes hard-to-classify points, it can interact strongly with synthetic samples: “too-easy” synthetic points may have little effect, while poorly generated synthetic points can dominate the gradient. Similarly when labels are written in $y' \in \{-1, +1\}$, the exponential loss becomes $\ell(\boldsymbol{\theta}; \mathbf{x}, y') = \exp(-y'f_{\boldsymbol{\theta}}(\mathbf{x}))$.

11 Related Classifiers

In this section, we review several common classifiers and relate them to the empirical risk minimization (ERM) framework used in this paper. Many discriminative methods, such as logistic regression, support vector machines, and boosting, can be written as minimizing an empirical average loss (with regularization), and therefore fall directly within our setting.

In contrast, some classical procedures are not naturally expressed as minimizing a fixed discriminative risk over a decision function. For example, linear discriminant analysis (LDA) is derived from a generative Gaussian model and applies the plug-in Bayes rule after estimating distributional parameters; although this corresponds to likelihood optimization over generative parameters, it is not a standard discriminative ERM formulation.

11.1 Discriminative classifiers in the ERM framework

Logistic regression. Logistic regression is a probabilistic linear classifier for binary outcomes that models the log-odds of the positive class as a linear function of features. Logistic regression also sits naturally inside the generalized linear model (GLM) framework via the logit link for binomial data.

Given data $\{(\mathbf{x}_i, y_i)\}_{i=1}^n$ with $y_i \in \{0, 1\}$, logistic regression models

$$\mathbb{P}_{\boldsymbol{\theta}}(y = 1 \mid \mathbf{x}) = \sigma(\boldsymbol{\theta}^\top \mathbf{x}), \quad \sigma(u) = \frac{1}{1 + e^{-u}}.$$

The negative log-likelihood corresponds to the logistic (cross-entropy) loss

$$\ell(\boldsymbol{\theta}; \mathbf{x}_i, y_i) = -y_i \log \sigma(\boldsymbol{\theta}^\top \mathbf{x}_i) - (1 - y_i) \log (1 - \sigma(\boldsymbol{\theta}^\top \mathbf{x}_i)),$$

and the estimator is an empirical risk minimizer

$$\hat{\boldsymbol{\theta}} \in \arg \min_{\boldsymbol{\theta} \in \Theta} \frac{1}{n} \sum_{i=1}^n \ell(\boldsymbol{\theta}; \mathbf{x}_i, y_i).$$

Common extensions of logistic regression still fit the same empirical risk minimization framework. Main extensions include Softmax Logistic Regression for $K > 2$ classes, Penalized Logistic Regression for high-dimensional settings and Kernel Logistic Regression for learning nonlinear decision boundaries.

Support vector machine (SVM). Support Vector Machines originated from the maximum-margin idea: learn a separating hyperplane that maximizes the margin between

classes. Early foundational formulations include [Boser et al. \(1992\)](#) and [Cortes and Vapnik \(1995\)](#).

In the binary case with labels $y_i \in \{0, 1\}$, the (soft-margin) SVM can be written as regularized empirical risk minimization with the hinge loss:

$$(\hat{\mathbf{w}}, \hat{b}) \in \arg \min_{\mathbf{w}, b} \frac{\lambda}{2} \|\mathbf{w}\|_2^2 + \frac{1}{n} \sum_{i=1}^n \max\left\{0, 1 - (2y_i - 1)(\mathbf{w}^\top \phi(\mathbf{x}_i) + b)\right\}.$$

where $\phi(\cdot)$ is a feature map and $\lambda > 0$ controls regularization. This is equivalent (up to reparameterization) to the classic constrained soft-margin form:

$$\min_{\mathbf{w}, b, \xi \geq 0} \frac{1}{2} \|\mathbf{w}\|_2^2 + C \sum_{i=1}^n \xi_i \quad \text{s.t.} \quad \begin{cases} \mathbf{w}^\top \phi(\mathbf{x}_i) + b \geq 1 - \xi_i & \text{if } y_i = 1, \\ \mathbf{w}^\top \phi(\mathbf{x}_i) + b \leq -1 + \xi_i & \text{if } y_i = 0. \end{cases}$$

Boosting. Boosting is an ensemble methodology that builds a strong predictor by combining many “weak” base learners. The original theoretical foundation is [Schapire \(1990\)](#), which formalized why boosting can work in principle. A widely used practical instantiation is AdaBoost, derived by [Freund and Schapire \(1997\)](#) in their decision-theoretic online learning framework and then applied to boosting.

A common view is that boosting learns an additive model

$$F_M(\mathbf{x}) = \sum_{m=1}^M \alpha_m h_m(\mathbf{x}), \quad h_m \in \mathcal{H},$$

by (approximately) minimizing an empirical risk

$$\hat{R}(F) = \frac{1}{n} \sum_{i=1}^n L(y_i, F(\mathbf{x}_i)),$$

using a greedy or stagewise procedure (choosing the next h_m and step size α_m to reduce \hat{R}).

In particular, AdaBoost can be interpreted as stagewise minimization of the exponential loss

$$L(y, F) = \exp\{-yF\}, \quad y \in \{-1, +1\},$$

which induces the familiar reweighting scheme: at iteration m , examples receive weights $\mathbf{w}_i^{(m)} \propto \exp\{-y_i F_{m-1}(\mathbf{x}_i)\}$, so misclassified or low-margin points are emphasized when fitting the next weak learner.

Random forest. Random Forests are an ensemble of decision trees built with two main sources of randomness, bootstrap resampling of the training set (bagging) and random feature selection at each split. The results are then aggregated through majority vote for classification (Breiman, 2001). The method explicitly builds on bagging and is closely related to the random subspace idea for constructing tree ensembles.

While a random forest is an ensemble rather than a single parametric ERM, it fits the empirical-risk minimization view at two levels. First, each decision tree is built by greedy minimization of a node-wise empirical loss. For a node containing samples S , a split rule s partitions S into children $S_L(s)$ and $S_R(s)$, and a CART-style tree selects

$$s^* \in \arg \min_{s \in \mathcal{S}} \frac{|S_L(s)|}{|S|} I(S_L(s)) + \frac{|S_R(s)|}{|S|} I(S_R(s)),$$

where $I(\cdot)$ is an impurity, e.g., Gini or entropy for classification. Random forests introduce additional randomness by fitting each tree on a bootstrap resample of the training data and by restricting \mathcal{S} at each node to splits over a random subset of features. Second, the forest aggregates B trees to form the predictor

$$\hat{f}(\mathbf{x}) = \frac{1}{B} \sum_{b=1}^B f_b(\mathbf{x}) \quad (\text{regression}), \quad \hat{y}(\mathbf{x}) = \text{majority_vote}\{f_b(\mathbf{x})\}_{b=1}^B \quad (\text{classification}),$$

which reduces prediction loss primarily through variance reduction from averaging de-correlated trees.

Neural networks. Neural networks for classification trace back to the perceptron, a linear threshold model for binary classification introduced by Rosenblatt (1958). Modern

multi-layer perceptrons (MLPs) extend this to multiple nonlinear hidden layers. Their practical success was enabled by efficient gradient-based training via backpropagation.

Given data $\{(\mathbf{x}_i, y_i)\}_{i=1}^n$, a neural network classifier is a parametric function $f_{\boldsymbol{\theta}}$ (e.g., an MLP) producing logits $s_{\boldsymbol{\theta}}(\mathbf{x}) \in \mathbb{R}^K$. A standard probabilistic classifier uses the softmax model

$$p_{\boldsymbol{\theta}}(y = k \mid \mathbf{x}) = \frac{\exp(s_{\boldsymbol{\theta},k}(\mathbf{x}))}{\sum_{j=1}^K \exp(s_{\boldsymbol{\theta},j}(\mathbf{x}))}.$$

Training fits the empirical-risk framework by minimizing a regularized empirical loss:

$$\hat{\boldsymbol{\theta}} \in \arg \min_{\boldsymbol{\theta}} \frac{1}{n} \sum_{i=1}^n \ell(y_i, s_{\boldsymbol{\theta}}(\mathbf{x}_i)) + \lambda \Omega(\boldsymbol{\theta}),$$

where ℓ is typically the cross-entropy (negative log-likelihood under the softmax model) and Ω is a regularizer (e.g., $\|\boldsymbol{\theta}\|_2^2$). In practice, $\hat{\boldsymbol{\theta}}$ is often found by stochastic gradient methods using backpropagation.

11.2 Generative classification

Linear Discriminant analysis. LDA is a classical generative classifier that models each class as a multivariate Gaussian distribution sharing a common covariance matrix. Assume K classes $y \in \{1, \dots, K\}$ and $\mathbf{x} \in \mathbb{R}^d$. LDA assumes

$$\mathbf{x} \mid (y = k) \sim \mathcal{N}(\mu_k, \Sigma), \quad \mathbb{P}(y = k) = \pi_k,$$

with shared Σ across classes. The parameters are typically estimated by maximum likelihood (equivalently, minimizing the negative log-likelihood over the generative parameters), after which the classifier is obtained via the plug-in Bayes rule:

$$\hat{y}(\mathbf{x}) = \arg \max_{k \in \{1, \dots, K\}} \delta_k(\mathbf{x}),$$

with the usual linear discriminant scores $\delta_k(\mathbf{x})$. Thus, LDA aligns with an ERM view over *generative* parameters, but it is not naturally expressed as minimizing a fixed *discriminative* loss $\frac{1}{n} \sum_{i=1}^n \ell(y_i, f(\mathbf{x}_i))$ over a decision function f of the form emphasized in our framework.

12 Related Synthetic Sample Generators

In this section, we briefly review the related synthetic data generators. These generators span both classical resampling-based approaches and modern model-based generative methods.

12.1 Classical Resampling and Interpolation Methods

12.1.1 Bootstrap and Reweighting

The bootstrap is a general-purpose resampling method introduced by [Efron and Tibshirani \(1994\)](#) for approximating sampling distributions and constructing uncertainty estimates. In its basic form, given a dataset of size n , one (i) draws a bootstrap resample by sampling n observations with replacement, (ii) fits the model or computes the statistic on the resample, and (iii) repeats this procedure B times to obtain an empirical distribution of the estimator (or predictions). In imbalanced learning, bootstrap-style resampling is often used as a simple data-level intervention: by resampling within each class, one can create approximately balanced training sets.

Beyond the classical bootstrap, several variants improve statistical behavior or scalability, such as the Bayesian bootstrap ([Rubin, 1981](#)) and the bag of little bootstraps for massive datasets ([Kleiner et al., 2014](#)).

Reweighting addresses imbalance by modifying the training objective rather than generating new samples: one assigns class- or example-dependent weights and minimizes a weighted empirical risk, often choosing weights inversely proportional to class frequency or according to a misclassification cost matrix. At the level of the objective, resampling and reweighting are closely connected: duplicating an example in a resampled dataset is equivalent to assigning it a larger weight in a weighted empirical risk, and importance weights can be

implemented either by passing weights to the learner or by appropriate resampling schemes (Chen, Yang, Yu, Shi and Chen, 2024).

As a baseline “generator,” bootstrap-based oversampling has important drawbacks: it creates duplicates rather than new minority information, which can increase overfitting (He and Garcia, 2009). It can also be sensitive to noise or outliers, since a rare noisy point may be selected multiple times and thus receive inflated influence (Chen, Yang, Yu, Shi and Chen, 2024).

12.1.2 SMOTE and Variants

SMOTE (Synthetic Minority Over-sampling Technique) is one of the most widely used synthetic oversampling methods for imbalanced classification. It was introduced by Chawla et al. (2002) as an alternative to naive minority replication, with the goal of expanding the minority region in feature space and improving classifier performance. Conceptually, SMOTE treats “synthetic data generation” as interpolation rather than duplication: it creates new minority samples between existing minority points and their neighbors. For a desired oversampling rate, SMOTE repeatedly: (i) selects a minority instance \mathbf{x} , (ii) finds its k nearest minority neighbors, (iii) randomly chooses one neighbor $\mathbf{x}_{(j)}$, and (iv) generates a synthetic point by linear interpolation

$$\mathbf{x}_{\text{new}} = \mathbf{x} + \gamma(\mathbf{x}_{(j)} - \mathbf{x}), \quad \gamma \sim \text{Uniform}(0, 1),$$

so the synthetic example lies on the line segment between \mathbf{x} and a minority neighbor. This procedure is applied until the required number of synthetic minority samples is produced.

Many SMOTE variants modify where and how interpolation occurs to better target difficult regions or reduce noise. Borderline-SMOTE oversamples primarily minority points near the decision boundary (“borderline” instances), motivated by the idea that these are more informative yet more error-prone (Han et al., 2005). ADASYN (Adaptive Synthetic

Sampling) further makes the number of generated synthetic points adaptive, producing more samples in regions where minority points are harder to learn (He et al., 2008). Also, more recent work incorporates structure in the minority distribution. For example, k-means SMOTE uses clustering to guide where synthetic samples are most helpful while aiming to avoid generating unnecessary noise (Last et al., 2017).

A key advantage of SMOTE over naive random oversampling is that it generates new minority samples by interpolation rather than duplicating existing points, which can reduce overfitting relative to simple replication-based oversampling, and it can also fill in the interior of minority clusters to make them easier for a classifier to model. On the downside, because SMOTE interpolates from existing minority points, if some minority instances are noisy or outliers, the algorithm can generate additional synthetic samples around these abnormal points, effectively propagating noise and hurting classification (Matharaarachchi et al., 2024). Moreover, SMOTE generates points along line segments between neighbors (i.e., within the convex hull implied by observed minority samples). When the true minority support is non-convex (e.g., two separated regions or curved manifolds), interpolation can place synthetic samples in low-density regions or even inside majority regions, thereby degrading the decision boundary.

12.2 Deep Generative Models

12.2.1 Generative Adversarial Network (GAN)

Generative Adversarial Network (GAN) is a class of implicit generative models introduced by Goodfellow et al. (2014), where a generator learns to synthesize samples that resemble the training data while a discriminator learns to distinguish real from generated samples. Learning proceeds as a two-player minimax game.

The GAN can be summarized as follows. Let $\mathbf{z} \sim p(\mathbf{z})$ be a noise source (e.g., $\mathbf{z} \sim \mathcal{N}(0, I)$),

$G_{\theta}(\mathbf{z})$ be the generator, and $D_{\phi}(\mathbf{x}) \in (0, 1)$ be the discriminator output interpreted as the probability that \mathbf{x} is real. The original GAN objective (Goodfellow et al., 2014) is the minimax game

$$\min_{\theta} \max_{\phi} V(\phi, \theta) = \mathbb{E}_{\mathbf{x} \sim p_{\text{data}}} [\log D_{\phi}(\mathbf{x})] + \mathbb{E}_{\mathbf{z} \sim p(\mathbf{z})} [\log (1 - D_{\phi}(G_{\theta}(\mathbf{z})))] .$$

Training alternates between updating ϕ to increase $V(\phi, \theta)$ (improving discrimination) and updating θ to decrease $V(\phi, \theta)$ (fooling the discriminator), typically via stochastic gradient steps on mini-batches. After convergence, synthetic sampling is performed by drawing $\mathbf{z} \sim p(\mathbf{z})$ and outputting $\mathbf{x} = G_{\theta}(\mathbf{z})$.

Many GAN variants modify architecture, conditioning, divergence or optimization to improve stability and fidelity. For example, DCGAN established convolutional architectural guidelines for stable image GAN training (Radford et al., 2015). Conditional GAN (cGAN) conditions both G and D on label information y to generate $p(\mathbf{x}|y)$ (Mirza and Osindero, 2014). InfoGAN adds a mutual-information term to encourage disentangled and interpretable latent factors (Chen et al., 2016).

12.2.2 Variational Autoencoders (VAEs)

Variational Autoencoders (VAEs) are latent variable generative models that combine probabilistic modeling with neural-network encoder-decoder parameterizations. They were popularized by Kingma and Welling (2013), which showed how to train deep latent variable models efficiently with gradient methods. At a high level, a VAE learns (i) a generative model that maps latent variables to data, and (ii) an inference (recognition) model that approximates the intractable posterior over latents given data.

Variational autoencoders posit a latent variable model

$$p_{\theta}(\mathbf{x}, \mathbf{z}) = p(\mathbf{z})p_{\theta}(\mathbf{x} | \mathbf{z}),$$

typically with a simple prior $p(\mathbf{z}) = \mathcal{N}(0, I)$. Since the posterior $p_{\theta}(\mathbf{z} | \mathbf{x})$ is generally intractable, VAEs introduce an amortized variational approximation $q_{\phi}(\mathbf{z} | \mathbf{x})$ and maximize the evidence lower bound (ELBO):

$$\log p_{\theta}(\mathbf{x}) \geq \mathcal{L}(\theta, \phi; \mathbf{x}) := \mathbb{E}_{q_{\phi}(\mathbf{z}|\mathbf{x})}[\log p_{\theta}(\mathbf{x} | \mathbf{z})] - \text{KL}(q_{\phi}(\mathbf{z} | \mathbf{x}) || p(\mathbf{z})).$$

Training proceeds by stochastic gradient ascent on $\sum_{i=1}^n \mathcal{L}(\theta, \phi; \mathbf{x}_i)$. For continuous latents (e.g., a Gaussian encoder), the reparameterization trick writes a sample as

$$\mathbf{z} = \mu_{\phi}(\mathbf{x}) + \sigma_{\phi}(\mathbf{x}) \odot \varepsilon, \quad \varepsilon \sim \mathcal{N}(0, I),$$

so Monte Carlo estimates of $\nabla_{\theta, \phi} \mathcal{L}(\theta, \phi; \mathbf{x})$ can be backpropagated through the stochastic node. After training, synthetic sampling is performed by drawing $\mathbf{z} \sim p(\mathbf{z})$ and then drawing $\mathbf{x} \sim p_{\theta}(\mathbf{x} | \mathbf{z})$.

Many VAE variants improve expressiveness, conditioning, or sample quality. IWAE tightens the ELBO by using an importance-weighted bound with multiple samples from $q_{\phi}(\mathbf{z}|\mathbf{x})$, improving density modeling and learned representations (Burda et al., 2015). β -VAE modifies the KL term to encourage disentangled latent factors (Higgins et al., 2017). Conditional VAE (CVAE) conditions generation on side information y to model $p_{\theta}(x|y)$ via latent variable formulations, supporting controlled prediction (Sohn et al., 2015).

12.2.3 Diffusion Models

Diffusion models are generative models that learn to sample from a data distribution by reversing a gradual noising process. The original diffusion-probabilistic framing is often traced to Sohl-Dickstein et al. (2015), who proposed transforming data into noise through a Markov diffusion and learning the reverse-time dynamics for generation. A highly influential modern formulation is DDPM (Denoising Diffusion Probabilistic Models) (Ho et al., 2020), which showed that diffusion models can produce high-quality image samples using a denoising training objective closely related to score matching, without adversarial training.

The basic steps of DDPM can be summarized as follows. Let $\mathbf{x}_0 \sim p_{\text{data}}$ and choose a variance schedule $\{\beta_t\}_{t=1}^T$ with $\alpha_t = 1 - \beta_t$ and $\bar{\alpha}_t = \prod_{s=1}^t \alpha_s$.

(1) *Forward diffusion (noising)*. Define the Markov chain

$$q(\mathbf{x}_t | \mathbf{x}_{t-1}) = \mathcal{N}(\sqrt{\alpha_t} \mathbf{x}_{t-1}, \beta_t I),$$

which implies the closed form marginal

$$q(\mathbf{x}_t | \mathbf{x}_0) = \mathcal{N}(\sqrt{\bar{\alpha}_t} \mathbf{x}_0, (1 - \bar{\alpha}_t) I), \quad \text{equivalently} \quad \mathbf{x}_t = \sqrt{\bar{\alpha}_t} \mathbf{x}_0 + \sqrt{1 - \bar{\alpha}_t} \varepsilon, \quad \varepsilon \sim \mathcal{N}(0, I).$$

(2) *Learn the reverse denoiser*. Parameterize a network $\varepsilon_{\theta}(\mathbf{x}_t, t)$ to predict the injected noise and train via the (simplified) denoising objective

$$\min_{\theta} \mathbb{E}_{\substack{t \sim \text{Unif}\{1, \dots, T\} \\ \mathbf{x}_0 \sim p_{\text{data}} \\ \varepsilon \sim \mathcal{N}(0, I)}} \|\varepsilon - \varepsilon_{\theta}(\mathbf{x}_t, t)\|_2^2.$$

This corresponds to a Gaussian reverse kernel

$$p_{\theta}(\mathbf{x}_{t-1} | \mathbf{x}_t) = \mathcal{N}(\mu_{\theta}(\mathbf{x}_t, t), \Sigma_t),$$

with a common parameterization

$$\mu_{\theta}(\mathbf{x}_t, t) = \frac{1}{\sqrt{\alpha_t}} \left(\mathbf{x}_t - \frac{\beta_t}{\sqrt{1 - \bar{\alpha}_t}} \varepsilon_{\theta}(\mathbf{x}_t, t) \right),$$

and Σ_t chosen as $\beta_t I$ or learned or modified.

(3) *Sampling (generation)*. Draw $\mathbf{x}_T \sim \mathcal{N}(0, I)$ and iterate for $t = T, \dots, 1$:

$$\mathbf{x}_{t-1} = \mu_{\theta}(\mathbf{x}_t, t) + \Sigma_t^{1/2} \mathbf{z}, \quad \mathbf{z} \sim \mathcal{N}(0, I),$$

yielding \mathbf{x}_0 as the synthetic sample.

There are many variants and extensions of diffusion models. For example, a major unifying view is score-based diffusion via SDEs, which formulates diffusion in continuous time and connects sampling to solving a reverse-time SDE (Song, Sohl-Dickstein, Kingma, Kumar,

Ermon and Poole, 2020). To address slow sampling, DDIM (denoising diffusion implicit models) introduces a non-Markovian formulation that can sample in far fewer steps while using the same training procedure as DDPMs (Song, Meng and Ermon, 2020). For efficiency at high resolution, Latent Diffusion Models (LDMs) perform diffusion in a learned latent space to reduce computation while maintaining strong synthesis performance (Rombach et al., 2022).

12.2.4 Flow Matching

Flow Matching is a training approach for continuous normalizing flows (CNFs) that learns a time-dependent vector field whose ODE transports a simple base distribution (e.g., Gaussian noise) to the data distribution. It was introduced by Lipman et al. (2022), with the key idea that instead of maximizing likelihood via expensive ODE simulation, one can train the CNF by regressing the model’s vector field to a known conditional velocity field induced by a chosen probability path connecting noise to data.

Let π_0 be a base distribution on \mathbb{R}^d (e.g., $\mathcal{N}(0, I)$) and $\pi_1 = p_{\text{data}}$. Choose a family of intermediate distributions $\{\rho_t\}_{t \in [0,1]}$ (a “probability path”) such that $\rho_0 = \pi_0$ and $\rho_1 = \pi_1$. A common construction specifies a conditional path $\mathbf{x}_t = \Psi_t(\mathbf{x}_0, \mathbf{x}_1, \epsilon)$ with $\mathbf{x}_0 \sim \pi_0$, $\mathbf{x}_1 \sim \pi_1$, and auxiliary noise ϵ (e.g., $\epsilon \sim \mathcal{N}(0, I)$ for Gaussian paths). This induces a conditional distribution $\rho_t(\cdot | \mathbf{x}_1)$ and an associated conditional velocity field $u_t(\mathbf{x} | \mathbf{x}_1)$ (or $u_t(\mathbf{x} | \mathbf{x}_0, \mathbf{x}_1)$), often available in closed form for the chosen path. Flow Matching trains a neural vector field $v_\theta(\mathbf{x}, t)$ by the regression objective

$$\min_{\theta} \mathbb{E}_{t \sim \text{Unif}[0,1]} \mathbb{E}_{\mathbf{x}_1 \sim \pi_1} \mathbb{E}_{\mathbf{x} \sim \rho_t(\cdot | \mathbf{x}_1)} \left\| v_\theta(\mathbf{x}, t) - u_t(\mathbf{x} | \mathbf{x}_1) \right\|_2^2.$$

After training, generation is performed by deterministic ODE sampling: draw $\mathbf{x}(0) \sim \pi_0$ and solve

$$\frac{d\mathbf{x}}{dt} = v_\theta(\mathbf{x}(t), t), \quad t \in [0, 1],$$

to obtain a synthetic sample $\mathbf{x}(1)$.

12.3 Large Language Models

Attention-based large language models (LLMs) use the Transformer architecture, built around self-attention to model and generate sequences. The foundational paper is [Vaswani et al. \(2017\)](#), which introduced multi-head self-attention as a fully parallel alternative to recurrence or convolutions for sequence modeling. Building on this architecture, modern LLMs are typically trained as auto-regressive models, where generation is done token-by-token.

An attention-based LLM defines an explicit probability model over token sequences $\mathbf{x}_{1:T}$ (e.g., words, subwords, or bytes) by the autoregressive factorization

$$p_{\theta}(\mathbf{x}_{1:T}) = \prod_{t=1}^T p_{\theta}(\mathbf{x}_t \mid \mathbf{x}_{<t}).$$

Given a training corpus $\{\mathbf{x}_{1:T_i}^{(i)}\}_{i=1}^n$, parameters θ are learned by maximum likelihood (equivalently, minimizing cross-entropy):

$$\hat{\theta} \in \arg \max_{\theta} \sum_{i=1}^n \sum_{t=1}^{T_i} \log p_{\theta}(\mathbf{x}_t^{(i)} \mid \mathbf{x}_{<t}^{(i)}).$$

The conditionals $p_{\theta}(\cdot \mid \mathbf{x}_{<t})$ are produced by a Transformer decoder with causal self-attention. Writing the hidden states as $H \in \mathbb{R}^{t \times d}$, each attention layer forms $Q = HW_Q$, $K = HW_K$, $V = HW_V$ and computes

$$\text{Attn}(Q, K, V) = \text{softmax} \left(\frac{QK^{\top}}{\sqrt{d_k}} + M \right) V,$$

where M is a causal mask (future positions set to $-\infty$), and multi-head attention concatenates several such heads.

After training, the LLM can generate synthetic sequences by sampling from the learned distribution p_{θ} . Starting from a prompt or a prefix $\mathbf{x}_{1:t_0}$, the model outputs a categorical

distribution over the next token:

$$\pi_t(\cdot) = p_{\hat{\theta}}(\mathbf{x}_t = \cdot \mid \mathbf{x}_{<t}).$$

A synthetic token is then drawn by a sampling rule such as ancestral sampling ($\mathbf{x}_t \sim \text{Categorical}(\pi_t)$) or temperature sampling ($\mathbf{x}_t \sim \text{Categorical}(\text{softmax}(\text{logits}/\tau))$). Appending the sampled token yields a longer prefix $\mathbf{x}_{1:t}$, and the process is repeated until an end-of-sequence token or a length cap is reached. The resulting sequence $\tilde{\mathbf{x}}_{1:\tilde{T}}$ is a synthetic sample from $p_{\hat{\theta}}$ or from the conditional distribution $p_{\hat{\theta}}(\cdot \mid \mathbf{x}_{1:t_0})$ when a prompt is used to steer attributes such as class, style, or covariates.

13 Details of Examples

In this section, we present the detailed calculations of the examples in the main paper.

13.1 Details of Example 1

Toy Collinear Example: The details of this example are split into following cases:

- **(Same Direction)** When $s = +1$, the direction of $\nabla\psi(\boldsymbol{\theta}^*)$ and $\nabla\phi(\boldsymbol{\theta}^*)$ are the same.

Then we select δ_n as

$$\delta_n = \frac{2}{\sqrt{\log n_1} - 2} \quad \Rightarrow \quad \tilde{n} = \frac{\sqrt{\log n_1}}{\sqrt{\log n_1} - 2}(n_0 - n_1).$$

Then we have

$$\mathbf{b}(\boldsymbol{\theta}) = \left(\frac{n_0}{n_0 + n_1 + \tilde{n}} - \frac{1}{2} + \frac{\tilde{n}}{n_0 + n_1 + \tilde{n}} \frac{1}{\sqrt{\log n_1}} \right) \nabla\phi(\boldsymbol{\theta}) = 0.$$

Hence,

$$T_1 = T_2 = 0, \quad T_3 = \Theta_P(n_0^{-1}) \quad \Rightarrow \quad \mathcal{R}(\hat{\boldsymbol{\theta}}) - \mathcal{R}(\boldsymbol{\theta}^*) = \Theta_P(n_0^{-1}).$$

- **(Opposite Direction)** Similarly, when $s = -1$, the direction of $\nabla\psi(\boldsymbol{\theta}^*)$ and $\nabla\phi(\boldsymbol{\theta}^*)$ are the opposite. Then we select δ_n as

$$\delta_n = \frac{-2}{\sqrt{\log n_1 + 2}} \quad \Rightarrow \quad \tilde{n} = \frac{\sqrt{\log n_1}}{\sqrt{\log n_1 + 2}}(n_0 - n_1).$$

Then we still have $\mathbf{b}(\boldsymbol{\theta}^*) = 0$ and

$$T_1 = T_2 = 0, \quad T_3 = \Theta_P(n_0^{-1}) \quad \Rightarrow \quad \mathcal{R}(\hat{\boldsymbol{\theta}}) - \mathcal{R}(\boldsymbol{\theta}^*) = \Theta_P(n_0^{-1}).$$

- **(Exactly Synthesizing $\tilde{n} = n_0 - n_1$)** In contrast, consider the above two cases but now simply generate $\tilde{n} = n_0 - n_1$ synthetic samples. Then, for the same and opposite direction settings,

$$\mathbf{b}(\boldsymbol{\theta}^*) = \left(\pi_0 - \frac{1}{2} + \frac{\tilde{n}}{n_0 + n_1 + \tilde{n}} \frac{s}{\sqrt{\log n_1}} \right) \nabla\phi(\boldsymbol{\theta}^*) = s \frac{n_0 - n_1}{2n_0} \frac{1}{\sqrt{\log n_1}} \nabla\phi(\boldsymbol{\theta}^*).$$

Therefore,

$$T_1 \asymp (\log n_1)^{-1}, \quad T_2 = \Theta_P((n_0 \log n_1)^{-1/2}), \quad T_3 = \Theta_P(n_0^{-1}),$$

and thus we have

$$\mathcal{R}(\hat{\boldsymbol{\theta}}) - \mathcal{R}(\boldsymbol{\theta}^*) = \Theta_P((\log n_1)^{-1}).$$

13.2 Details of Example 2

Two-Dimensional Gaussian Example:

We consider a two dimensional Gaussian case where the majority follows $\mathbf{x}|y = 0 \sim \mathcal{P}_0 = \mathcal{N}(0, I_2)$ while the minority $\mathbf{x}|y = 1 \sim \mathcal{P}_1 = \mathcal{N}(\boldsymbol{\mu}_1, I_2)$. The synthetic data are generated from $\tilde{\mathbf{x}} \sim \mathcal{P}_{\text{syn}} = \mathcal{N}(\boldsymbol{\mu}_s, I_2)$. We consider the mean squared loss $\ell(f_{\boldsymbol{\theta}}(\mathbf{x}), y) = (\boldsymbol{\theta}^\top \mathbf{x} - y)^2$. Generally, when $\mathbf{x} \sim \mathcal{N}(\boldsymbol{\mu}, I)$, the risk is

$$\mathbb{E}_{\mathcal{N}(\boldsymbol{\mu}, I)} \ell(\boldsymbol{\theta}; \mathbf{x}, y) = \mathbb{E}(\boldsymbol{\theta}^\top \mathbf{x} - y)^2 = \boldsymbol{\theta}^\top \boldsymbol{\theta} + (\boldsymbol{\theta}^\top \boldsymbol{\mu} - y)^2.$$

Thus the balanced risk

$$\begin{aligned}\mathcal{R}(\boldsymbol{\theta}) &= \frac{1}{2}\mathbb{E}_{\mathcal{P}_0}\ell(\boldsymbol{\theta}; \mathbf{x}, 0) + \frac{1}{2}\mathbb{E}_{\mathcal{P}_1}\ell(\boldsymbol{\theta}; \mathbf{x}, 1) = \boldsymbol{\theta}^\top \boldsymbol{\theta} + \frac{1}{2}(\boldsymbol{\theta}^\top \boldsymbol{\mu}_1 - 1)^2, \\ \nabla \mathcal{R}(\boldsymbol{\theta}) &= 2\boldsymbol{\theta} + (\boldsymbol{\theta}^\top \boldsymbol{\mu}_1 - 1)\boldsymbol{\mu}_1 = 0 \quad \Rightarrow \quad \boldsymbol{\theta}^* = (\boldsymbol{\mu}_1 \boldsymbol{\mu}_1^\top + 2I)^{-1} \boldsymbol{\mu}_1.\end{aligned}$$

Then,

$$\nabla \phi(\boldsymbol{\theta}) = -2(\boldsymbol{\theta}^\top \boldsymbol{\mu}_1 - 1)\boldsymbol{\mu}_1, \quad \nabla \psi(\boldsymbol{\theta}) = 2(\boldsymbol{\theta}^\top \boldsymbol{\mu}_s - 1)\boldsymbol{\mu}_s - 2(\boldsymbol{\theta}^\top \boldsymbol{\mu}_1 - 1)\boldsymbol{\mu}_1. \quad (7)$$

- **Aligned Synthetic Bias Case.** For the aligned bias case, we select $\boldsymbol{\mu}_1 = (\mu, 0)^\top$ and $\boldsymbol{\mu}_s = (a, 0)^\top$, where $a \neq \left\{\mu, \frac{2}{\mu}\right\}$. By equation (7), two gradients are exactly aligned

$$\nabla \phi(\boldsymbol{\theta}^*) = \left(\frac{4\mu}{\mu^2 + 2}, 0\right)^\top, \quad \nabla \psi(\boldsymbol{\theta}^*) = \left(\frac{2(\mu a - 2)(a - \mu)}{\mu^2 + 2}, 0\right)^\top.$$

By empirical estimation, we have

$$\hat{\boldsymbol{\theta}} - \tilde{\boldsymbol{\theta}} = O_P\left((n_0 + n_1 + \tilde{n})^{-1/2}\right).$$

Here we choose \tilde{n} to enforce $\tilde{\boldsymbol{\theta}} = \boldsymbol{\theta}^*$, then the excess risk is consistent by Taylor expansion

$$\mathcal{R}(\hat{\boldsymbol{\theta}}) - \mathcal{R}(\boldsymbol{\theta}^*) = \mathcal{R}(\hat{\boldsymbol{\theta}}) - \mathcal{R}(\tilde{\boldsymbol{\theta}}) \lesssim \frac{1}{2}\lambda_{\max}(\nabla^2 \mathcal{R}(\boldsymbol{\theta}^*))\|\hat{\boldsymbol{\theta}} - \tilde{\boldsymbol{\theta}}\|^2 = O_P\left((n_0 + n_1 + \tilde{n})^{-1}\right).$$

To solve the corresponding synthetic size, $\tilde{\boldsymbol{\theta}} = \boldsymbol{\theta}^*$ implies $\nabla \tilde{\mathcal{R}}(\boldsymbol{\theta}^*) = 0$. Calculation gives

$$\begin{aligned}\nabla \tilde{\mathcal{R}}(\boldsymbol{\theta}^*) &= 2\boldsymbol{\theta}^* + 2\pi_1(\boldsymbol{\theta}^{*T} \boldsymbol{\mu}_1 - 1)\boldsymbol{\mu}_1 + 2\tilde{\pi}(\boldsymbol{\theta}^{*T} \boldsymbol{\mu}_s - 1)\boldsymbol{\mu}_s \\ &= \left(\frac{2\mu}{\mu^2 + 2}, 0\right)^\top + \left(\frac{-4\pi_1\mu}{\mu^2 + 2}, 0\right)^\top + \left(\frac{2\tilde{\pi}(\mu a - \mu^2 - 2)a}{\mu^2 + 2}, 0\right)^\top = 0.\end{aligned}$$

Solving this gives

$$\tilde{n} = \frac{\mu(n_0 - n_1)}{a(\mu^2 + 2) - \mu(a^2 + 1)}.$$

For example, when $\mu = 1$, $a = \frac{1}{2}$, this value is $\tilde{n} = 4(n_0 - n_1)$, which is far away from the balanced synthetic size $n_0 - n_1$.

- **Sub-Optimal Synthetic Size** $n_0 - n_1$. In the previous case, if we still choose the balanced synthetic size $\tilde{n} = n_0 - n_1$, the excess risk is not consistent anymore. The population risk

$$\tilde{\mathcal{R}}(\boldsymbol{\theta}) = \boldsymbol{\theta}^\top \boldsymbol{\theta} + \pi_1(\boldsymbol{\theta}_1 \mu - 1)^2 + \tilde{\pi}(\boldsymbol{\theta}_1 a - 1)^2.$$

Therefore,

$$\nabla \tilde{\mathcal{R}}(\boldsymbol{\theta}) = 0 \Rightarrow \begin{cases} \boldsymbol{\theta}_1 + \pi_1(\boldsymbol{\theta}_1 \mu - 1)\mu + \tilde{\pi}(\boldsymbol{\theta}_1 a - 1)a = 0, \\ \boldsymbol{\theta}_2 = 0, \end{cases} \Rightarrow \tilde{\boldsymbol{\theta}} = \left(\frac{\mu\pi_1 + a\tilde{\pi}}{1 + \pi_1\mu^2 + \tilde{\pi}a^2}, 0 \right)^\top$$

Define $\frac{n_1}{n_0} \rightarrow \rho$, where $\rho \geq 0$. Therefore, $\pi_0 \rightarrow \frac{1}{2}$, $\pi_1 \rightarrow \frac{\rho}{2}$ and $\tilde{\pi} \rightarrow \frac{1-\rho}{2}$. The Hessian for the risk

$$\nabla^2 \mathcal{R}(\boldsymbol{\theta}) = \begin{pmatrix} \mu^2 + 2 & 0 \\ 0 & 2 \end{pmatrix} \succeq 2I,$$

thus $\mathcal{R}(\boldsymbol{\theta})$ is 2-strongly convex and thus $\mathcal{R}(\boldsymbol{\theta}) - \mathcal{R}(\boldsymbol{\theta}^*) \geq \|\boldsymbol{\theta} - \boldsymbol{\theta}^*\|^2$. Therefore,

$$\lim \mathcal{R}(\tilde{\boldsymbol{\theta}}) - \mathcal{R}(\boldsymbol{\theta}^*) \geq \lim \|\tilde{\boldsymbol{\theta}} - \boldsymbol{\theta}^*\|^2 = \left(\frac{\mu\pi_1 + a\tilde{\pi}}{1 + \pi_1\mu^2 + \tilde{\pi}a^2} - \frac{\mu}{\mu^2 + 2} \right)^2 = c > 0,$$

here for $a \neq \frac{\mu^2+2}{\mu}$ when $\rho = 0$. Also by empirical estimation and Taylor expansion

$$\mathcal{R}(\hat{\boldsymbol{\theta}}) - \mathcal{R}(\tilde{\boldsymbol{\theta}}) = O_P\left(\frac{1}{n_0 + n_1 + \tilde{n}}\right),$$

we have

$$\mathcal{R}(\hat{\boldsymbol{\theta}}) - \mathcal{R}(\boldsymbol{\theta}^*) = \mathcal{R}(\hat{\boldsymbol{\theta}}) - \mathcal{R}(\tilde{\boldsymbol{\theta}}) + \mathcal{R}(\tilde{\boldsymbol{\theta}}) - \mathcal{R}(\boldsymbol{\theta}^*) \rightarrow c > 0$$

in probability.

- **Orthogonal Synthetic Bias.** Construct $\boldsymbol{\mu}_1 = (\mu, 0)^\top$ and $\boldsymbol{\mu}_s = (\mu, \mu)$ with $\mu^2 \leq 2$, we have the orthogonal synthetic bias

$$\nabla \phi(\boldsymbol{\theta}^*) = \left(\frac{4\mu}{\mu^2 + 2}, 0 \right)^\top, \quad \nabla \psi(\boldsymbol{\theta}^*) = \left(0, -\frac{4\mu}{\mu^2 + 2} \right)^\top.$$

Solving the balanced minimizer

$$\nabla \mathcal{R}(\boldsymbol{\theta}) = 0 \Rightarrow \boldsymbol{\theta}^* = \left(\frac{\mu}{\mu^2 + 2}, 0 \right)^\top \Rightarrow \mathcal{R}(\boldsymbol{\theta}^*) = \frac{1}{\mu^2 + 2}.$$

Thus, the excess risk for any $\boldsymbol{\theta}$ satisfies

$$\mathcal{R}(\boldsymbol{\theta}) - \mathcal{R}(\boldsymbol{\theta}^*) = \boldsymbol{\theta}_1^2 + \boldsymbol{\theta}_2^2 + \frac{1}{2}(\boldsymbol{\theta}_1\mu - 1)^2 - \frac{1}{\mu^2 + 2} \geq \boldsymbol{\theta}_2^2.$$

Then for $\tilde{\boldsymbol{\theta}}$,

$$\begin{aligned} \nabla \tilde{\mathcal{R}}(\boldsymbol{\theta}) = 0 \Rightarrow & \begin{cases} \boldsymbol{\theta}_1 + \pi_1(\boldsymbol{\theta}_1\mu - 1)\mu + \tilde{\pi}\mu(\mu\boldsymbol{\theta}_1 + \mu\boldsymbol{\theta}_2 - 1) = 0, \\ \boldsymbol{\theta}_2 + \tilde{\pi}\mu(\mu\boldsymbol{\theta}_1 + \mu\boldsymbol{\theta}_2 - 1) = 0, \end{cases} \\ & \Rightarrow \tilde{\boldsymbol{\theta}}_2 = \frac{\tilde{\pi}\mu}{1 + \pi_1\mu^2 + 2\tilde{\pi}\mu^2 + \pi_1\pi_2\mu^4} \end{aligned}$$

Thus for any non-diminishing synthetic size ($\lim \tilde{\pi} \geq \tau > 0$), we have $\lim \tilde{\boldsymbol{\theta}}_2 \geq c > 0$.

By similar steps in the last example,

$$\mathcal{R}(\hat{\boldsymbol{\theta}}) - \mathcal{R}(\boldsymbol{\theta}^*) = \mathcal{R}(\hat{\boldsymbol{\theta}}) - \mathcal{R}(\tilde{\boldsymbol{\theta}}) + \mathcal{R}(\tilde{\boldsymbol{\theta}}) - \mathcal{R}(\boldsymbol{\theta}^*) \rightarrow c > 0$$

in probability.

- **Arbitrary Direction.** For any direction $\nabla \psi(\boldsymbol{\theta}^*)$, we can always make a projection onto $\nabla \phi(\boldsymbol{\theta}^*)$ and an orthogonal vector. As long as the projection onto the orthogonal vector is $o_P(1)$, we can always find some proper synthetic size to make the excess risk consistent.

13.3 Details of Example 3

For the mean shift model, we use labels $y \in \{0, 1\}$ with class prior

$$\mathbb{P}(y = 1) = \pi \quad \mathbb{P}(y = 0) = 1 - \pi,$$

allowing π to be arbitrarily imbalanced. Let $\boldsymbol{\xi} \in \mathbb{R}^d$ be a random vector from any distribution such that 1) $\boldsymbol{\xi}$ has bounded support almost surely and 2) $\boldsymbol{\xi}$ is mean zero and with

full-rank covariance. Conditioned on y , features follow symmetric shifts of the common noise distribution $\boldsymbol{\xi}$:

$$\mathbf{x}|(y = 1) \sim \boldsymbol{\mu} + \boldsymbol{\xi} \quad \mathbf{x}|(y = 0) \sim -\boldsymbol{\mu} + \boldsymbol{\xi}.$$

We consider the linear classifier with squared loss

$$f_{\boldsymbol{\theta}}(\mathbf{x}) = \boldsymbol{\theta}^\top \mathbf{x} \quad \ell(\boldsymbol{\theta}; \mathbf{x}, y) = (y - 1/2 - \boldsymbol{\theta}^\top \mathbf{x})^2.$$

This model isolates how class imbalance interacts with the geometry of the population risk and provides a clean setting to see when rebalancing via synthetic data is inherently unnecessary. We then have the following theorem.

Proposition 1 (Local symmetry for mean shift model). *Under the mean shift model, for any distribution of $\boldsymbol{\xi}$ satisfying the above conditions, the balanced minimizer has a closed form solution, and majority-minority bias cancels.*

$$\boldsymbol{\theta}^* = \frac{1}{2} \left[\boldsymbol{\mu} \boldsymbol{\mu}^\top + \mathbb{E}[\boldsymbol{\xi} \boldsymbol{\xi}^\top] \right]^{-1} \boldsymbol{\mu}, \quad \nabla \phi(\boldsymbol{\theta}^*) = 0.$$

Proposition 1 shows that, under the mean shift model, the balanced risk minimizer admits a closed form expression and, crucially, the majority–minority bias cancels at the optimum $\nabla \phi(\boldsymbol{\theta}^*) = 0$. This is precisely the local symmetry property discussed earlier. As a result, even under severe imbalance, adding synthetic minority samples cannot improve the estimator’s performance under any realistic generator.

13.4 Details of Example 4

For the logistic regression model, we continue to use the label convention $y = \{0, 1\}$. The data are generated from a sigmoid Bernoulli model without intercept:

$$\mathbf{x} \sim p(\mathbf{x}), \quad \mathbb{P}(y = 1 | \mathbf{x}) = \sigma(\mathbf{x}^\top \boldsymbol{\theta}_{\text{true}}), \quad \mathbb{P}(y = 0 | \mathbf{x}) = 1 - \sigma(\mathbf{x}^\top \boldsymbol{\theta}_{\text{true}}).$$

Under this formulation, the logistic loss can be written as

$$\ell(\boldsymbol{\theta}; \mathbf{x}, y) = \log(1 + \exp\{\boldsymbol{\theta}^\top \mathbf{x}\}) - y\mathbf{x}^\top \boldsymbol{\theta}.$$

Our goal in this subsection is to identify conditions on $p(\mathbf{x})$ under which class imbalance does not induce a first-order shift in the balanced risk optimum, implying that synthetic minority augmentation is not expected to help.

Proposition 2 (Local symmetry for Sigmoid Bernoulli model). *Any data generating distribution $p(\mathbf{x})$ satisfying the following condition gives a canceled majority-minority bias*

$$\mathbb{E}_{p(\mathbf{x})} \left[\mathbf{x}\sigma(\boldsymbol{\theta}_{\text{true}}^\top \mathbf{x}) \left(1 - \sigma(\boldsymbol{\theta}_{\text{true}}^\top \mathbf{x})\right) \right] = 0 \quad \Rightarrow \quad \nabla\phi(\boldsymbol{\theta}^*) = 0. \quad (8)$$

Proposition 2 provides a sufficient condition on the feature distribution $p(\mathbf{x})$ under which the majority–minority bias cancels at the balanced risk minimizer, i.e., $\nabla\phi(\boldsymbol{\theta}^*) = 0$. Intuitively, this condition enforces a form of local symmetry: the weighted contribution of features to the gradient through $\mathbb{E}_{p(\mathbf{x})} \left[\mathbf{x}\sigma(\boldsymbol{\theta}_{\text{true}}^\top \mathbf{x}) \left(1 - \sigma(\boldsymbol{\theta}_{\text{true}}^\top \mathbf{x})\right) \right] = 0$ averages out, so changing class proportions does not create a first-order perturbation of the target solution. Consequently, imbalance is not the bottleneck in this regime, and adding synthetic minority samples cannot improve excess risk under realistic generators. To demonstrate that this situation is not pathological, we next construct concrete examples of $p(\mathbf{x})$ that satisfy the condition and illustrate how the cancellation can occur in practice.

Example 5 (One-Dimensional Discrete Case). *Under the sigmoid Bernoulli logistic regression model, suppose the covariate is generated from the discrete distribution*

$$x = \begin{cases} -a & \text{with probability } \alpha; \\ b & \text{with probability } 1 - \alpha; \end{cases} \quad (9)$$

Here $a, b, \alpha > 0$. Let $\boldsymbol{\theta}_{\text{true}} = c > 0$. Then the condition in equation (8) is

$$\mathbb{E}_{p(x)} [x\sigma(cx)(1 - \sigma(cx))] = -\alpha a\sigma(ca)(1 - \sigma(ca)) + (1 - \alpha)b\sigma(cb)(1 - \sigma(cb)) = 0$$

The condition is satisfied as long as the probability α satisfies

$$\alpha = \frac{b\sigma(cb)(1 - \sigma(cb))}{a\sigma(ca)(1 - \sigma(ca)) + b\sigma(cb)(1 - \sigma(cb))}. \quad (10)$$

Also, the imbalance of this problem can have any severity:

$$\mathbb{P}(y = 1) = \mathbb{E}_{p(\mathbf{x})} [\sigma(c\mathbf{x})] = \alpha(1 - \sigma(ca)) + (1 - \alpha)\sigma(cb) \xrightarrow{a \rightarrow \infty} 0. \quad (11)$$

Thus, we can construct any imbalance for this problem by creating constants a and b , instead of just a naive balancing case.

Example 6 (Multivariate Case). Suppose the true parameter is

$$\boldsymbol{\theta}_{\text{true}} = c \cdot \mathbf{v}, \quad \|\mathbf{v}\| = 1, \quad c > 0.$$

And the covariates are generated from the distribution

$$\mathbf{x} = T\mathbf{v} + W,$$

where T follows the distribution of x in equation (9) in example 5. W is a mean zero random noise of any distribution with bounded support and full-rank covariance in the orthogonal space of \mathbf{v} such that $\mathbf{v}^\top W = 0$ almost surely. Also, W is independent of T . Therefore, we have

$$\boldsymbol{\theta}_{\text{true}}^\top \mathbf{x} = c\mathbf{v}^\top (T\mathbf{v} + W) = cT.$$

Then the condition (8) is

$$\begin{aligned} \mathbb{E}_{p(\mathbf{x})} [(T\mathbf{v} + W)\sigma(cT)(1 - \sigma(cT))] &= \mathbf{v}\mathbb{E}_{p(\mathbf{x})} [T\sigma(cT)(1 - \sigma(cT))] \\ &= -\alpha a\sigma(ca)(1 - \sigma(ca)) + (1 - \alpha)b\sigma(cb)(1 - \sigma(cb)) = 0. \end{aligned}$$

Similar to example 5, the condition (8) holds as long as the probability α satisfies equation (10), while the imbalance can still be any severe because equation (11) still holds.

14 Proofs

14.1 Proof of Theorem 1

By the first order optimality

$$\|\nabla\tilde{\mathcal{R}}(\boldsymbol{\theta}^*)\| = \|\nabla\tilde{\mathcal{R}}(\boldsymbol{\theta}^*) - \nabla\tilde{\mathcal{R}}(\tilde{\boldsymbol{\theta}})\| \leq M\|\boldsymbol{\theta}^* - \tilde{\boldsymbol{\theta}}\|,$$

where the last step is from the M -smoothness of $\tilde{\mathcal{R}}(\boldsymbol{\theta})$ at $\tilde{\boldsymbol{\theta}}$. Thus we have the lower bound for parameter

$$\|\boldsymbol{\theta}^* - \tilde{\boldsymbol{\theta}}\| \geq \frac{1}{M}\|\nabla\tilde{\mathcal{R}}(\boldsymbol{\theta}^*)\|. \quad (12)$$

The balanced risk $\mathcal{R}(\boldsymbol{\theta})$ is μ -strongly convex near the minimizer $\boldsymbol{\theta}^*$, that is

$$\mathcal{R}(\boldsymbol{\theta}) - \mathcal{R}(\boldsymbol{\theta}^*) \geq \frac{\mu}{2}\|\boldsymbol{\theta} - \boldsymbol{\theta}^*\|^2.$$

Combining equation (12), we have

$$\mathcal{R}(\tilde{\boldsymbol{\theta}}) - \mathcal{R}(\boldsymbol{\theta}^*) \geq \frac{\mu}{2}\|\tilde{\boldsymbol{\theta}} - \boldsymbol{\theta}^*\|^2 \geq \frac{\mu}{2M^2}\|\nabla\tilde{\mathcal{R}}(\boldsymbol{\theta}^*)\|^2.$$

Recall the relationship combined with first order optimality

$$\nabla\tilde{\mathcal{R}}(\boldsymbol{\theta}^*) = \nabla\mathcal{R}(\boldsymbol{\theta}^*) + \left(\pi_0 - \frac{1}{2}\right)\nabla\phi(\boldsymbol{\theta}^*) + \tilde{\pi}\nabla\psi(\boldsymbol{\theta}^*) = \left(\pi_0 - \frac{1}{2}\right)\nabla\phi(\boldsymbol{\theta}^*) + \tilde{\pi}\nabla\psi(\boldsymbol{\theta}^*).$$

Thus we have

$$\mathcal{R}(\tilde{\boldsymbol{\theta}}) - \mathcal{R}(\boldsymbol{\theta}^*) \geq \frac{\mu}{2M^2}\left\|\left(\pi_0 - \frac{1}{2}\right)\nabla\phi(\boldsymbol{\theta}^*) + \tilde{\pi}\nabla\psi(\boldsymbol{\theta}^*)\right\|^2. \quad (13)$$

Next we analyze $|\mathcal{R}(\hat{\boldsymbol{\theta}}) - \mathcal{R}(\tilde{\boldsymbol{\theta}})|$. We first show that $\hat{\boldsymbol{\theta}}$ and $\tilde{\boldsymbol{\theta}}$ are close to each other. For fixed $\epsilon > 0$, define the set

$$A_\epsilon := \{\boldsymbol{\theta} \in \Theta : \|\boldsymbol{\theta} - \tilde{\boldsymbol{\theta}}\| \geq \epsilon\}.$$

Thus it is easy to verify that

$$\inf_{\boldsymbol{\theta} \in A_\epsilon} (\tilde{\mathcal{R}}(\boldsymbol{\theta}) - \tilde{\mathcal{R}}(\tilde{\boldsymbol{\theta}})) > 0.$$

Then, define the set

$$E_n = \left\{ \sup_{\boldsymbol{\theta} \in \Theta} \left| \hat{\mathcal{R}}(\boldsymbol{\theta}) - \tilde{\mathcal{R}}(\boldsymbol{\theta}) \right| \leq \inf_{\boldsymbol{\theta} \in A_\epsilon} \left(\tilde{\mathcal{R}}(\boldsymbol{\theta}) - \tilde{\mathcal{R}}(\tilde{\boldsymbol{\theta}}) \right) / 3 \right\}. \quad (14)$$

By definition, we have

$$\begin{aligned} \left| \hat{\mathcal{R}}(\boldsymbol{\theta}) - \tilde{\mathcal{R}}(\boldsymbol{\theta}) \right| &\leq \pi_0 \left| \frac{1}{n_0} \sum_{i=1}^{n_0} \ell(f_{\boldsymbol{\theta}}(\mathbf{x}_i^{(0)}), 0) - \mathbb{E}_{\mathcal{P}_0} \ell(\boldsymbol{\theta}; \mathbf{x}, 0) \right| \\ &+ \pi_1 \left| \frac{1}{n_1} \sum_{i=1}^{n_1} \ell(f_{\boldsymbol{\theta}}(\mathbf{x}_i^{(1)}), 1) - \mathbb{E}_{\mathcal{P}_1} \ell(\boldsymbol{\theta}; \mathbf{x}, 1) \right| + \tilde{\pi} \left| \frac{1}{\tilde{n}} \sum_{i=1}^{\tilde{n}} \ell(f_{\boldsymbol{\theta}}(\tilde{\mathbf{x}}_i), 1) - \mathbb{E}_{\mathcal{P}_{\text{syn}}} \ell(\boldsymbol{\theta}; \mathbf{x}, 1) \right|. \end{aligned} \quad (15)$$

For the first two terms, we have compact $\boldsymbol{\theta}$, continuous ℓ and bounded loss, thus by Uniform Law of Large Numbers (e.g. Lemma 2.4 in [Newey and McFadden \(1994\)](#)), the uniform convergence holds that

$$\begin{aligned} \sup_{\boldsymbol{\theta} \in \Theta} \left| \frac{1}{n_0} \sum_{i=1}^{n_0} \ell(\boldsymbol{\theta}; \mathbf{x}_i^{(0)}, 0) - \mathbb{E}_{\mathcal{P}_0} \ell(\boldsymbol{\theta}; \mathbf{x}, 0) \right| &\xrightarrow{P} 0, \\ \sup_{\boldsymbol{\theta} \in \Theta} \left| \frac{1}{n_1} \sum_{i=1}^{n_1} \ell(\boldsymbol{\theta}; \mathbf{x}_i^{(1)}, 1) - \mathbb{E}_{\mathcal{P}_1} \ell(\boldsymbol{\theta}; \mathbf{x}, 1) \right| &\xrightarrow{P} 0. \end{aligned}$$

For the third term, if the synthetic size $\tilde{n} \rightarrow \infty$, we similarly have

$$\sup_{\boldsymbol{\theta} \in \Theta} \left| \frac{1}{\tilde{n}} \sum_{i=1}^{\tilde{n}} \ell(\boldsymbol{\theta}; \tilde{\mathbf{x}}_i, 1) - \mathbb{E}_{\mathcal{P}_{\text{syn}}} \ell(\boldsymbol{\theta}; \mathbf{x}, 1) \right| \xrightarrow{P} 0,$$

while if the synthetic size is bounded by some large constant $\tilde{n} \leq M$, we have $\tilde{\pi} \rightarrow 0$.

Combined with the bounded loss, we still have the convergence in probability

$$\tilde{\pi} \sup_{\boldsymbol{\theta} \in \Theta} \left| \frac{1}{\tilde{n}} \sum_{i=1}^{\tilde{n}} \ell(\boldsymbol{\theta}; \tilde{\mathbf{x}}_i, 1) - \mathbb{E}_{\mathcal{P}_{\text{syn}}} \ell(\boldsymbol{\theta}; \mathbf{x}, 1) \right| \xrightarrow{P} 0.$$

Thus combining the three terms and equation (15), we have the uniform convergence

$$\sup_{\boldsymbol{\theta} \in \Theta} \left| \hat{\mathcal{R}}(\boldsymbol{\theta}) - \tilde{\mathcal{R}}(\boldsymbol{\theta}) \right| \xrightarrow{P} 0.$$

Therefore, the set (14) satisfies

$$P(E_n) \rightarrow 1,$$

considering $\inf_{\boldsymbol{\theta} \in A_\epsilon} (\tilde{\mathcal{R}}(\boldsymbol{\theta}) - \tilde{\mathcal{R}}(\tilde{\boldsymbol{\theta}})) / 3$ is a fixed positive number. To show the parameter convergence, suppose for contradiction that on event E_n , we have $\hat{\boldsymbol{\theta}} \in A_\epsilon$. Then by the definition of E_n , we have

$$\begin{aligned} \hat{\mathcal{R}}(\hat{\boldsymbol{\theta}}) &\geq \tilde{\mathcal{R}}(\hat{\boldsymbol{\theta}}) - \frac{1}{3} \inf_{\boldsymbol{\theta} \in A_\epsilon} (\tilde{\mathcal{R}}(\boldsymbol{\theta}) - \tilde{\mathcal{R}}(\tilde{\boldsymbol{\theta}})) = \tilde{\mathcal{R}}(\hat{\boldsymbol{\theta}}) - \tilde{\mathcal{R}}(\tilde{\boldsymbol{\theta}}) + \tilde{\mathcal{R}}(\tilde{\boldsymbol{\theta}}) - \frac{1}{3} \inf_{\boldsymbol{\theta} \in A_\epsilon} (\tilde{\mathcal{R}}(\boldsymbol{\theta}) - \tilde{\mathcal{R}}(\tilde{\boldsymbol{\theta}})) \\ &\geq \tilde{\mathcal{R}}(\tilde{\boldsymbol{\theta}}) + \frac{2}{3} \inf_{\boldsymbol{\theta} \in A_\epsilon} (\tilde{\mathcal{R}}(\boldsymbol{\theta}) - \tilde{\mathcal{R}}(\tilde{\boldsymbol{\theta}})). \end{aligned}$$

Also by definition,

$$\hat{\mathcal{R}}(\tilde{\boldsymbol{\theta}}) \leq \tilde{\mathcal{R}}(\tilde{\boldsymbol{\theta}}) + \frac{1}{3} \inf_{\boldsymbol{\theta} \in A_\epsilon} (\tilde{\mathcal{R}}(\boldsymbol{\theta}) - \tilde{\mathcal{R}}(\tilde{\boldsymbol{\theta}})).$$

Then we conclude $\hat{\mathcal{R}}(\hat{\boldsymbol{\theta}}) > \hat{\mathcal{R}}(\tilde{\boldsymbol{\theta}})$, which contradicts the fact that $\hat{\boldsymbol{\theta}}$ is the minimizer of $\hat{\mathcal{R}}(\boldsymbol{\theta})$.

Therefore, under event E_n , we have $\hat{\boldsymbol{\theta}} \notin A_\epsilon$. That is $\|\hat{\boldsymbol{\theta}} - \tilde{\boldsymbol{\theta}}\| \leq \epsilon$ on E_n . Thus

$$\mathbb{P}(\|\hat{\boldsymbol{\theta}} - \tilde{\boldsymbol{\theta}}\| > \epsilon) \leq \mathbb{P}(E_n^c) \rightarrow 0.$$

That is the parameter convergence

$$\|\hat{\boldsymbol{\theta}} - \tilde{\boldsymbol{\theta}}\| \xrightarrow{P} 0.$$

Considering $\mathcal{R}(\boldsymbol{\theta})$ is continuous, for any $\eta > 0$, $\exists \delta > 0$ s.t. for $\|\boldsymbol{\theta} - \tilde{\boldsymbol{\theta}}\| \leq \delta$ we have $|\mathcal{R}(\boldsymbol{\theta}) - \mathcal{R}(\tilde{\boldsymbol{\theta}})| \leq \eta$. Thus

$$\mathbb{P}(|\mathcal{R}(\hat{\boldsymbol{\theta}}) - \mathcal{R}(\tilde{\boldsymbol{\theta}})| > \eta) \leq \mathbb{P}(\|\hat{\boldsymbol{\theta}} - \tilde{\boldsymbol{\theta}}\| > \delta) \rightarrow 0.$$

That is,

$$|\mathcal{R}(\hat{\boldsymbol{\theta}}) - \mathcal{R}(\tilde{\boldsymbol{\theta}})| = o_P(1). \tag{16}$$

Thus, combining equations (13) and (16), we have

$$\begin{aligned} \mathcal{R}(\hat{\boldsymbol{\theta}}) - \mathcal{R}(\boldsymbol{\theta}^*) &= \mathcal{R}(\hat{\boldsymbol{\theta}}) - \mathcal{R}(\tilde{\boldsymbol{\theta}}) + \mathcal{R}(\tilde{\boldsymbol{\theta}}) - \mathcal{R}(\boldsymbol{\theta}^*) \\ &\geq \frac{\mu}{2M^2} \left\| \left(\pi_0 - \frac{1}{2} \right) \nabla \phi(\boldsymbol{\theta}^*) + \tilde{\pi} \nabla \psi(\boldsymbol{\theta}^*) \right\|^2 + o_P(1). \end{aligned}$$

14.2 Proof of Theorem 2

We start by making a decomposition to the excess risk:

$$\mathcal{R}(\hat{\boldsymbol{\theta}}) - \mathcal{R}(\boldsymbol{\theta}^*) = (\mathcal{R}(\hat{\boldsymbol{\theta}}) - \mathcal{R}(\tilde{\boldsymbol{\theta}})) + (\mathcal{R}(\tilde{\boldsymbol{\theta}}) - \mathcal{R}(\boldsymbol{\theta}^*)). \quad (17)$$

We first give an upper bound for the population risk $\mathcal{R}(\tilde{\boldsymbol{\theta}}) - \mathcal{R}(\boldsymbol{\theta}^*)$. For function $F(\mathbf{x})$ that is differentiable and has minimizer \mathbf{x}^* , satisfying

$$F(\mathbf{x}^*) \geq F(\mathbf{x}) + \nabla F(\mathbf{x})^\top (\mathbf{x}^* - \mathbf{x}) + \frac{\mu}{2} \|\mathbf{x}^* - \mathbf{x}\|^2,$$

we have

$$\begin{aligned} F(\mathbf{x}) - F(\mathbf{x}^*) &\leq \nabla F(\mathbf{x})^\top (\mathbf{x} - \mathbf{x}^*) - \frac{\mu}{2} \|\mathbf{x} - \mathbf{x}^*\|^2 \\ &\leq \frac{1}{2\mu} \|\nabla F(\mathbf{x})\|^2 + \frac{\mu}{2} \|\mathbf{x} - \mathbf{x}^*\|^2 - \frac{\mu}{2} \|\mathbf{x} - \mathbf{x}^*\|^2 = \frac{1}{2\mu} \|\nabla F(\mathbf{x})\|^2, \end{aligned} \quad (18)$$

where the second inequality is from the fact that $0 \leq \|\frac{1}{\sqrt{\mu}} \nabla F(\mathbf{x}) - \sqrt{\mu}(\mathbf{x} - \mathbf{x}^*)\|^2$.

Applying equation (18) on the balanced risk \mathcal{R} gives

$$\mathcal{R}(\tilde{\boldsymbol{\theta}}) - \mathcal{R}(\boldsymbol{\theta}^*) \leq \frac{1}{2\mu} \|\nabla \mathcal{R}(\tilde{\boldsymbol{\theta}})\|^2. \quad (19)$$

For the synthetic risk, we can write it into the form

$$\tilde{\mathcal{R}}(\boldsymbol{\theta}) = \mathcal{R}(\boldsymbol{\theta}) + \left(\pi_0 - \frac{1}{2}\right) \phi(\boldsymbol{\theta}) + \tilde{\pi} \psi(\boldsymbol{\theta}),$$

Take derivative to both sides gives

$$\nabla \tilde{\mathcal{R}}(\boldsymbol{\theta}) = \nabla \mathcal{R}(\boldsymbol{\theta}) + \left(\pi_0 - \frac{1}{2}\right) \nabla \phi(\boldsymbol{\theta}) + \tilde{\pi} \nabla \psi(\boldsymbol{\theta}).$$

Considering $\tilde{\boldsymbol{\theta}}$ is the minimizer of $\tilde{\mathcal{R}}(\boldsymbol{\theta})$, plugging in and by first order optimality,

$$0 = \nabla \tilde{\mathcal{R}}(\tilde{\boldsymbol{\theta}}) = \nabla \mathcal{R}(\tilde{\boldsymbol{\theta}}) + \left(\pi_0 - \frac{1}{2}\right) \nabla \phi(\tilde{\boldsymbol{\theta}}) + \tilde{\pi} \nabla \psi(\tilde{\boldsymbol{\theta}}).$$

Take norms

$$\|\nabla \mathcal{R}(\tilde{\boldsymbol{\theta}})\| = \left\| \left(\pi_0 - \frac{1}{2}\right) \nabla \phi(\tilde{\boldsymbol{\theta}}) + \tilde{\pi} \nabla \psi(\tilde{\boldsymbol{\theta}}) \right\|. \quad (20)$$

Combining equation (19), we have the bound

$$\mathcal{R}(\tilde{\theta}) - \mathcal{R}(\theta^*) \leq \frac{1}{2\mu} \left\| \left(\pi_0 - \frac{1}{2} \right) \nabla \phi(\tilde{\theta}) + \tilde{\pi} \nabla \psi(\tilde{\theta}) \right\|. \quad (21)$$

Further by the quadratic growth assumption, it holds that

$$\|\tilde{\theta} - \theta^*\| \leq \sqrt{\frac{1}{2\mu L}} \left\| \left(\pi_0 - \frac{1}{2} \right) \nabla \phi(\tilde{\theta}) + \tilde{\pi} \nabla \psi(\tilde{\theta}) \right\| \quad (22)$$

With this upper bound, we then give a representation for $\tilde{\theta} - \theta^*$. Take derivative at $\tilde{\theta}$ for equation (2) gives

$$0 = \nabla \tilde{\mathcal{R}}(\tilde{\theta}) = \nabla \mathcal{R}(\tilde{\theta}) + \left(\pi_0 - \frac{1}{2} \right) \nabla \phi(\tilde{\theta}) + \tilde{\pi} \nabla \psi(\tilde{\theta}). \quad (23)$$

Standard Taylor expansion gives

$$0 = \nabla \tilde{\mathcal{R}}(\tilde{\theta}) = \nabla \tilde{\mathcal{R}}(\theta^*) + \nabla^2 \tilde{\mathcal{R}}(\theta^*) (\tilde{\theta} - \theta^*) + r_1, \quad (24)$$

where the remainder has the integral form

$$r_1 = \int_0^1 \left(\nabla^2 \tilde{\mathcal{R}}(\theta^* + t(\tilde{\theta} - \theta^*)) - \nabla^2 \tilde{\mathcal{R}}(\theta^*) \right)^\top (\tilde{\theta} - \theta^*) dt.$$

By Assumption (A4), we have the Lipschitzness

$$\left\| \nabla^2 \tilde{\mathcal{R}}(\theta^* + t(\tilde{\theta} - \theta^*)) - \nabla^2 \tilde{\mathcal{R}}(\theta^*) \right\| \leq L \|\tilde{\theta} - \theta^*\|.$$

Thus we have the remainder term satisfying

$$\|r_1\| = O(\|\tilde{\theta} - \theta^*\|).$$

Recall the expression in equation (4). Taking derivative gives

$$\nabla \tilde{\mathcal{R}}(\theta) = \nabla \mathcal{R}(\theta) + b(\theta).$$

Taking θ^* and by the first order optimality, we have

$$\nabla \tilde{\mathcal{R}}(\theta^*) = \nabla \mathcal{R}(\theta^*) + b(\theta^*) = b(\theta^*).$$

Also, taking second derivative to equation (4) and at θ^* , we have

$$\nabla^2 \tilde{\mathcal{R}}(\theta^*) = \nabla^2 \mathcal{R}(\theta^*) + \nabla b(\theta^*).$$

Plugging back in equation (24), we have

$$0 = b(\theta^*) + \left(\nabla^2 \mathcal{R}(\theta^*) + \nabla b(\theta^*) \right) (\tilde{\theta} - \theta^*) + r_1.$$

Solving the equation gives a representation

$$\begin{aligned} & \tilde{\theta} - \theta^* \\ &= - \left[\nabla^2 \mathcal{R}(\theta^*) + \left(\pi_0 - \frac{1}{2} \right) \nabla^2 \phi(\theta^*) + \tilde{\pi} \nabla^2 \psi(\theta^*) \right]^{-1} \left[\left(\pi_0 - \frac{1}{2} \right) \nabla \phi(\theta^*) + \tilde{\pi} \nabla \psi(\theta^*) \right] + \mathbf{r}, \end{aligned} \quad (25)$$

where $\|\mathbf{r}\| = O(\|\tilde{\theta} - \theta^*\|^2) = O\left(\left\| \left(\pi_0 - \frac{1}{2} \right) \nabla \phi(\tilde{\theta}) + \tilde{\pi} \nabla \psi(\tilde{\theta}) \right\|^2\right)$ because the smallest eigenvalue of $\nabla^2 \mathcal{R}(\theta^*) + \left(\pi_0 - \frac{1}{2} \right) \nabla^2 \phi(\theta^*) + \tilde{\pi} \nabla^2 \psi(\theta^*)$ is lower bounded by assumption $\nabla^2 \tilde{\mathcal{R}}(\theta) \succeq \lambda I$.

For the second term in equation (17), standard Taylor expansion gives

$$\mathcal{R}(\tilde{\theta}) - \mathcal{R}(\theta^*) = \nabla \mathcal{R}(\theta^*) (\tilde{\theta} - \theta^*) + \frac{1}{2} (\tilde{\theta} - \theta^*)^\top \nabla^2 \mathcal{R}(\theta^*) (\tilde{\theta} - \theta^*) + O(\|\tilde{\theta} - \theta^*\|^3) \quad (26)$$

Combining equation (26) and the representation in equation (25) gives a representation for the second term in equation (17)

$$\begin{aligned} \mathcal{R}(\tilde{\theta}) - \mathcal{R}(\theta^*) &= \frac{1}{2} \mathbf{b}(\theta^*)^\top \left(\nabla^2 \mathcal{R}(\theta^*) + \nabla \mathbf{b}(\theta^*) \right)^{-1} \nabla^2 \mathcal{R}(\theta^*) \left(\nabla^2 \mathcal{R}(\theta^*) + \nabla \mathbf{b}(\theta^*) \right)^{-1} \mathbf{b}(\theta^*) \\ &\quad + O_P \left(\left\| \left(\pi_0 - \frac{1}{2} \right) \nabla \phi(\tilde{\theta}) + \tilde{\pi} \nabla \psi(\tilde{\theta}) \right\|^3 \right) \end{aligned} \quad (27)$$

To give a representation for the first term in equation (17), we need a representation for $\hat{\theta} - \tilde{\theta}$. We first give an upper bound for $\|\hat{\theta} - \tilde{\theta}\|$. By first order optimality and Taylor expansion,

$$0 = \nabla \hat{\mathcal{R}}(\hat{\theta}) = \nabla \hat{\mathcal{R}}(\tilde{\theta}) + \nabla^2 \hat{\mathcal{R}}(\tilde{\theta}) (\hat{\theta} - \tilde{\theta}) + \mathbf{r}_4,$$

where the remainder term satisfies $\|\mathbf{r}_4\| = O(\|\hat{\boldsymbol{\theta}} - \tilde{\boldsymbol{\theta}}\|^2)$. By matrix concentration, we have the minimal eigenvalue of Hessian matrix $|\lambda_{\min}(\nabla^2 \hat{\mathcal{R}}(\boldsymbol{\theta})) - \lambda_{\min}(\nabla^2 \tilde{\mathcal{R}}(\boldsymbol{\theta}))| \rightarrow 0$ in probability and $\nabla^2 \tilde{\mathcal{R}}(\boldsymbol{\theta}) \succeq \lambda I$ by assumption. Thus, for large enough n_0 and n_1 , we have $\lambda_{\min}(\nabla^2 \hat{\mathcal{R}}(\tilde{\boldsymbol{\theta}})) > \frac{\lambda}{c} > 0$ for some constant $c > 0$ in probability. Therefore $\nabla^2 \hat{\mathcal{R}}(\tilde{\boldsymbol{\theta}})$ is invertible and the norm satisfies $\left\| [\nabla^2 \hat{\mathcal{R}}(\tilde{\boldsymbol{\theta}})]^{-1} \right\| \leq \frac{c}{\lambda}$. That is,

$$\hat{\boldsymbol{\theta}} - \tilde{\boldsymbol{\theta}} = - [\nabla^2 \hat{\mathcal{R}}(\tilde{\boldsymbol{\theta}})]^{-1} \nabla \hat{\mathcal{R}}(\tilde{\boldsymbol{\theta}}) + \mathbf{r}_5, \quad (28)$$

where $\|\mathbf{r}_5\| = O(\|\hat{\boldsymbol{\theta}} - \tilde{\boldsymbol{\theta}}\|^2)$.

By optimality, $\mathbb{E} \nabla \hat{\mathcal{R}}(\tilde{\boldsymbol{\theta}}) = \nabla \tilde{\mathcal{R}}(\tilde{\boldsymbol{\theta}}) = 0$. Therefore,

$$\begin{aligned} \|\nabla \hat{\mathcal{R}}(\tilde{\boldsymbol{\theta}})\| &= \left\| \frac{\pi_0}{n_0} \sum_{i=1}^{n_0} \nabla \ell(\boldsymbol{\theta}; \mathbf{x}_i, 0) + \frac{\pi_1}{n_1} \sum_{i=1}^{n_1} \nabla \ell(\boldsymbol{\theta}; \mathbf{x}_i, 1) + \frac{\tilde{\pi}}{\tilde{n}} \sum_{i=1}^{\tilde{n}} \nabla \ell(\boldsymbol{\theta}; \tilde{\mathbf{x}}_i, 1) - \mathbb{E} \nabla \hat{\mathcal{R}}(\tilde{\boldsymbol{\theta}}) \right\| \\ &\leq \pi_0 \left\| \frac{1}{n_0} \sum_{i=1}^{n_0} \nabla \ell(\boldsymbol{\theta}; \mathbf{x}_i, 0) - \mathbb{E}_{\mathcal{P}_0} [\nabla \ell(\boldsymbol{\theta}; \mathbf{x}, 0)] \right\| + \pi_1 \left\| \frac{1}{n_1} \sum_{i=1}^{n_1} \nabla \ell(\boldsymbol{\theta}; \mathbf{x}_i, 1) - \mathbb{E}_{\mathcal{P}_1} [\nabla \ell(\boldsymbol{\theta}; \mathbf{x}, 1)] \right\| \\ &\quad + \tilde{\pi} \left\| \frac{1}{\tilde{n}} \sum_{i=1}^{\tilde{n}} \nabla \ell(\boldsymbol{\theta}; \tilde{\mathbf{x}}_i, 1) - \mathbb{E}_{\mathcal{P}_{\text{syn}}} [\nabla \ell(\boldsymbol{\theta}; \tilde{\mathbf{x}}, 1)] \right\| \end{aligned} \quad (29)$$

By union bound and Hoeffding's inequality, for fixed $\boldsymbol{\theta}$,

$$\begin{aligned} &\mathbb{P} \left(\left\| \frac{1}{n_0} \sum_{i=1}^{n_0} \nabla \ell(\boldsymbol{\theta}; \mathbf{x}_i, 0) - \mathbb{E}_{\mathcal{P}_0} \nabla \ell(\boldsymbol{\theta}; \mathbf{x}, 0) \right\| > t \right) \\ &\leq \mathbb{P} \left(\exists i \in [d], \text{ s.t. } \left| \left[\frac{1}{n_0} \sum_{i=1}^{n_0} \nabla \ell(\boldsymbol{\theta}; \mathbf{x}_i, 0) \right]_i - [\mathbb{E}_{\mathcal{P}_0} \nabla \ell(\boldsymbol{\theta}; \mathbf{x}, 0)]_i \right| > \frac{t}{\sqrt{d}} \right) \\ &\leq \sum_{i=1}^d \mathbb{P} \left(\left| \left[\frac{1}{n_0} \sum_{i=1}^{n_0} \nabla \ell(\boldsymbol{\theta}; \mathbf{x}_i, 0) \right]_i - [\mathbb{E}_{\mathcal{P}_0} \nabla \ell(\boldsymbol{\theta}; \mathbf{x}, 0)]_i \right| > \frac{t}{\sqrt{d}} \right) \leq 2d \exp \left\{ -\frac{2t^2 n_0}{dB} \right\}, \end{aligned} \quad (30)$$

where $B > 0$ is a constant from bounded support assumption. Thus

$$\begin{aligned} &\mathbb{P} \left(\pi_0 \left\| \frac{1}{n_0} \sum_{i=1}^{n_0} \nabla \ell(\boldsymbol{\theta}; \mathbf{x}_i, 0) - \mathbb{E}_{\mathcal{P}_0} \nabla \ell(\boldsymbol{\theta}; \mathbf{x}, 0) \right\| > t \right) \\ &= \mathbb{P} \left(\left\| \frac{1}{n_0} \sum_{i=1}^{n_0} \nabla \ell(\boldsymbol{\theta}; \mathbf{x}_i, 0) - \mathbb{E}_{\mathcal{P}_0} \nabla \ell(\boldsymbol{\theta}; \mathbf{x}, 0) \right\| > \frac{t}{\pi_0} \right) \leq 2d \exp \left\{ -\frac{2t^2 (n_0 + n_1 + \tilde{n})^2}{dB n_0} \right\}. \end{aligned} \quad (31)$$

Therefore, with probability at least $1 - \delta$,

$$\pi_0 \left\| \frac{1}{n_0} \sum_{i=1}^{n_0} \nabla \ell(\boldsymbol{\theta}; \mathbf{x}_i, 0) - \mathbb{E}_{\mathcal{P}_0} \nabla \ell(\boldsymbol{\theta}; \mathbf{x}, 0) \right\| \leq \sqrt{\frac{Bd \log(2d/\delta)}{2}} \frac{\sqrt{n_0}}{n_0 + n_1 + \tilde{n}}.$$

That is, we have

$$\pi_0 \left\| \frac{1}{n_0} \sum_{i=1}^{n_0} \nabla \ell(\boldsymbol{\theta}; \mathbf{x}_i, 0) - \mathbb{E}_{\mathcal{P}_0} \nabla \ell(\boldsymbol{\theta}; \mathbf{x}, 0) \right\| = O_P \left(\frac{\sqrt{n_0}}{n_0 + n_1 + \tilde{n}} \right). \quad (32)$$

By essentially the same procedure with equation (30), one can have

$$\mathbb{P} \left(\pi_1 \left\| \frac{1}{n_1} \sum_{i=1}^{n_1} \nabla \ell(\boldsymbol{\theta}; \mathbf{x}_i, 1) - \mathbb{E}_{\mathcal{P}_1} \nabla \ell(\boldsymbol{\theta}; \mathbf{x}, 1) \right\| > t \right) \leq 2d \exp \left\{ -\frac{2t^2(n_0 + n_1 + \tilde{n})^2}{Bdn_1} \right\},$$

$$\mathbb{P} \left(\tilde{\pi} \left\| \frac{1}{\tilde{n}} \sum_{i=1}^{\tilde{n}} \nabla \ell(\boldsymbol{\theta}; \tilde{\mathbf{x}}_i, 1) - \mathbb{E}_{\mathcal{P}_{\text{syn}}} \nabla \ell(\boldsymbol{\theta}; \tilde{\mathbf{x}}, 1) \right\| > t \right) \leq 2d \exp \left\{ -\frac{2t^2(n_0 + n_1 + \tilde{n})^2}{Bd\tilde{n}} \right\},$$

that is

$$\pi_1 \left\| \frac{1}{n_1} \sum_{i=1}^{n_1} \nabla \ell(\boldsymbol{\theta}; \mathbf{x}_i, 1) - \mathbb{E}_{\mathcal{P}_1} \nabla \ell(\boldsymbol{\theta}; \mathbf{x}, 1) \right\| = O_P \left(\frac{\sqrt{n_1}}{n_0 + n_1 + \tilde{n}} \right). \quad (33)$$

$$\tilde{\pi} \left\| \frac{1}{\tilde{n}} \sum_{i=1}^{\tilde{n}} \nabla \ell(\boldsymbol{\theta}; \tilde{\mathbf{x}}_i, 1) - \mathbb{E}_{\mathcal{P}_{\text{syn}}} \nabla \ell(\boldsymbol{\theta}; \tilde{\mathbf{x}}, 1) \right\| = O_P \left(\frac{\sqrt{\tilde{n}}}{n_0 + n_1 + \tilde{n}} \right). \quad (34)$$

Combining equation (30), (32), (33) and (34), we have

$$\|\nabla \hat{\mathcal{R}}(\tilde{\boldsymbol{\theta}})\| = O_P \left(\frac{1}{\sqrt{n_0 + n_1 + \tilde{n}}} \right)$$

Also equation (28) gives

$$\|\hat{\boldsymbol{\theta}} - \tilde{\boldsymbol{\theta}}\| \leq \left\| [\nabla^2 \hat{\mathcal{R}}(\tilde{\boldsymbol{\theta}})]^{-1} \right\| \|\nabla \hat{\mathcal{R}}(\tilde{\boldsymbol{\theta}})\| + c \|\hat{\boldsymbol{\theta}} - \tilde{\boldsymbol{\theta}}\|^2 \quad (35)$$

Therefore, solving equation (35), we have

$$\|\hat{\boldsymbol{\theta}} - \tilde{\boldsymbol{\theta}}\| = O_P \left(\frac{1}{\sqrt{n_0 + n_1 + \tilde{n}}} \right). \quad (36)$$

To give a representation for $\hat{\boldsymbol{\theta}} - \tilde{\boldsymbol{\theta}}$, we need to study the expansion of probability density functions for sample average. Let $\mathbf{x}_i, i = 1, \dots, n$ be i.i.d. d -dimensional random vectors with finite mean $\boldsymbol{\mu}$, positive definite covariance matrix Σ and bounded support. Define

$$W_n = \sqrt{n} \Sigma^{-\frac{1}{2}} (\bar{\mathbf{x}}_n - \boldsymbol{\mu}), \quad \bar{\mathbf{x}}_n = \frac{1}{n} \sum_{i=1}^n \mathbf{x}_i. \quad (37)$$

Denote the probability density function of W_n as $f_n(\mathbf{x})$ for $\mathbf{x} \in \mathbb{R}^d$, and denote the density of d -dimensional standard Gaussian random vector $\mathcal{N}(0, I_d)$ as $\phi_d(\mathbf{x})$. By standard multivariate Berry-Esseen local limit theorem (for example [Bobkov and Götze \(2024\)](#)), we have the uniform bound on the density

$$\sup_{\mathbf{x}} |f_n(\mathbf{x}) - \phi_d(\mathbf{x})| \lesssim \frac{1}{\sqrt{n}} \quad (38)$$

For notational simplicity, we define $b_n := \frac{c}{\sqrt{n}}$ with a constant $c > 0$ such that $\sup_{\mathbf{x}} |f_n(\mathbf{x}) - \phi_d(\mathbf{x})| \leq \frac{c}{\sqrt{n}}$, and two sets

$$A_n = \left\{ \mathbf{x} \in \mathbb{R}^d : \phi_d(\mathbf{x}) \geq 2b_n \right\}, \quad B_n := A_n^c = \left\{ \mathbf{x} \in \mathbb{R}^d : \phi_d(\mathbf{x}) < 2b_n \right\}.$$

Also, we define

$$h_n := f_n - \phi_d, \quad h_n^+ = \max(f_n - \phi_d, 0), \quad h_n^- = \max(\phi_d - f_n, 0).$$

Therefore, simply we have

$$\int f_n = \int \phi_d = 1 \Rightarrow \int h_n = 0.$$

Also, we have

$$h_n = h_n^+ - h_n^-, \quad \text{and} \quad |h_n| = h_n^+ + h_n^-.$$

Combining above we also have

$$\int h_n^+ - h_n^- = 0 \Rightarrow \int h_n^+ = \int h_n^-.$$

Therefore, we have the total variation satisfying

$$TV(f_n, \phi_d) = \frac{1}{2} \int |h_n| = \frac{1}{2} \int h_n^+ + \frac{1}{2} \int h_n^- = \int h_n^- = \int_{A_n} h_n^- + \int_{B_n} h_n^-. \quad (39)$$

Under the set A_n , by the Berry-Esseen bound (38), which is uniform in x , we have $h_n^- \leq b_n$.

Under the set B_n , considering two distributions are positive, we have $h_n^- \leq \phi_d$. That is

$$h_n^-(x) \leq \begin{cases} b_n & \mathbf{x} \in A_n \\ \phi_d & \mathbf{x} \in B_n \end{cases} \quad (40)$$

Combining equations (39) and (40), the total variation can be upper bounded by

$$TV(f_n, \phi_d) \leq b_n |A_n| + \int_{B_n} \phi_d. \quad (41)$$

Therefore, we can study the two terms in equation (41) separately. For the first term, we only need to derive the volume $|A_n|$. By the definition of A_n , we solve the equation

$$\phi_d(\mathbf{x}) = (2\pi)^{-\frac{d}{2}} \exp\left\{-\frac{\|\mathbf{x}\|^2}{2}\right\} \geq 2b_n = \frac{2c}{\sqrt{n}}.$$

The solution of the equation satisfies $\|\mathbf{x}\|^2 \leq \log n - \log(2\pi)^{d/2}c$, which is positive for large enough n . Therefore, the set A_n satisfies that

$$|A_n| = O\left((\log n)^{\frac{d}{2}}\right) \Rightarrow b_n |A_n| = O\left(\frac{(\log n)^{\frac{d}{2}}}{\sqrt{n}}\right) \rightarrow 0. \quad (42)$$

For the second term in equation (41), we have

$$\int_{B_n} \phi_d(\mathbf{x}) d\mathbf{x} = \int_{\|\mathbf{x}\|^2 \geq \log n - \log(2\pi)^{d/2}c} \phi_d(\mathbf{x}) d\mathbf{x}.$$

By standard tail bound for multivariate Gaussian (e.g. $\int_{\|\mathbf{x}\| > r} \phi_d(\mathbf{x}) d\mathbf{x} \leq c_d r^{d-2} e^{-\frac{r^2}{2}}$ for large enough r), we have

$$\int_{B_n} \phi_d(\mathbf{x}) d\mathbf{x} \leq c \frac{(\log n)^{\frac{d-2}{2}}}{\sqrt{n}} \rightarrow 0. \quad (43)$$

Combining equations (41), (42) and (43) gives the convergence of total variation distance

$$TV(f_n, \phi_d) \leq c \frac{(\log n)^{\frac{d}{2}}}{\sqrt{n}} + c \frac{(\log n)^{\frac{d-2}{2}}}{\sqrt{n}} \rightarrow 0.$$

Therefore, by maximal coupling principle, there exists a coupling between W_n and Z such that

$$\mathbb{P}(W_n \neq Z) = TV(f_n, \phi_d).$$

That is

$$\mathbb{P}\left(\|W_n - Z\| > \frac{c}{n}\right) \leq TV(f_n, \phi_d) \rightarrow 0.$$

That is, we can write

$$W_n = Z + \mathbf{r}, \quad \|\mathbf{r}\| = O_P\left(\frac{1}{n}\right),$$

for some Z having marginal distribution ϕ_d . Recall the definition of W_n , we solve for the sample average as

$$\bar{\mathbf{x}}_n = \boldsymbol{\mu} + \frac{1}{\sqrt{n}}\Sigma^{\frac{1}{2}}Z + \mathbf{r}, \quad \|\mathbf{r}\| = O_P\left(\frac{1}{n}\right). \quad (44)$$

Now we are ready to give a representation for $\hat{\boldsymbol{\theta}} - \tilde{\boldsymbol{\theta}}$. By optimality and Taylor expansion

$$0 = \nabla \hat{\mathcal{R}}(\hat{\boldsymbol{\theta}}) = \nabla \hat{\mathcal{R}}(\tilde{\boldsymbol{\theta}}) + \nabla^2 \hat{\mathcal{R}}(\tilde{\boldsymbol{\theta}})(\hat{\boldsymbol{\theta}} - \tilde{\boldsymbol{\theta}}) + O(\|\hat{\boldsymbol{\theta}} - \tilde{\boldsymbol{\theta}}\|^2)$$

By the convergence of sample mean to expectation and applying equation (44),

$$\begin{aligned} 0 &= \nabla \tilde{\mathcal{R}}(\tilde{\boldsymbol{\theta}}) + \frac{1}{n_0 + n_1 + \tilde{n}} \left[\sqrt{n_0}\Sigma_0^{\frac{1}{2}}Z_1 + \sqrt{n_1}\Sigma_1^{\frac{1}{2}}Z_2 + \sqrt{\tilde{n}}\tilde{\Sigma}^{\frac{1}{2}}Z_3 \right] + O_P\left(\frac{1}{n_0 + n_1 + \tilde{n}}\right) \\ &+ \nabla^2 \tilde{\mathcal{R}}(\tilde{\boldsymbol{\theta}})(\hat{\boldsymbol{\theta}} - \tilde{\boldsymbol{\theta}}) + O_P\left(\left(\frac{1}{\sqrt{n_0 + n_1 + \tilde{n}}}\right) \|\hat{\boldsymbol{\theta}} - \tilde{\boldsymbol{\theta}}\|\right) + O(\|\hat{\boldsymbol{\theta}} - \tilde{\boldsymbol{\theta}}\|^2) \\ &= \frac{1}{n_0 + n_1 + \tilde{n}} \left[\sqrt{n_0}\Sigma_0^{\frac{1}{2}}Z_1 + \sqrt{n_1}\Sigma_1^{\frac{1}{2}}Z_2 + \sqrt{\tilde{n}}\tilde{\Sigma}^{\frac{1}{2}}Z_3 \right] + \nabla^2 \tilde{\mathcal{R}}(\tilde{\boldsymbol{\theta}})(\hat{\boldsymbol{\theta}} - \tilde{\boldsymbol{\theta}}) + O_P\left(\frac{1}{n_0 + n_1 + \tilde{n}}\right), \end{aligned}$$

where Z_1 , Z_2 and Z_3 are independent d -dimensional standard Gaussian random vectors.

Considering these are three independent Gaussians, we can combine them into one Gaussian, that is

$$0 = \frac{1}{n_0 + n_1 + \tilde{n}} \left(n_0\Sigma_0 + n_1\Sigma_1 + \tilde{n}\tilde{\Sigma} \right)^{\frac{1}{2}} Z + \nabla^2 \tilde{\mathcal{R}}(\tilde{\boldsymbol{\theta}})(\hat{\boldsymbol{\theta}} - \tilde{\boldsymbol{\theta}}) + O_P\left(\frac{1}{n_0 + n_1 + \tilde{n}}\right), \quad (45)$$

where the Gaussian $Z \sim \mathcal{N}(0, I_d)$. Solving for $\hat{\boldsymbol{\theta}} - \tilde{\boldsymbol{\theta}}$ gives the representation

$$\hat{\boldsymbol{\theta}} - \tilde{\boldsymbol{\theta}} = -\frac{1}{n_0 + n_1 + \tilde{n}} \left[\nabla^2 \tilde{\mathcal{R}}(\tilde{\boldsymbol{\theta}}) \right]^{-1} \left(n_0\Sigma_0 + n_1\Sigma_1 + \tilde{n}\tilde{\Sigma} \right)^{\frac{1}{2}} Z + O_P\left(\frac{1}{n_0 + n_1 + \tilde{n}}\right). \quad (46)$$

Taylor expansion, combining equation (20) and (46) gives a representation for the first term

in equation (17),

$$\begin{aligned}
\mathcal{R}(\hat{\boldsymbol{\theta}}) - \mathcal{R}(\tilde{\boldsymbol{\theta}}) &= \nabla \mathcal{R}(\tilde{\boldsymbol{\theta}})^\top (\hat{\boldsymbol{\theta}} - \tilde{\boldsymbol{\theta}}) + \frac{1}{2} (\hat{\boldsymbol{\theta}} - \tilde{\boldsymbol{\theta}})^\top \nabla^2 \mathcal{R}(\tilde{\boldsymbol{\theta}}) (\hat{\boldsymbol{\theta}} - \tilde{\boldsymbol{\theta}}) + O(\|\hat{\boldsymbol{\theta}} - \tilde{\boldsymbol{\theta}}\|^3) \\
&= \frac{1}{\sqrt{n_0 + n_1 + \tilde{n}}} \nabla \mathcal{R}(\tilde{\boldsymbol{\theta}})^\top [\nabla^2 \tilde{\mathcal{R}}(\tilde{\boldsymbol{\theta}})]^{-1} \Sigma^{\frac{1}{2}} Z \\
&\quad + \frac{1}{2(n_0 + n_1 + \tilde{n})} Z^\top \Sigma^{\frac{1}{2}} [\nabla^2 \tilde{\mathcal{R}}(\tilde{\boldsymbol{\theta}})]^{-1} \nabla^2 \mathcal{R}(\tilde{\boldsymbol{\theta}}) [\nabla^2 \tilde{\mathcal{R}}(\tilde{\boldsymbol{\theta}})]^{-1} \Sigma^{\frac{1}{2}} Z \\
&\quad + O_P \left((n_0 + n_1 + \tilde{n})^{-\frac{3}{2}} + \frac{\|\mathbf{b}(\tilde{\boldsymbol{\theta}})\|}{n_0 + n_1 + \tilde{n}} \right), \tag{47}
\end{aligned}$$

where

$$\Sigma = \frac{n_0 \Sigma_0 + n_1 \Sigma_1 + \tilde{n} \tilde{\Sigma}}{n_0 + n_1 + \tilde{n}}.$$

Combining equations (17), (27) and (47) gives

$$\begin{aligned}
\mathcal{R}(\hat{\boldsymbol{\theta}}) - \mathcal{R}(\boldsymbol{\theta}^*) &= \frac{1}{2} \mathbf{b}(\boldsymbol{\theta}^*)^\top (\nabla^2 \mathcal{R}(\boldsymbol{\theta}^*) + \nabla \mathbf{b}(\boldsymbol{\theta}^*))^{-1} \nabla^2 \mathcal{R}(\boldsymbol{\theta}^*) (\nabla^2 \mathcal{R}(\boldsymbol{\theta}^*) + \nabla \mathbf{b}(\boldsymbol{\theta}^*))^{-1} \mathbf{b}(\boldsymbol{\theta}^*) \\
&\quad + \frac{1}{n_0 + n_1 + \tilde{n}} \nabla \mathcal{R}(\tilde{\boldsymbol{\theta}})^\top [\nabla^2 \tilde{\mathcal{R}}(\tilde{\boldsymbol{\theta}})]^{-1} (n_0 \Sigma_0(\tilde{\boldsymbol{\theta}}) + n_1 \Sigma_1(\tilde{\boldsymbol{\theta}}) + \tilde{n} \tilde{\Sigma}(\tilde{\boldsymbol{\theta}}))^{\frac{1}{2}} Z \\
&\quad + \frac{1}{2(n_0 + n_1 + \tilde{n})^2} Z^\top \Sigma(\tilde{\boldsymbol{\theta}})^{\frac{1}{2}} [\nabla^2 \tilde{\mathcal{R}}(\tilde{\boldsymbol{\theta}})]^{-1} \nabla^2 \mathcal{R}(\tilde{\boldsymbol{\theta}}) [\nabla^2 \tilde{\mathcal{R}}(\tilde{\boldsymbol{\theta}})]^{-1} \Sigma(\tilde{\boldsymbol{\theta}})^{\frac{1}{2}} Z \\
&\quad + O_P \left(\|\mathbf{b}(\tilde{\boldsymbol{\theta}})\| + (n_0 + n_1 + \tilde{n})^{-\frac{3}{2}} + \frac{\|\mathbf{b}(\tilde{\boldsymbol{\theta}})\|}{n_0 + n_1 + \tilde{n}} \right), \tag{48}
\end{aligned}$$

Next, we need to get rid of $\tilde{\boldsymbol{\theta}}$ in the final representation. For $\nabla \mathcal{R}(\tilde{\boldsymbol{\theta}})$, by Taylor expansion,

$$\nabla \mathcal{R}(\tilde{\boldsymbol{\theta}}) = \nabla \mathcal{R}(\boldsymbol{\theta}^*) + \nabla^2 \mathcal{R}(\boldsymbol{\theta}^*) (\tilde{\boldsymbol{\theta}} - \boldsymbol{\theta}^*) + \mathbf{r}_6 = \nabla^2 \mathcal{R}(\boldsymbol{\theta}^*) (\tilde{\boldsymbol{\theta}} - \boldsymbol{\theta}^*) + \mathbf{r}_6,$$

where $\|\mathbf{r}_6\| = O(\|\tilde{\boldsymbol{\theta}} - \boldsymbol{\theta}^*\|^2)$. Then combining equations (22) and (25) gives a representation

$$\nabla \mathcal{R}(\tilde{\boldsymbol{\theta}}) = -\nabla^2 \mathcal{R}(\boldsymbol{\theta}^*) [\nabla^2 \mathcal{R}(\boldsymbol{\theta}^*) + \nabla \mathbf{b}(\boldsymbol{\theta}^*)]^{-1} \left[\left(\pi_0 - \frac{1}{2} \right) \nabla \phi(\boldsymbol{\theta}^*) + \tilde{\pi} \nabla \psi(\boldsymbol{\theta}^*) \right] + \mathbf{r}, \tag{49}$$

where $\|\mathbf{r}\| = O(\|\mathbf{b}(\tilde{\boldsymbol{\theta}})\|^2)$.

For the term $[\nabla^2 \tilde{\mathcal{R}}(\tilde{\boldsymbol{\theta}})]^{-1}$, the inverse satisfies,

$$[\nabla^2 \tilde{\mathcal{R}}(\tilde{\boldsymbol{\theta}})]^{-1} - [\nabla^2 \tilde{\mathcal{R}}(\boldsymbol{\theta}^*)]^{-1} = [\nabla^2 \tilde{\mathcal{R}}(\boldsymbol{\theta}^*)]^{-1} [\nabla^2 \tilde{\mathcal{R}}(\boldsymbol{\theta}^*) - \nabla^2 \tilde{\mathcal{R}}(\tilde{\boldsymbol{\theta}})] [\nabla^2 \tilde{\mathcal{R}}(\tilde{\boldsymbol{\theta}})]^{-1},$$

Thus, taking norms,

$$\begin{aligned} \left\| [\nabla^2 \tilde{\mathcal{R}}(\tilde{\boldsymbol{\theta}})]^{-1} - [\nabla^2 \tilde{\mathcal{R}}(\boldsymbol{\theta}^*)]^{-1} \right\| &= \left\| [\nabla^2 \tilde{\mathcal{R}}(\boldsymbol{\theta}^*)]^{-1} \right\| \left\| \nabla^2 \tilde{\mathcal{R}}(\boldsymbol{\theta}^*) - \nabla^2 \tilde{\mathcal{R}}(\tilde{\boldsymbol{\theta}}) \right\| \left\| [\nabla^2 \tilde{\mathcal{R}}(\tilde{\boldsymbol{\theta}})]^{-1} \right\| \\ &\leq \frac{L}{\lambda^2} \|\tilde{\boldsymbol{\theta}} - \boldsymbol{\theta}^*\|. \end{aligned}$$

Therefore, we can write

$$[\nabla^2 \tilde{\mathcal{R}}(\tilde{\boldsymbol{\theta}})]^{-1} = [\nabla^2 \tilde{\mathcal{R}}(\boldsymbol{\theta}^*)]^{-1} + \mathbf{r} = [\nabla^2 \mathcal{R}(\boldsymbol{\theta}^*) + \nabla \mathbf{b}(\boldsymbol{\theta}^*)]^{-1} + \mathbf{r}, \quad (50)$$

where $\|\mathbf{r}\| \leq \frac{L}{\lambda^2} \|\tilde{\boldsymbol{\theta}} - \boldsymbol{\theta}^*\| = O(\|\mathbf{b}(\tilde{\boldsymbol{\theta}})\|)$.

For the term $(n_0 \Sigma_0(\tilde{\boldsymbol{\theta}}) + n_1 \Sigma_1(\tilde{\boldsymbol{\theta}}) + \tilde{n} \tilde{\Sigma}(\tilde{\boldsymbol{\theta}}))^{\frac{1}{2}}$, denote $\Sigma(\boldsymbol{\theta}) = n_0 \Sigma_0(\boldsymbol{\theta}) + n_1 \Sigma_1(\boldsymbol{\theta}) + \tilde{n} \tilde{\Sigma}(\boldsymbol{\theta})$ for brevity. By assumption, $\Sigma(\boldsymbol{\theta}) \succ \lambda I$ and is Lipschitz. By simple algebra, we have the Sylvester type equation

$$\Sigma(\tilde{\boldsymbol{\theta}})^{\frac{1}{2}} (\Sigma(\tilde{\boldsymbol{\theta}})^{\frac{1}{2}} - \Sigma(\boldsymbol{\theta}^*)^{\frac{1}{2}}) + (\Sigma(\tilde{\boldsymbol{\theta}})^{\frac{1}{2}} - \Sigma(\boldsymbol{\theta}^*)^{\frac{1}{2}}) \Sigma(\boldsymbol{\theta}^*)^{\frac{1}{2}} = \Sigma(\tilde{\boldsymbol{\theta}}) - \Sigma(\boldsymbol{\theta}^*).$$

We need to solve this equation to give a representation for $\Sigma(\tilde{\boldsymbol{\theta}})^{\frac{1}{2}}$. Define

$$F(t) := e^{-t\Sigma(\tilde{\boldsymbol{\theta}})^{1/2}} (\Sigma(\tilde{\boldsymbol{\theta}})^{\frac{1}{2}} - \Sigma(\boldsymbol{\theta}^*)^{\frac{1}{2}}) e^{-t\Sigma(\boldsymbol{\theta}^*)^{1/2}}.$$

Take derivative to t ,

$$\begin{aligned} \frac{d}{dt} F(t) &= e^{-t\Sigma(\tilde{\boldsymbol{\theta}})^{1/2}} \left[\Sigma(\tilde{\boldsymbol{\theta}})^{\frac{1}{2}} (\Sigma(\tilde{\boldsymbol{\theta}})^{\frac{1}{2}} - \Sigma(\boldsymbol{\theta}^*)^{\frac{1}{2}}) - (\Sigma(\tilde{\boldsymbol{\theta}})^{\frac{1}{2}} - \Sigma(\boldsymbol{\theta}^*)^{\frac{1}{2}}) \Sigma(\boldsymbol{\theta}^*)^{\frac{1}{2}} \right] e^{-t\Sigma(\boldsymbol{\theta}^*)^{1/2}} \\ &= e^{-t\Sigma(\tilde{\boldsymbol{\theta}})^{1/2}} \left[\Sigma(\tilde{\boldsymbol{\theta}}) - \Sigma(\boldsymbol{\theta}^*) \right] e^{-t\Sigma(\boldsymbol{\theta}^*)^{1/2}}. \end{aligned}$$

Then take integral on $[0, T]$, we have

$$F(T) - F(0) = - \int_0^T e^{-t\Sigma(\tilde{\boldsymbol{\theta}})^{1/2}} \left[\Sigma(\tilde{\boldsymbol{\theta}}) - \Sigma(\boldsymbol{\theta}^*) \right] e^{-t\Sigma(\boldsymbol{\theta}^*)^{1/2}} dt.$$

By definition of $F(t)$, we have

$$\|F(t)\| \leq \left\| e^{-t\Sigma(\tilde{\boldsymbol{\theta}})^{1/2}} \right\| \left\| \Sigma(\tilde{\boldsymbol{\theta}})^{\frac{1}{2}} - \Sigma(\boldsymbol{\theta}^*)^{\frac{1}{2}} \right\| \left\| e^{-t\Sigma(\boldsymbol{\theta}^*)^{1/2}} \right\| \leq \left\| e^{-t\sqrt{\lambda}} \right\|^2 \left\| \Sigma(\tilde{\boldsymbol{\theta}})^{\frac{1}{2}} - \Sigma(\boldsymbol{\theta}^*)^{\frac{1}{2}} \right\| \rightarrow 0,$$

when $t \rightarrow \infty$. Also,

$$F(0) = \Sigma(\tilde{\boldsymbol{\theta}})^{\frac{1}{2}} - \Sigma(\boldsymbol{\theta}^*)^{\frac{1}{2}}.$$

Therefore, taking $T \rightarrow \infty$ in the integral gives

$$\Sigma(\tilde{\boldsymbol{\theta}})^{\frac{1}{2}} - \Sigma(\boldsymbol{\theta}^*)^{\frac{1}{2}} = - \int_0^\infty e^{-t\Sigma(\tilde{\boldsymbol{\theta}})^{1/2}} \left[\Sigma(\tilde{\boldsymbol{\theta}}) - \Sigma(\boldsymbol{\theta}^*) \right] e^{-t\Sigma(\boldsymbol{\theta}^*)^{1/2}} dt.$$

That is, we have the norm,

$$\begin{aligned} \left\| \Sigma(\tilde{\boldsymbol{\theta}})^{\frac{1}{2}} - \Sigma(\boldsymbol{\theta}^*)^{\frac{1}{2}} \right\| &= \int_0^\infty \left\| e^{-t\Sigma(\tilde{\boldsymbol{\theta}})^{1/2}} \right\| \left\| \Sigma(\tilde{\boldsymbol{\theta}}) - \Sigma(\boldsymbol{\theta}^*) \right\| \left\| e^{-t\Sigma(\boldsymbol{\theta}^*)^{1/2}} \right\| dt \\ &\leq \int_0^\infty e^{-2t\sqrt{\lambda}} dt \left\| \Sigma(\tilde{\boldsymbol{\theta}}) - \Sigma(\boldsymbol{\theta}^*) \right\| \leq \frac{1}{2\sqrt{\lambda}} \left\| \Sigma(\tilde{\boldsymbol{\theta}}) - \Sigma(\boldsymbol{\theta}^*) \right\| \\ &\leq \frac{L}{2\sqrt{\lambda}} \left\| \tilde{\boldsymbol{\theta}} - \boldsymbol{\theta}^* \right\| = O\left(\left\| \mathbf{b}(\tilde{\boldsymbol{\theta}}) \right\|\right). \end{aligned}$$

That is, we can write

$$\Sigma(\tilde{\boldsymbol{\theta}})^{\frac{1}{2}} = \Sigma(\boldsymbol{\theta}^*)^{\frac{1}{2}} + \mathbf{r}_7, \quad (51)$$

where $\|\mathbf{r}_7\| = O\left(\left\| \mathbf{b}(\tilde{\boldsymbol{\theta}}) \right\|\right)$.

Then, combine the representation in equations (49), (50) and (51), we have a representation without $\tilde{\boldsymbol{\theta}}$ for the second term (denoted as T_2 for brevity) in equation (48):

$$T_2 = - \frac{\mathbf{b}(\boldsymbol{\theta}^*) \left[\nabla^2 \mathcal{R}(\boldsymbol{\theta}^*) + \nabla \mathbf{b}(\boldsymbol{\theta}^*) \right]^{-1} \nabla^2 \mathcal{R}(\boldsymbol{\theta}^*) \left[\nabla^2 \mathcal{R}(\boldsymbol{\theta}^*) + \nabla \mathbf{b}(\boldsymbol{\theta}^*) \right]^{-1} \Sigma(\boldsymbol{\theta}^*)^{\frac{1}{2}} Z}{n_0 + n_1 + \tilde{n}} + \mathbf{r}, \quad (52)$$

where $\|\mathbf{r}\| = O_P\left(\frac{1}{\sqrt{n_0 + n_1 + \tilde{n}}} \left\| \mathbf{b}(\tilde{\boldsymbol{\theta}}) \right\|^2\right)$.

For the third term (denoted as T_3) in the representation (48), plugging in the equations (50), (51), and together with lipschitz condition of $\nabla^2 \mathcal{R}(\boldsymbol{\theta})$, we have

$$T_3 = \frac{Z^\top \Sigma(\boldsymbol{\theta}^*)^{\frac{1}{2}} \left[\nabla^2 \mathcal{R}(\boldsymbol{\theta}^*) + \nabla \mathbf{b}(\boldsymbol{\theta}^*) \right]^{-1} \nabla^2 \mathcal{R}(\boldsymbol{\theta}^*) \left[\nabla^2 \mathcal{R}(\boldsymbol{\theta}^*) + \nabla \mathbf{b}(\boldsymbol{\theta}^*) \right]^{-1} \Sigma(\boldsymbol{\theta}^*)^{\frac{1}{2}} Z}{2(n_0 + n_1 + \tilde{n})^2} + \mathbf{r}, \quad (53)$$

where $\|\mathbf{r}\| = O_P\left(\left\| \mathbf{b}(\tilde{\boldsymbol{\theta}}) \right\|\right)$.

Finally, combine the representation for the second and third terms (equations (52) and (53)), we have

$$\begin{aligned}\mathcal{R}(\hat{\boldsymbol{\theta}}) - \mathcal{R}(\boldsymbol{\theta}^*) &= \frac{1}{2} \mathbf{b}(\boldsymbol{\theta}^*)^\top \left(\nabla^2 \mathcal{R}(\boldsymbol{\theta}^*) + \nabla \mathbf{b}(\boldsymbol{\theta}^*) \right)^{-1} \nabla^2 \mathcal{R}(\boldsymbol{\theta}^*) \left(\nabla^2 \mathcal{R}(\boldsymbol{\theta}^*) + \nabla \mathbf{b}(\boldsymbol{\theta}^*) \right)^{-1} \mathbf{b}(\boldsymbol{\theta}^*) \\ &- \frac{1}{n_0 + n_1 + \tilde{n}} \mathbf{b}(\boldsymbol{\theta}^*) \left[\nabla^2 \mathcal{R}(\boldsymbol{\theta}^*) + \nabla \mathbf{b}(\boldsymbol{\theta}^*) \right]^{-1} \nabla^2 \mathcal{R}(\boldsymbol{\theta}^*) \left[\nabla^2 \mathcal{R}(\boldsymbol{\theta}^*) + \nabla \mathbf{b}(\boldsymbol{\theta}^*) \right]^{-1} \Sigma(\boldsymbol{\theta}^*)^{\frac{1}{2}} Z \\ &+ \frac{1}{2(n_0 + n_1 + \tilde{n})^2} Z^\top \Sigma(\boldsymbol{\theta}^*)^{\frac{1}{2}} \left[\nabla^2 \mathcal{R}(\boldsymbol{\theta}^*) + \nabla \mathbf{b}(\boldsymbol{\theta}^*) \right]^{-1} \nabla^2 \mathcal{R}(\boldsymbol{\theta}^*) \left[\nabla^2 \mathcal{R}(\boldsymbol{\theta}^*) + \nabla \mathbf{b}(\boldsymbol{\theta}^*) \right]^{-1} \Sigma(\boldsymbol{\theta}^*)^{\frac{1}{2}} Z + R,\end{aligned}$$

where the remainder term R satisfies

$$R = O_P \left(\|\mathbf{b}(\tilde{\boldsymbol{\theta}})\|^3 + (n_0 + n_1 + \tilde{n})^{-\frac{3}{2}} + \frac{1}{n_0 + n_1 + \tilde{n}} \|\mathbf{b}(\tilde{\boldsymbol{\theta}})\| + \frac{1}{\sqrt{n_0 + n_1 + \tilde{n}}} \|\mathbf{b}(\tilde{\boldsymbol{\theta}})\|^2 \right).$$

For the remaining term, by integral form of Taylor expansion,

$$\begin{aligned}0 &= \nabla \tilde{\mathcal{R}}(\tilde{\boldsymbol{\theta}}) = \nabla \tilde{\mathcal{R}}(\boldsymbol{\theta}^*) + \left(\int_0^1 \nabla^2 \tilde{\mathcal{R}}(\boldsymbol{\theta}^* + t(\tilde{\boldsymbol{\theta}} - \boldsymbol{\theta}^*)) dt \right) (\tilde{\boldsymbol{\theta}} - \boldsymbol{\theta}^*) \\ &= \mathbf{b}(\boldsymbol{\theta}^*) + \left(\int_0^1 \nabla^2 \tilde{\mathcal{R}}(\boldsymbol{\theta}^* + t(\tilde{\boldsymbol{\theta}} - \boldsymbol{\theta}^*)) dt \right) (\tilde{\boldsymbol{\theta}} - \boldsymbol{\theta}^*).\end{aligned}$$

Therefore, by positive definite $\nabla^2 \mathcal{R}(\boldsymbol{\theta})$ assumption,

$$\|\tilde{\boldsymbol{\theta}} - \boldsymbol{\theta}^*\| \leq \left\| \left(\int_0^1 \nabla^2 \tilde{\mathcal{R}}(\boldsymbol{\theta}^* + t(\tilde{\boldsymbol{\theta}} - \boldsymbol{\theta}^*)) dt \right)^{-1} \right\| \|\mathbf{b}(\boldsymbol{\theta}^*)\| \lesssim \|\mathbf{b}(\boldsymbol{\theta}^*)\|.$$

Again by integral mean value theorem

$$\mathbf{b}(\tilde{\boldsymbol{\theta}}) = \mathbf{b}(\boldsymbol{\theta}^*) + \left(\int_0^1 \nabla \mathbf{b}(\boldsymbol{\theta}^* + t(\tilde{\boldsymbol{\theta}} - \boldsymbol{\theta}^*)) dt \right) (\tilde{\boldsymbol{\theta}} - \boldsymbol{\theta}^*).$$

By finite $\|\nabla \mathbf{b}(\boldsymbol{\theta})\|$ assumption, we have

$$\left\| \int_0^1 \nabla \mathbf{b}(\boldsymbol{\theta}^* + t(\tilde{\boldsymbol{\theta}} - \boldsymbol{\theta}^*)) dt \right\| \leq \sup \|\nabla \mathbf{b}(\boldsymbol{\theta})\| < \infty.$$

That is

$$\|\mathbf{b}(\tilde{\boldsymbol{\theta}})\| \lesssim \|\mathbf{b}(\boldsymbol{\theta}^*)\| + \left\| \int_0^1 \nabla \mathbf{b}(\boldsymbol{\theta}^* + t(\tilde{\boldsymbol{\theta}} - \boldsymbol{\theta}^*)) dt \right\| \|\tilde{\boldsymbol{\theta}} - \boldsymbol{\theta}^*\| \lesssim \|\mathbf{b}(\boldsymbol{\theta}^*)\|.$$

We thus can get rid of $\tilde{\boldsymbol{\theta}}$ in the remaining term by bounding it as

$$R = O_P \left(\|\mathbf{b}(\boldsymbol{\theta}^*)\|^3 + (n_0 + n_1 + \tilde{n})^{-\frac{3}{2}} + \frac{1}{n_0 + n_1 + \tilde{n}} \|\mathbf{b}(\boldsymbol{\theta}^*)\| + \frac{1}{\sqrt{n_0 + n_1 + \tilde{n}}} \|\mathbf{b}(\boldsymbol{\theta}^*)\|^2 \right).$$

We then finish the proof.

14.3 Proof of Theorem 3

By the choice of \mathcal{C} , the synthetic size within \mathcal{C} satisfies

$$\left(\frac{n_0}{n_0 + n_1 + \tilde{n}} - \frac{1}{2}\right)^2 \ll \frac{1}{n_0}.$$

Applying the decomposition in Theorem 2 (and the same order bounds used in the proof of Theorem 4),

$$T_1 \asymp \|\mathbf{b}(\boldsymbol{\theta}^*)\|^2, \quad |T_2| = \Theta_P\left(\frac{1}{\sqrt{n_0}}\|\mathbf{b}(\boldsymbol{\theta}^*)\|\right), \quad T_3 = \Theta_P\left(\frac{1}{n_0}\right). \quad (54)$$

By the projection detailed in equation (59), the norm satisfies

$$\begin{aligned} \|\mathbf{b}(\boldsymbol{\theta}^*)\|^2 &= \left(\pi_0 - \frac{1}{2} + \alpha\tilde{\pi}\frac{\|\nabla\psi(\boldsymbol{\theta}^*)\|}{\|\nabla\phi(\boldsymbol{\theta}^*)\|}\right)^2 \|\nabla\phi(\boldsymbol{\theta}^*)\|^2 + \beta^2\tilde{\pi}^2\|\nabla\psi(\boldsymbol{\theta}^*)\|^2 \\ &= \left(\pi_0 - \frac{1}{2}\right)^2 \|\nabla\phi(\boldsymbol{\theta}^*)\|^2 + 2\alpha\tilde{\pi}\left(\pi_0 - \frac{1}{2}\right)\|\nabla\phi(\boldsymbol{\theta}^*)\|\|\nabla\psi(\boldsymbol{\theta}^*)\| \\ &\quad + \alpha^2\tilde{\pi}^2\|\nabla\psi(\boldsymbol{\theta}^*)\|^2 + \beta^2\tilde{\pi}^2\|\nabla\psi(\boldsymbol{\theta}^*)\|^2, \end{aligned}$$

Combining the definition of \mathcal{C} and the synthetic generator quality $\|\nabla\psi(\boldsymbol{\theta}^*)\| \ll \frac{1}{\sqrt{n_0}}$, we have

$$\|\mathbf{b}(\boldsymbol{\theta}^*)\| \ll \frac{1}{\sqrt{n_0}}.$$

Together with equation (54), it holds that

$$T_1 \ll \frac{1}{n_0}, \quad |T_2| \ll \Theta_P\left(\frac{1}{n_0}\right), \quad T_3 = \Theta_P\left(\frac{1}{n_0}\right).$$

We thus finish the proof by noting all terms are small terms compared with T_3 .

14.4 Proof of Theorem 4

For the normalized expected loss gradient difference between synthetic data and minority data, we can make a projection, such that

$$\frac{\nabla\psi(\boldsymbol{\theta}^*)}{\|\nabla\psi(\boldsymbol{\theta}^*)\|} = \alpha\frac{\nabla\phi(\boldsymbol{\theta}^*)}{\|\nabla\phi(\boldsymbol{\theta}^*)\|} + \beta\mathbf{u},$$

where \mathbf{u} is a unit vector ($\|\mathbf{u}\| = 1$) with direction depending on $\nabla\psi(\boldsymbol{\theta}^*)$, and we have orthogonality $\mathbf{u}^\top \nabla\phi(\boldsymbol{\theta}^*) = 0$. It is easy to verify that here

$$\alpha = \cos \angle (\nabla\phi(\boldsymbol{\theta}^*), \nabla\psi(\boldsymbol{\theta}^*)), \quad \beta = \sin \angle (\nabla\phi(\boldsymbol{\theta}^*), \nabla\psi(\boldsymbol{\theta}^*)).$$

Therefore,

$$\nabla\psi(\boldsymbol{\theta}^*) = \alpha \frac{\|\nabla\psi(\boldsymbol{\theta}^*)\|}{\|\nabla\phi(\boldsymbol{\theta}^*)\|} \nabla\phi(\boldsymbol{\theta}^*) + \beta \|\nabla\psi(\boldsymbol{\theta}^*)\| \mathbf{u}, \quad (55)$$

Recall the first term

$$T_1 = \frac{1}{2} \mathbf{b}(\boldsymbol{\theta}^*)^\top \left(\nabla^2 \mathcal{R}(\boldsymbol{\theta}^*) + \nabla \mathbf{b}(\boldsymbol{\theta}^*) \right)^{-1} \nabla^2 \mathcal{R}(\boldsymbol{\theta}^*) \left(\nabla^2 \mathcal{R}(\boldsymbol{\theta}^*) + \nabla \mathbf{b}(\boldsymbol{\theta}^*) \right)^{-1} \mathbf{b}(\boldsymbol{\theta}^*), \quad (56)$$

we have

$$\nabla^2 \mathcal{R}(\boldsymbol{\theta}^*) + \nabla \mathbf{b}(\boldsymbol{\theta}^*) = \nabla^2 \mathcal{R}(\boldsymbol{\theta}^*) + \left(\pi_0 - \frac{1}{2} \right) \nabla^2 \phi(\boldsymbol{\theta}^*) + \tilde{\pi} \nabla^2 \psi(\boldsymbol{\theta}^*).$$

By assumption, we have

$$\lambda_{\min} \left(\nabla^2 \mathcal{R}(\boldsymbol{\theta}^*) + \nabla \mathbf{b}(\boldsymbol{\theta}^*) \right) \geq \lambda,$$

which is lower bounded by a constant. Therefore, the first term in Theorem 2 satisfies

$$T_1 \lesssim \|\mathbf{b}(\boldsymbol{\theta}^*)\|^2. \quad (57)$$

For the lower bound of the first term, we have by assumption on bounded $\|\nabla \mathbf{b}(\boldsymbol{\theta}^*)\|$ and both of them are fixed numbers that

$$\lambda_{\max} \left(\nabla^2 \mathcal{R}(\boldsymbol{\theta}^*) + \nabla \mathbf{b}(\boldsymbol{\theta}^*) \right) \leq c \lambda_{\max} \left(\nabla^2 \mathcal{R}(\boldsymbol{\theta}^*) \right),$$

which is a constant. Therefore, by the representation of the first term (56), we have

$$T_1 \geq \frac{\lambda}{c \lambda_{\max} \left(\nabla^2 \mathcal{R}(\boldsymbol{\theta}^*) \right)^2} \mathbf{b}(\boldsymbol{\theta}^*)^\top \mathbf{b}(\boldsymbol{\theta}^*) \gtrsim \|\mathbf{b}(\boldsymbol{\theta}^*)\|^2. \quad (58)$$

Therefore, combining equation (57) and (58) gives

$$T_1 \asymp \|\mathbf{b}(\boldsymbol{\theta}^*)\|^2.$$

We then analyze the term $\|\mathbf{b}(\boldsymbol{\theta}^*)\|^2$. By equation (55), it holds that

$$\mathbf{b}(\boldsymbol{\theta}^*) = \left(\pi_0 - \frac{1}{2} + \alpha \tilde{\pi} \frac{\|\nabla\psi(\boldsymbol{\theta}^*)\|}{\|\nabla\phi(\boldsymbol{\theta}^*)\|} \right) \cdot \nabla\phi(\boldsymbol{\theta}^*) + \beta \tilde{\pi} \|\nabla\psi(\boldsymbol{\theta}^*)\| \cdot \mathbf{u}. \quad (59)$$

Taking norms and setting synthetic size as

$$\tilde{n} = \frac{n_0 - n_1 + O_P(\sqrt{n_0})}{1 - 2\|\nabla\psi(\boldsymbol{\theta}^*)\|/\|\nabla\phi(\boldsymbol{\theta}^*)\|\alpha + O_P(1/\sqrt{n_0})},$$

we have

$$\left\| \left(\pi_0 - \frac{1}{2} + \alpha \tilde{\pi} \frac{\|\nabla\psi(\boldsymbol{\theta}^*)\|}{\|\nabla\phi(\boldsymbol{\theta}^*)\|} \right) \cdot \nabla\phi(\boldsymbol{\theta}^*) \right\| = O_P\left(\frac{1}{\sqrt{n_0}}\right),$$

while the second term

$$\|\beta \tilde{\pi} \|\nabla\psi(\boldsymbol{\theta}^*)\| \cdot \mathbf{u}\| = O_P\left(\frac{1}{\sqrt{n_0}}\right),$$

where the inequality follows by the assumption

$$\beta = \sin \angle(\nabla\phi(\boldsymbol{\theta}^*), \nabla\psi(\boldsymbol{\theta}^*)) \lesssim \frac{1}{\|\nabla\psi(\boldsymbol{\theta}^*)\|\sqrt{n_0}}.$$

Combining, we have

$$\|\mathbf{b}(\boldsymbol{\theta}^*)\|^2 \lesssim \left\| \left(\pi_0 - \frac{1}{2} + \alpha \tilde{\pi} \frac{\|\nabla\psi(\boldsymbol{\theta}^*)\|}{\|\nabla\phi(\boldsymbol{\theta}^*)\|} \right) \cdot \nabla\phi(\boldsymbol{\theta}^*) \right\|^2 + \|\beta \tilde{\pi} \|\nabla\psi(\boldsymbol{\theta}^*)\| \cdot \mathbf{u}\|^2 = O_P\left(\frac{1}{n_0}\right),$$

Similarly, it is easy to show that the second and third term follows that

$$|T_2| = \Theta_P\left(\frac{1}{\sqrt{n_0}}\|\mathbf{b}(\boldsymbol{\theta}^*)\|\right) \lesssim \Theta_P\left(\frac{1}{n_0}\right), \quad T_3 = \Theta_P\left(\frac{1}{n_0}\right).$$

Therefore, the excess risk satisfies

$$\mathcal{R}(\hat{\boldsymbol{\theta}}) - \mathcal{R}(\boldsymbol{\theta}^*) = \Theta_P\left(\frac{1}{n_0}\right).$$

For the second statement, simply plugging in the synthetic size $\tilde{n} = n_0 - n_1$ gives

$$\mathbf{b}(\boldsymbol{\theta}^*) = \alpha \frac{n_0 - n_1}{2n_0} \frac{\|\nabla\psi(\boldsymbol{\theta}^*)\|}{\|\nabla\phi(\boldsymbol{\theta}^*)\|} \cdot \nabla\phi(\boldsymbol{\theta}^*) + \beta \frac{n_0 - n_1}{2n_0} \|\nabla\psi(\boldsymbol{\theta}^*)\| \cdot \mathbf{u}.$$

Taking norms and squaring both sides,

$$\|\mathbf{b}(\boldsymbol{\theta}^*)\|^2 = \alpha^2 \left(\frac{n_0 - n_1}{2n_0} \right)^2 \|\nabla\psi(\boldsymbol{\theta}^*)\|^2 + \beta^2 \left(\frac{n_0 - n_1}{2n_0} \right)^2 \|\nabla\psi(\boldsymbol{\theta}^*)\|^2 \asymp \|\nabla\psi(\boldsymbol{\theta}^*)\|^2.$$

That is, it follows that

$$T_1 \asymp \|\nabla\psi(\boldsymbol{\theta}^*)\|^2, \quad |T_2| = \Theta_P \left(\frac{1}{\sqrt{n_0}} \|\nabla\psi(\boldsymbol{\theta}^*)\| \right), \quad T_3 = \Theta_P \left(\frac{1}{n_0} \right).$$

Finally, we have the excess risk

$$\mathcal{R}(\hat{\boldsymbol{\theta}}) - \mathcal{R}(\boldsymbol{\theta}^*) = \Theta_P \left(\|\nabla\psi(\boldsymbol{\theta}^*)\|^2 \right) \gg \Theta_P \left(\frac{1}{n_0} \right).$$

We then finish the proof.

14.5 Proof of Theorem 5

By similar procedure with proof of theorem 4, we make projection

$$\frac{\nabla\psi(\boldsymbol{\theta}^*)}{\|\nabla\psi(\boldsymbol{\theta}^*)\|} = \alpha \frac{\nabla\phi(\boldsymbol{\theta}^*)}{\|\nabla\phi(\boldsymbol{\theta}^*)\|} + \beta \mathbf{u},$$

where \mathbf{u} is a unit vector ($\|\mathbf{u}\| = 1$) with direction depending on $\nabla\psi(\boldsymbol{\theta}^*)$, and we have orthogonality $\mathbf{u}^\top \nabla\phi(\boldsymbol{\theta}^*) = 0$. That is,

$$\nabla\psi(\boldsymbol{\theta}^*) = \alpha \frac{\|\nabla\psi(\boldsymbol{\theta}^*)\|}{\|\nabla\phi(\boldsymbol{\theta}^*)\|} \nabla\phi(\boldsymbol{\theta}^*) + \beta \|\nabla\psi(\boldsymbol{\theta}^*)\| \mathbf{u},$$

Plugging in gives

$$\mathbf{b}(\boldsymbol{\theta}^*) = \left(\pi_0 - \frac{1}{2} + \alpha \tilde{\pi} \frac{\|\nabla\psi(\boldsymbol{\theta}^*)\|}{\|\nabla\phi(\boldsymbol{\theta}^*)\|} \right) \nabla\phi(\boldsymbol{\theta}^*) + \beta \tilde{\pi} \|\nabla\psi(\boldsymbol{\theta}^*)\| \mathbf{u}.$$

With the selection of

$$\tilde{n} = \frac{n_0 - n_1 + (n_0 + n_1)o(1)}{1 - 2\|\nabla\psi(\boldsymbol{\theta}^*)\|/\|\nabla\phi(\boldsymbol{\theta}^*)\|\alpha + o(1)},$$

we have

$$\pi_0 - \frac{1}{2} + \alpha \tilde{\pi} \frac{\|\nabla\psi(\boldsymbol{\theta}^*)\|}{\|\nabla\phi(\boldsymbol{\theta}^*)\|} = o_P(1).$$

Also by assumption, $\beta = o(1)$. Therefore, we have the total synthetic bias

$$\|\mathbf{b}(\boldsymbol{\theta}^*)\| = o_P(1).$$

By previous analysis of the excess risk, we have

$$\mathcal{R}(\hat{\boldsymbol{\theta}}) - \mathcal{R}(\boldsymbol{\theta}^*) = o_P(1).$$

If we still choose synthetic size $\tilde{n} = n_0 - n_1$, it holds that

$$\liminf_{n_0, n_1 \rightarrow \infty} \|\mathbf{b}(\boldsymbol{\theta}^*)\| \geq \liminf_{n_0, n_1 \rightarrow \infty} \left| \alpha \left(\frac{1}{2} - \frac{n_1}{2n_0} \right) \right| \|\nabla\psi(\boldsymbol{\theta}^*)\| \geq c > 0.$$

Thus by Theorem 1, the excess risk

$$\liminf_{n_0, n_1 \rightarrow \infty} \mathcal{R}(\hat{\boldsymbol{\theta}}) - \mathcal{R}(\boldsymbol{\theta}^*) \geq c > 0,$$

in probability.

When synthetic direction is not aligned such that $\sin \angle(\nabla\phi(\boldsymbol{\theta}^*), \nabla\psi(\boldsymbol{\theta}^*)) > c > 0$ in probability, and $\tilde{n}/n_0 \rightarrow \rho$, we have $\tilde{\pi} \rightarrow \frac{\rho}{1+\rho+n_1/n_0}$, $\pi_0 \rightarrow \frac{1}{1+\rho+n_1/n_0}$. Therefore,

$$\|\mathbf{b}(\boldsymbol{\theta}^*)\|^2 = \left(\pi_0 - \frac{1}{2} + \alpha\tilde{\pi} \frac{\|\nabla\psi(\boldsymbol{\theta}^*)\|}{\|\nabla\phi(\boldsymbol{\theta}^*)\|} \right)^2 \|\nabla\phi(\boldsymbol{\theta}^*)\|^2 + \beta^2 \tilde{\pi}^2 \|\nabla\psi(\boldsymbol{\theta}^*)\|^2 \|\mathbf{u}\|^2 \gtrsim c$$

Thus by Theorem 1, the excess risk satisfies

$$\mathcal{R}(\hat{\boldsymbol{\theta}}) - \mathcal{R}(\boldsymbol{\theta}^*) \geq c + o_P(1).$$

14.6 Proof of Theorem 6

For diminishing synthetic size $\tilde{n} = O(\sqrt{n_0}/\|\nabla\psi(\boldsymbol{\theta}^*)\|)$, under $\nabla\phi(\boldsymbol{\theta}^*) = 0$ and a realistic generator, we have

$$\mathbf{b}(\boldsymbol{\theta}^*) = \tilde{\pi}\nabla\psi(\boldsymbol{\theta}^*) \quad \Rightarrow \quad \|\mathbf{b}(\boldsymbol{\theta}^*)\| = \frac{\tilde{n}}{n_0 + n_1 + \tilde{n}} \|\nabla\psi(\boldsymbol{\theta}^*)\| = O(n_0^{-1/2}).$$

From previous analysis for Theorem 2, it holds that

$$T_1 \asymp \|\mathbf{b}(\boldsymbol{\theta}^*)\|^2, \quad T_2 = \Theta_P \left(\frac{\|\mathbf{b}(\boldsymbol{\theta}^*)\|}{\sqrt{n_0 + n_1 + \tilde{n}}} \right), \quad T_3 = \Theta_P \left(\frac{1}{n_0 + n_1 + \tilde{n}} \right),$$

and remaining term R is smaller order term under this setting. Thus, we conclude that

$$\mathcal{R}(\hat{\boldsymbol{\theta}}) - \mathcal{R}(\boldsymbol{\theta}^*) = O_P(n_0^{-1}).$$

For the non-diminishing synthetic size $\tilde{n} \gtrsim n_0$, we have

$$\|\mathbf{b}(\boldsymbol{\theta}^*)\| = \frac{\tilde{n}}{n_0 + n_1 + \tilde{n}} \|\nabla\psi(\boldsymbol{\theta}^*)\| \gtrsim \|\nabla\psi(\boldsymbol{\theta}^*)\|.$$

Similarly by the order analysis of Theorem 2,

$$\mathcal{R}(\hat{\boldsymbol{\theta}}) - \mathcal{R}(\boldsymbol{\theta}^*) = \Theta_P(\|\mathbf{b}(\boldsymbol{\theta}^*)\|^2) \gtrsim \Omega_P(\|\nabla\psi(\boldsymbol{\theta}^*)\|^2) \gg \Theta_P(n_0^{-1}).$$

14.7 Proof of Proposition 1

For the squared loss, we have

$$f_{\boldsymbol{\theta}}(\mathbf{x}) = \boldsymbol{\theta}^\top \mathbf{x}, \quad \ell(\boldsymbol{\theta}; \mathbf{x}, y) = (y - 1/2 - \boldsymbol{\theta}^\top \mathbf{x})^2, \quad \nabla\ell(\boldsymbol{\theta}; \mathbf{x}, y) = -2(y - 1/2 - \boldsymbol{\theta}^\top \mathbf{x})\mathbf{x}.$$

Thus for the population of majority,

$$\mathbb{E}_{\mathcal{P}_0} \nabla\ell(\boldsymbol{\theta}; \mathbf{x}, 0) = \mathbb{E}_{\mathcal{P}_0} [(1 + 2\boldsymbol{\theta}^\top \mathbf{x})\mathbf{x}] = 2(\boldsymbol{\mu}\boldsymbol{\mu}^\top + \mathbb{E}[\boldsymbol{\xi}\boldsymbol{\xi}^\top])\boldsymbol{\theta} - \boldsymbol{\mu}.$$

Similarly for minority

$$\mathbb{E}_{\mathcal{P}_1} \nabla\ell(\boldsymbol{\theta}; \mathbf{x}, 1) = \mathbb{E}_{\mathcal{P}_1} [(2\boldsymbol{\theta}^\top \mathbf{x} - 1)\mathbf{x}] = 2(\boldsymbol{\mu}\boldsymbol{\mu}^\top + \mathbb{E}[\boldsymbol{\xi}\boldsymbol{\xi}^\top])\boldsymbol{\theta} - \boldsymbol{\mu}.$$

Thus the derivative of the balanced risk is

$$\nabla\mathcal{R}(\boldsymbol{\theta}) = \frac{1}{2}\mathbb{E}_{\mathcal{P}_0} \nabla\ell(\boldsymbol{\theta}; \mathbf{x}, 0) + \frac{1}{2}\mathbb{E}_{\mathcal{P}_1} \nabla\ell(\boldsymbol{\theta}; \mathbf{x}, 1) = 2(\boldsymbol{\mu}\boldsymbol{\mu}^\top + \mathbb{E}[\boldsymbol{\xi}\boldsymbol{\xi}^\top])\boldsymbol{\theta} - \boldsymbol{\mu} = 0.$$

Solving gives the minimum

$$\boldsymbol{\theta}^* = \frac{1}{2} [\boldsymbol{\mu}\boldsymbol{\mu}^\top + \mathbb{E}[\boldsymbol{\xi}\boldsymbol{\xi}^\top]]^{-1} \boldsymbol{\mu}.$$

Also, plugging in gives the majority-minority bias cancels

$$\nabla\phi(\boldsymbol{\theta}^*) = \mathbb{E}_{\mathcal{P}_0} \nabla\ell(\boldsymbol{\theta}; \mathbf{x}, 0) - \mathbb{E}_{\mathcal{P}_1} \nabla\ell(\boldsymbol{\theta}; \mathbf{x}, 1) = 0.$$

14.8 Proof of Proposition 2

Under the data generating mechanism of sigmoid Bernoulli model, the class conditionals are

$$\begin{aligned}\mathcal{P}_1 &\sim \mathbb{P}(\mathbf{x} \mid y = 1) = \frac{\mathbb{P}(y = 1 \mid \mathbf{x})p(\mathbf{x})}{\mathbb{P}(y = 1)} = \frac{p(\mathbf{x})\sigma(\boldsymbol{\theta}_{\text{true}}^\top \mathbf{x})}{\mathbb{P}(y = 1)}, \\ \mathcal{P}_0 &\sim \mathbb{P}(\mathbf{x} \mid y = 0) = \frac{\mathbb{P}(y = 0 \mid \mathbf{x})p(\mathbf{x})}{\mathbb{P}(y = 0)} = \frac{p(\mathbf{x})(1 - \sigma(\boldsymbol{\theta}_{\text{true}}^\top \mathbf{x}))}{\mathbb{P}(y = 0)},\end{aligned}$$

where

$$\begin{aligned}\mathbb{P}(y = 1) &= \int \mathbb{P}(\mathbf{x}, y = 1) = \int \mathbb{P}(y = 1 \mid \mathbf{x})p(\mathbf{x}) = \mathbb{E}_p[\sigma(\boldsymbol{\theta}_{\text{true}}^\top \mathbf{x})], \\ \mathbb{P}(y = 0) &= 1 - \mathbb{E}_p[\sigma(\boldsymbol{\theta}_{\text{true}}^\top \mathbf{x})].\end{aligned}$$

The derivative of the logistic loss is

$$\nabla \ell(\boldsymbol{\theta}; \mathbf{x}, y) = (\sigma(\boldsymbol{\theta}^\top \mathbf{x}) - y)\mathbf{x}.$$

Then for majority under the true parameter,

$$\begin{aligned}\mathbb{E}_{\mathcal{P}_0} \nabla \ell(\boldsymbol{\theta}_{\text{true}}; \mathbf{x}, 0) &= \mathbb{E}_{\mathcal{P}_0} \sigma(\boldsymbol{\theta}_{\text{true}}^\top \mathbf{x}) \mathbf{x} \\ &= \int \sigma(\boldsymbol{\theta}_{\text{true}}^\top \mathbf{x}) \mathbf{x} \frac{p(\mathbf{x})(1 - \sigma(\boldsymbol{\theta}_{\text{true}}^\top \mathbf{x}))}{\mathbb{P}(y = 0)} = \frac{1}{\mathbb{P}(y = 0)} \mathbb{E}_{p(\mathbf{x})} \left[\mathbf{x} \sigma(\boldsymbol{\theta}_{\text{true}}^\top \mathbf{x}) (1 - \sigma(\boldsymbol{\theta}_{\text{true}}^\top \mathbf{x})) \right].\end{aligned}$$

Similarly for minority

$$\mathbb{E}_{\mathcal{P}_1} \nabla \ell(\boldsymbol{\theta}_{\text{true}}; \mathbf{x}, 1) = -\frac{1}{\mathbb{P}(y = 1)} \mathbb{E}_{p(\mathbf{x})} \left[\mathbf{x} \sigma(\boldsymbol{\theta}_{\text{true}}^\top \mathbf{x}) (1 - \sigma(\boldsymbol{\theta}_{\text{true}}^\top \mathbf{x})) \right].$$

Then we conclude that $\boldsymbol{\theta}_{\text{true}}$ is the minimizer of the balanced risk by noticing

$$\begin{aligned}\nabla \mathcal{R}(\boldsymbol{\theta}_{\text{true}}) &= \frac{1}{2} \mathbb{E}_{\mathcal{P}_0} \nabla \ell(\boldsymbol{\theta}_{\text{true}}; \mathbf{x}, 0) + \frac{1}{2} \mathbb{E}_{\mathcal{P}_1} \nabla \ell(\boldsymbol{\theta}_{\text{true}}; \mathbf{x}, 1) \\ &= \frac{1}{2} \left(\frac{1}{\mathbb{P}(y = 0)} - \frac{1}{\mathbb{P}(y = 1)} \right) \mathbb{E}_{p(\mathbf{x})} \left[\mathbf{x} \sigma(\boldsymbol{\theta}_{\text{true}}^\top \mathbf{x}) (1 - \sigma(\boldsymbol{\theta}_{\text{true}}^\top \mathbf{x})) \right] = 0.\end{aligned}$$

By strong convexity around the minimizer of $\mathcal{R}(\boldsymbol{\theta})$, we have uniqueness of the minimizer, and thus $\boldsymbol{\theta}^* = \boldsymbol{\theta}_{\text{true}}$. Therefore the majority-minority difference cancels

$$\begin{aligned}\nabla \phi(\boldsymbol{\theta}^*) &= \mathbb{E}_{\mathcal{P}_0} \nabla \ell(\boldsymbol{\theta}_{\text{true}}; \mathbf{x}, 0) - \mathbb{E}_{\mathcal{P}_1} \nabla \ell(\boldsymbol{\theta}_{\text{true}}; \mathbf{x}, 1) \\ &= \left(\frac{1}{\mathbb{P}(y = 0)} + \frac{1}{\mathbb{P}(y = 1)} \right) \mathbb{E}_{p(\mathbf{x})} \left[\mathbf{x} \sigma(\boldsymbol{\theta}_{\text{true}}^\top \mathbf{x}) (1 - \sigma(\boldsymbol{\theta}_{\text{true}}^\top \mathbf{x})) \right] = 0.\end{aligned}$$

We thus finish the proof.

15 Additional Results and Details for Simulation Studies

15.1 Under Local Asymmetry

15.1.1 For Biased Synthetic Generator

In the local asymmetry case, we study the classification with directional alignment. To illustrate the directional-alignment phenomenon for biased synthetic generator discussed in Section 4.3 of the main paper, we consider a 2D Gaussian setting as in Example 2, with imbalance ratio $n_0/n_1 = 20$. For n_1 varying from 6 to 3200, we set $n_0 = 20n_1$, draw majority samples $\mathbf{x} \mid y = 0 \sim \mathcal{N}(0, I_2)$ and minority samples $\mathbf{x} \mid y = 1 \sim \mathcal{N}(\boldsymbol{\mu}_1, I_2)$ with $\boldsymbol{\mu}_1 = (\mu, 0)$ and $\mu = 1$. We augment the training data with \tilde{n} synthetic points labeled as minority, generated from a biased but directionally aligned generator $\mathbf{x}_{\text{syn}} \sim \mathcal{N}(\boldsymbol{\mu}_s, I_2)$ with $\boldsymbol{\mu}_s = (a, 0)$ and $a = 0.5$. For each repetition (100 Monte Carlo runs per n_1), we also generate a fresh balanced test set of size 5000 per class from the true distributions. We compare two fixed synthetic-size rules: the naive balancing choice $\tilde{n} = n_0 - n_1$ and the bias-canceling choice $\tilde{n} = 4(n_0 - n_1)$ (from the analysis of Example 2). On each augmented training set, we fit the linear predictor $\hat{\boldsymbol{\theta}} \in \mathbb{R}^2$ by least squares and evaluate (i) parameter error $\|\hat{\boldsymbol{\theta}} - \boldsymbol{\theta}^*\|_2$ and (ii) balanced excess risk $\mathcal{R}(\hat{\boldsymbol{\theta}}) - \mathcal{R}(\boldsymbol{\theta}^*)$, where $\mathcal{R}(\boldsymbol{\theta}) = \|\boldsymbol{\theta}\|_2^2 + \frac{1}{2}(\boldsymbol{\theta}^\top \boldsymbol{\mu}_1 - 1)^2$ and $\boldsymbol{\theta}^* = (\mu/(\mu^2 + 2), 0)$. Finally, we plot the mean and standard deviation of the excess risk and parameter error versus n_1 on log scales for the two choices of \tilde{n} . The results are reported in Figure 2 in the main paper.

15.1.2 For Consistent Synthetic Generators

For directional alignment with a realistic and consistent synthetic generator (Section 4.2 of the main paper), we simulate the same 2D Gaussian setup as above under imbalance $n_0/n_1 = 20$ and squared loss. For $n_1 \in [10, 500]$, we run 100 Monte Carlo repetitions. Synthetic minority samples are produced by a realistic, consistent, and directionally aligned generator: for a requested synthetic size k , draw $\mathbf{x}_{\text{syn}} \sim \mathcal{N}(\boldsymbol{\mu}_{\text{syn}}, I_2)$ with $\boldsymbol{\mu}_{\text{syn}} = \left(1 - (\log n_1)^{-1/2}\right) \boldsymbol{\mu}_1$, so that the synthetic mean approaches $\boldsymbol{\mu}_1$ as n_1 increases while remaining aligned with $\boldsymbol{\mu}_1$. We compare VTSS with the naive balancing rule $\tilde{n} = n_0 - n_1$, fit a least-squares predictor on the augmented training data, and evaluate both methods using population excess risk $\mathcal{R}(\hat{\boldsymbol{\theta}}) - \mathcal{R}(\boldsymbol{\theta}^*)$ and parameter error $\|\hat{\boldsymbol{\theta}} - \boldsymbol{\theta}^*\|_2$, reporting mean and empirical 95% confidence interval over repetitions as functions of n_1 . The results are shown in Figure 3 in the main paper.

15.2 Under Local Symmetry

15.2.1 Mean-Shift Model

To further illustrate local symmetry (Section 5 of the main paper), we conduct a simulation study based on the mean-shift model in Example 3. We generate imbalanced binary data in dimension $d = 20$ from $\mathbf{x} \mid y = 1 \sim \boldsymbol{\mu} + \boldsymbol{\xi}$, $\mathbf{x} \mid y = 0 \sim -\boldsymbol{\mu} + \boldsymbol{\xi}$, where $\boldsymbol{\mu} = \delta \mathbf{e}_1$ with $\delta = 1$ and $\mathbf{e}_1 = (1, 0, \dots, 0)^\top$. Here $\boldsymbol{\xi}$ has mean zero and identity covariance. We consider three choices of $\boldsymbol{\xi}$: (i) Uniform cube with independent coordinates $\xi_j \sim \text{Unif}[-\sqrt{3}, \sqrt{3}]$, (ii) Rademacher with $\xi_j \in \{-1, +1\}$ equally likely, and (iii) Uniform-on-sphere obtained by sampling $\mathbf{g} \sim \mathcal{N}(0, I_d)$ and setting $\boldsymbol{\xi} = \sqrt{d} \mathbf{g} / \|\mathbf{g}\|$. We start from an imbalanced training sample with $n_1 = 100$ and $n_0 = 2000$, and augment the minority class with $\tilde{n} = \text{round}(\gamma(n_0 - n_1))$ synthetic samples, where γ ranges over 20 values in $[0, 4]$. We fit a linear predictor under squared loss on the augmented sample and report the balanced

excess risk $\mathcal{R}(\hat{\theta}) - \mathcal{R}(\theta^*)$, where $\theta^* = \mu / (1 + \|\mu\|_2^2)$ and $\mathcal{R}(\theta)$ is evaluated in closed form under the population model. We compare four synthetic generators: (i) **Oracle**, which draws synthetic points from the true minority distribution $\mu + \xi$; (ii) **SMOTE**, which interpolates between minority neighbors (with $k = 5$); (iii) **Gaussian-fit**, which samples from $\mathcal{N}(\hat{\mu}_1, \hat{\Sigma})$ using the empirical minority mean and covariance estimate; and (iv) **Semi-Oracle**, which samples ξ from the true noise distribution but centers at the empirical minority mean $\hat{\mu}_1$ (i.e., $\hat{\mu}_1 + \xi$). Results are averaged over 100 Monte Carlo repetitions, and we plot the mean balanced excess risk across repetitions as a function of γ on a log scale. The results are reported in Figure 4 of the main paper.

We also examine the VTSS-selected multiplier γ^* in the same mean-shift setup. Rather than sweeping γ to plot excess-risk curves, we focus on the empirical distribution of the minimizer γ^* . For each noise distribution ξ (Uniform cube, Rademacher, Uniform sphere), we run 500 repetitions. In each repetition, we generate a fresh balanced validation set with 2000 samples per class and tune over a grid of 200 equally spaced candidates $\gamma \in [0, 2]$ (including $\gamma = 0$). For each candidate γ and each generator, we fit the least-squares predictor on the augmented training set and set γ^* to the minimizer of the validation loss. Figure 9 reports the empirical distribution of γ^* . VTSS selects a very small γ^* in the vast majority of runs and frequently chooses $\gamma^* = 0$ exactly. The intuition is that when synthetic augmentation provides no genuine benefit and can introduce mismatch-induced bias, the balanced validation objective typically does not decrease as γ increases. Hence, the minimizer is attained at (or near) the boundary $\gamma = 0$, allowing the procedure to automatically opt out of synthetic data in this regime.

15.2.2 Sigmoid Bernoulli Logistic Model

To further demonstrate a regime where class imbalance is not the bottleneck, we consider the sigmoid Bernoulli logistic model in Example 4 with dimension $d = 20$. We let $v = \mathbf{e}_1$

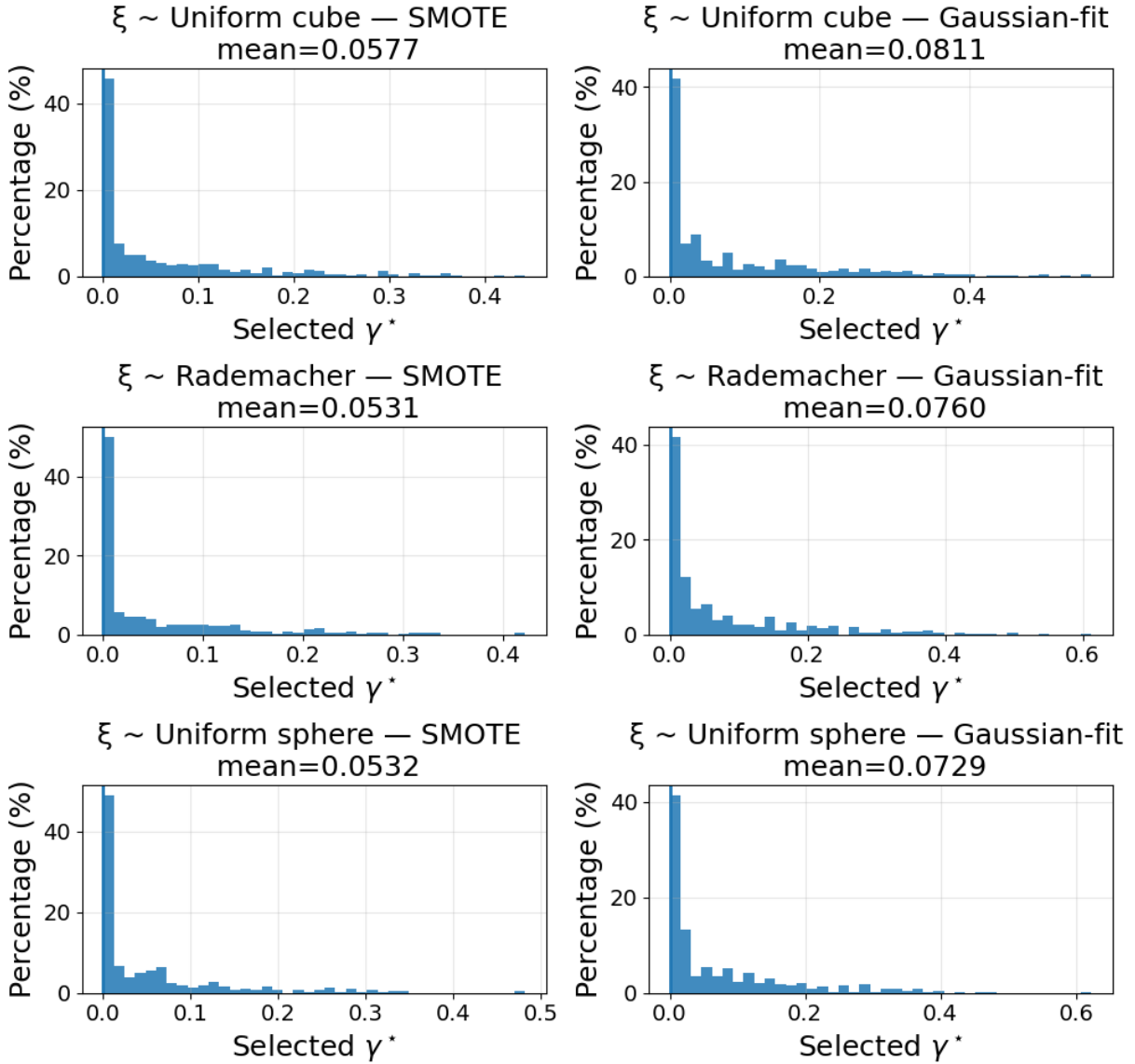


Figure 9: Histograms of the selected synthetic multiplier γ^* chosen by VTSS.

and $\boldsymbol{\theta}_{\text{true}} = c\mathbf{v}$ with $c = 1$, and generate covariates as $\mathbf{x} = T\mathbf{v} + W$, where $T \in \{-a, b\}$ with $a = 5$, $b = 1$, and $\mathbb{P}(T = -a) = \alpha$ chosen by the bias-cancellation formula (equation (10) in the Supplement). The noise W is orthogonal to \mathbf{v} (its first coordinate is identically zero) and has a symmetric, non-Gaussian mixture distribution in the remaining coordinates: $W_{2:d} = \mathbf{z} + s\boldsymbol{\mu}$ with $\mathbf{z} \sim \mathcal{N}(0, I)$, $s \in \{\pm 1\}$ equally likely, and $\boldsymbol{\mu}$ having its first three entries equal to 2.5 (others zero), making Gaussian-fit imperfect. Labels are drawn as $y \in \{0, 1\}$ with $\mathbb{P}(y = 1 \mid \mathbf{x}) = \sigma(\boldsymbol{\theta}_{\text{true}}^\top \mathbf{x})$. For each of 100 repetitions, we sample $n_{\text{train}} = 5000$

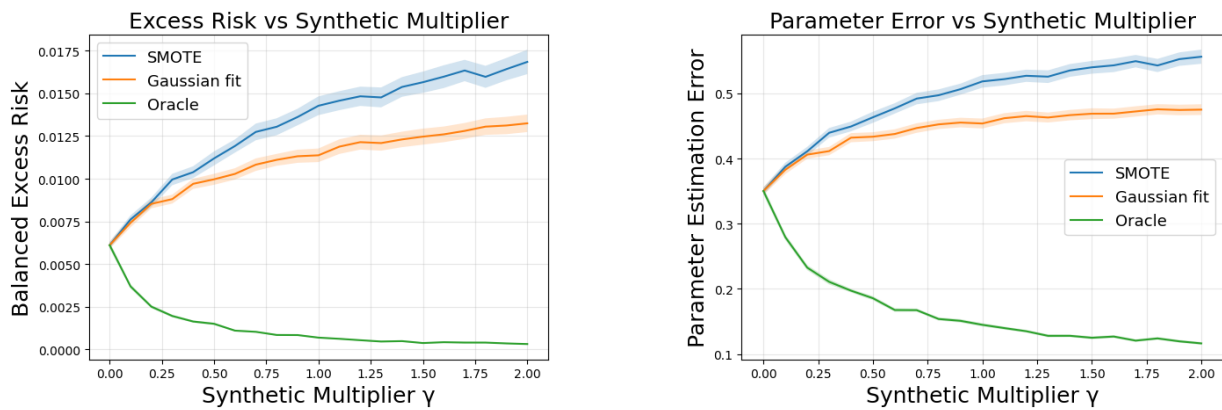


Figure 10: Synthetic augmentation does not help under a bias-cancellation sigmoid Bernoulli logistic model.

i.i.d. training pairs (\mathbf{x}, y) (with random realized class counts), define the minority class as the label with fewer observations, and augment only that minority class to size $n_1 + \tilde{n}$, where $\tilde{n} = \text{round}(\gamma(n_0 - n_1))$ and γ ranges over $[0, 2]$. We compare three generators for minority augmentation: SMOTE (nearest-neighbor interpolation with $k = 5$), Gaussian-fit (sampling from a fitted Gaussian using the minority empirical mean and covariance with a small ridge), and an Oracle generator that draws fresh (\mathbf{x}, y) from the true model and keeps only minority-labeled points. For each augmented dataset, we fit logistic regression and report (i) balanced excess logistic risk relative to $\boldsymbol{\theta}^*$ and (ii) parameter error $\|\hat{\boldsymbol{\theta}} - \boldsymbol{\theta}^*\|_2$, where $\boldsymbol{\theta}^*$ is obtained by fitting the same model on a large balanced sample of 20,000 per class.

Figure 10 shows that, for realistic generators such as SMOTE and Gaussian-fit, increasing γ does not reduce balanced excess risk or parameter error; in fact, performance typically worsens. In contrast, the Oracle generator improves monotonically, as expected.

15.2.3 Further Evaluation of VTSS

We consider two configurations in Section 7.3 in the main paper.

Linear classification (SMOTE + logistic regression). We generate imbalanced training data in $d = 5$ with ratio $r = n_0/n_1 = 20$ (in the plotted curve, $n_1 = 200$, $n_0 = 4000$, and $n_0 - n_1 = 3800$). The majority class is $\mathcal{N}(0, I)$, while the minority class is a balanced two-component Gaussian mixture, with each component having covariance I and means $\boldsymbol{\mu}_{\pm} = \delta \mathbf{e}_1 \pm \frac{\xi}{2} \mathbf{e}_2$. For each of 100 repetitions, we sweep \tilde{n} over a grid induced by $\gamma \in [0.6, 1.4]$ via $\tilde{n} = \text{round}(\gamma(n_0 - n_1))$, apply SMOTE to reach minority size $n_1 + \tilde{n}$, fit logistic regression, and evaluate balanced test log-loss on a fixed balanced test set (10,000 per class). VTSS chooses \tilde{n} in each repetition by minimizing the same balanced log-loss on a validation set, and we plot its average test loss as a horizontal reference line.

Nonlinear classification (perturbed sampling + kernel logistic). We use a non-Gaussian data-generating process in $d = 5$. For the majority class $y = 0$, we first draw a mixture indicator $z \sim \text{Bernoulli}(0.30)$, then sample the first two coordinates from a correlated Gaussian $(x_1, x_2) \sim \mathcal{N}\left((1.5 \cdot z, 0), \begin{pmatrix} 1 & 0.5 \\ 0.5 & 1 \end{pmatrix}\right)$, and sample the remaining coordinates i.i.d. as $x_{3:5} \sim \mathcal{N}(0, I_3)$. For the minority class $y = 1$, we generate a noisy ring in the (x_1, x_2) -plane by drawing an angle $\omega \sim \text{Unif}[0, 2\pi]$ and radius $r = 2.2 + \varepsilon_r$ with $\varepsilon_r \sim \mathcal{N}(0, 0.12^2)$, then setting $x_1 = \delta + r \cos \omega + \varepsilon_1$, $x_2 = r \sin \omega + \varepsilon_2$, with $\varepsilon_1, \varepsilon_2 \sim \mathcal{N}(0, 0.08^2)$ and $\delta = 4.8$. The remaining coordinates are small Gaussian noise $x_{3:5} \sim \mathcal{N}(0, 0.08^2 I_3)$. This simulation is a controlled nonlinear-boundary benchmark, designed to test whether VTSS can tune synthetic size when the generator introduces distributional blur. We embed the 2D structure in $d = 5$ by adding nuisance coordinates, reflecting the common setting where only a subset of features drives class separation. Synthetic data are generated by perturbed resampling: bootstrap minority points and add Gaussian jitter $\mathcal{N}(0, I)$. We train an RBF-kernel probabilistic classifier, sweep $\tilde{n} = \text{round}(\gamma(n_0 - n_1))$ over $\gamma \in [0.6, 1.4]$, and let VTSS pick \tilde{n} via validation minimization in each repetition.

The results are reported in Figure 5 of the main paper.